A change of pace: How fish alter kinematics with swim speed

A dissertation submitted by

Andrew David Clark

In partial fulfillment of the requirements for the degree of

Doctor of Philosophy

in

Biology

Tufts University

May 2025

©2025 Andrew David Clark

Advisor: Eric Tytell

Abstract

Fishes swim in diverse and complicated ways, but too often, we tend to reduce their swimming to simplified models, which facilitates analysis, but limits complexity. Even when scientists study complex behaviors, they often ignore how context can influence their results. Here, we aimed to address this gap in the literature by first challenging the form equals function model, then by quantifying various features of maneuvering, with an emphasis on how speed imkpacts kinematics. First, we compared steady swimming bluegill sunfish (*Lepomis macrochirus*) with steady swimming pumpkinseed sunfish (*Lepomis gibbosus*) to understand their forms and how their forms contribute to their kinematics. Based on prevailing thought, due to how morphologically similar the two species are, we should have found very few kinematic differences. However, we quantified signficantly different caudal fin kinematics that suggest these morphometrically similar species are functionally distinct. We also measured heart rate in bluegill to understand how it changes with swimming speed and maneuvering. By inserting electrodes into the fish's pericardial cavity and by filming and tracking their movements over time at a range of flow speeds, we concluded that heart rate changes on a very small scale as bluegill swim steadily at higher speeds, but that heart rate does not do a good job of capturing the costs of maneuvering. We also quantified fin and body kinematics during braking at various speeds. We observed distinct speed-related differences in how much force bluegill produce with their fins at increasing speeds, and also quantified how they handled stability during braking. Finally, we explored how bluegill solved the tradeoff between maximizing torque and minimizing moment of inertia during turning. Overall, we concluded that bluegill handle these tradeoffs differently at different turn speeds such that fast turns are not simply sped up slow turns, but are kinematically distinct.

Acknowledgement

As I look back at everything that has led me here and everyone that has supported me along the way, I cannot help but be immensely grateful for all of the wonderful people that have helped me grow into who I am today. To list everyone would be to write another dissertation, so I will do my best to be brief while trying to acknowledge everyone I can.

I have been so fortunate to have had the most incredible research mentors throughout my education and my career and I would like to start by thanking all of my mentors before I arrived at Tufts. Mr. Wardrop, you taught me to always fail gloriously and to use that failure to improve. Professor Golovchenko and Tamas, you gave me my first opportunity in an academic lab and helped me put my feet on the path I am now at the end of. Stacey, Andrew, Nick, Jake, Mary, James, Callin, and Susie, you fostered such a beautiful lab community and I could not have had a better environment in which to write my senior thesis or a better group to write it with. Andy, Nicolai, Callin, Jake, and Mary, you gave me the most incredible deep dive into research the summer after my senior year, and even though it was only for a short time, I will never forget it or the Andrew Allocation Calendar. Kevin and all of the St Andrews crew, you really gave me the most wonderful experience diving into evolutionary biology research. I am so grateful to have worked with all of you over the course of my career and will always fondly remember the time we spent together

I would also like to thank Tufts for being such a wonderful place to earn my PhD. The biology department could not be a more welcoming and supportive place and I am deeply grateful for all of the faculty, staff, and fellow students for always being there for me and helping me along the way. I also feel so fortunate to have been a part of the Tytell lab. Thank you Mike, Jerry, Ben, Yordano, Ming, and Olivia for being amazing colleagues and friends. Thank you Brendan, Emily, Stephen, Miru, and Paige for letting me join your undergraduate journies as a research mentor. Thank you Barry and Mimi for being such incredible and supportive mentors. Finally, thank you so much Eric. Thank you for believing in me and bringing me to Tufts. Thank you for supporting me and my projects throughout my time here. Thank you for putting up with my many puns and antics.

I am also very grateful for my partner Kelsey and her wonderful family. They have always made me feel welcome and supported and I have enjoyed every minute that I have been fortunate enough to spend with them. Kelsey, I love you and you are the most incredible person. Thank you for all of your support and for

believing in me when I didn't believe in myself. Every moment I spend with you means the world to me, and I can't wait to make even more memories together.

I would also like to thank my family. Without them I wouldn't be who I am today and I wouldn't have been able to complete this PhD. Bobby, Carroll, DD, and Poppy, you have always been there for me and I love you very much. I hope that one day I can live up to the examples you set. Mom, dad, thank you for loving and supporting me through all of the ups and downs. I could not be more grateful to be your son and I love you both very much. Phoebe, thank you for being such an awesome sister. I love you and your powerful and inspiring passion for the natural world and I cannot wait to see where it leads you! Finally, thank you Zeus for helping me through the pandemic. I love you and I miss you.

Finally, thanks to you who may be reading this. May you find what you are looking for in this dissertation and may it help you on your own journey through the wonderful world of fish biomechanics.

Table of contents

Introduction **2**

References 5

Chapter 1: Not a caudal relationship: Form does not fully drive function of the tail in bluegill and pumpkinseed **9**

Introduction 9

Methods 13

Results 18

Discussion 25

Contributions 27

References 28

Chapter 2: Bluegill increase their heart rate with swimming speed **32**

Introduction 32

Methods 35

Results 40

Discussion 46

Contributions 48

References 49

Chapter 3: Braking is about balance in addition to drag **52**

Introduction 52

Methods 54

Results 60

Discussion 71
Competing Interests 75
Funding 75
References 76

Chapter 4: Fast turns are not sped up slow turns: How bluegill sunfish change their kinematics with turn speed **81**

Introduction 81
Methods 84
Results 92
Discussion 101
Acknowledgements 105
Competing Interests 105
Funding 105
Data Availability 105
References 106

Prospectus **111**

The science 111
The PhD 113

List of Tables

1 Trial breakdown for morphometric analysis. AR stands for aspect ratio which was the body depth of each individual divided by its length. Numbers represent number of individuals per analysis. 13

2 Trial breakdown for lateral setup fins analysis. Numbers represent number of trials per flow speed. 15

1 Trial breakdown for lateral setup fins analysis. Numbers represent number of trials per car speed. 58

2 Trial breakdown for lateral setup fins analysis. Numbers represent number of trials per brake speed as defined by each trial's overall deceleration. 59

List of Figures

1 Phylogeny of *Lepomis* modified from Near and Koppelman (2009), Fig. 1.31. Near and Koppelman (2009) generated the phylogeny using a mixed-model Bayesian analysis of mitochondrial and nuclear DNA. They time-calibrated the phylogeny using fossils. It is calibrated against the geological time scale. 10

2 Pumpkinseed swam with a higher body frequency than bluegill. Preliminary data modified from Michaels (2024) shows that across a similar range of steady swimming speeds, pumpkinseed swam with a higher body frequency than bluegill. 12

3 Morphometrics. (A) We measured the depth. length, and dorsal fin position. (B) We also measured three widths along the body. Red lines denote measured distances. 14

4 Camera views. (A) Lateral orthogonal view. (B) Lateral off axis view. Yellow points represent SLEAP digitized points 16

5 Body shape was similar between the two species. The position of the dorsal fin divided by the total length of the fish as it relates to the aspect ratio (depth/length) of the fish for bluegill (blue) and pumpkinseed (orange). Solid lines denote linear fits. Fish sillouettes illustrate what high and low values signify on each axis. 19

6 Body width was similar for both species. Widths in bodylengths along the length of the fish for (A) between the pectoral fins, (B) at the middle of the body, and (C) at the peduncle. Solid lines denote means for each group. 20

7 The anal and caudal fins were larger for bluegill than pumpkinseed. Fin area normalized by body length for (A) one pectoral fin, (B) the dorsal fin, (C) the anal fin, and (D) the caudal fin. Solid lines represent each group's mean. Asterisks denote $p < 0.05$ (*) and $p < 0.001$ (**) 21

8 Tailbeat amplitude and frequency were different between the two species. (A) Tailbeat frequency over the range of tested flow speeds in bodylengths per second. (B, C) Amplitudes for both the snout (B) and the tail (C) over the range of flow speeds. Vertical lines represent the standard deviation and the two solid lines show a linear fit. 22

9 The side-to-side speed of the snout and tail was similar for the two species. Speed of both (A) the snout and (B) the tail over the range of tested flow speeds. Vertical lines represent the standard deviation and the two solid lines show the linear fits. 23

10 Caudal fin angular excursion and splay angle of the caudal fin was different among the species. (A) Tail fin angular excursion about the flow axis over the range of tested flow speeds. (B) Caudal fin splay angle as defined by the vectors from the middle of the peduncle to the top of the caudal fin and from the middle of the peduncle to the bottom of the caudal fin. Vertical lines represent the standard deviation and the two solid lines represent the linear fits 24

1 EKG setup. (A) Individual with the electrodes inserted into its pericardial cavity. (B) The electrodes we used with the tips shaved off. (C) Representative trace of a heart beat recorded from an individual during an experiment. Relevant peaks are labeled on the trace of the first beat where P is atrial depolarization, the QRS complex is ventricle depolarization, and T is ventricle repolarization. 36

2 Each individual changed their heart rate (A) and heart rate variability (B) differently with flow speed. Color denotes individual. Lines represent means within groups. 40

3 Maneuvering speed increased with flow speed. Color denotes individual. Lines represent means within groups. 41

4 Heart rate (A) and heart rate variability (B) did not significantly change with flow speed. Color denotes individual. Lines represent linear fits of the regression of heart rate or heart rate variability on maneuvering speed. 42

5 (A) Heart rate increased with flow speed during the ramp up (in red) and decreased with flow speed during the ramp down (in blue). (B) Heart rate variability did not change much with flow speed. Color denotes ramp direction. Lines represent means within groups. The 2.0 speed is shown in both panels because it is the plateau speed. 43

6 Maneuvering speed increased with flow speed. Color denotes ramp direction. Lines represent means within groups. 44

7 (A) Heart rate remained constant as maneuvering speed increased. (B) Heart rate variability also remaind constant as maneuvering speed increased. Color denotes individual. The lines represent linear fits of the regression of heart rate or heart rate variability on maneuvering speed. 45

1 (A, C) Stills from videos collected using the two lateral setup using a (A) lateral orthogonal and (C) lateral off axis camera. (B, D) Stills from videos collected using the two ventral setup using a (B) ventral orthogonal and (D) ventral off axis camera. Yellow points in A and C are SLEAP predicted points. Blue points in B and D are SLEAP predicted points with blue lines denoting the skeleton used during training. Point names in red are automatically predicted points, while point names in light blue are manually digitized points 56

2 (A) Snout velocity normalized by bodylength over the course of the trial. The vertical black line represents the mean total braking time after prey capture reported by Flammang and Lauder in their study (Flammang and Lauder (2009)) (B) The overall deceleration during each trial as elicted by its respective brake speed. The black lines represent the means. (C) The maximum velocity reached compared with how much distance the fish needed to stop. In all cases, dark blue is slow brakes, light turquoise is medium brakes, and red is fast brakes. 61

3 Fin forces from the pectoral fins. Body length normalized fin forces from both pectoral fins over time for slow (A), medium (B), and fast (C) brakes. (D) Total normalized fin force from both pectoral fins over time for slow, medium, and fast brakes. Colors denote individual and lines connect points from the same trial. Black lines in (C) are the means of each speed. . . 62

4 Forces from the dorsal, anal, and left pelvic fins over the time course of the brake for slow, medium, and fast brakes. Color represents individual with thin lines connecting trials and thick lines connecting individual means. Note the different y axis scales. 64

5 Total normalized impulse from the dorsal (A), anal (B), and left pelvic fins (C) for slow, medium, and fast brakes. Color represents individual with the black lines representing the means and standard deviations. Note the different y axis scales. 66

6 Normalized lateral surface area over the time course of the brake for slow, medium, and fast brakes. Color represents individual with thin lines connecting trials and thick lines connecting individual means. 67

7 The length of the trailing edge of the caudal fin for slow, medium, and fast brakes. Data are presented as means during the course of the brake broken up into five temporally equal portions. Color represents individual and the black lines show the means. 69

8 Body angle in degrees relative to the horizontal over the time course of the brake for slow, medium, and fast brakes. Negative values indicate the bluegill is pitched down while positive values indicate it is pitched up. Color represents individual with thin lines connecting trials and thick lines connecting individual means. 70

1 The programmable car elicits repeatable turns. (A) A 3D solidworks model of the system (available in supplementary material). (B) A bluegill swimming in the chamber. (C, D, E) I filmed using an orthogonal lateral camera (C), an orthogonal ventral camera (D), and an off axis ventral camera (E). The yellow points represent digitized points along the body. Light gray lines show the skeleton used for training (the snout to all other points to form a shallow tree). (F, G, H) Three consecutive turns show similar kinematics from the ventral view. . . 85

2 Mass was estimated using images of each bluegill. (A, B) Points were added to their respective locations along the length of the body (red dots). Lines were then drawn from vertical edge to vertical edge of the fish in the lateral view (A) and lateral edge to lateral edge of the fish in the ventral view (B) (light blue lines). FIJI was then used to measure each of the lines and the distance between them in the ventral view. The known length of the fish was used to set the scale. 87

3 Angular velocities were higher when the car reversed faster. (A) Changes in snout angle for both slow turns in blue and fast turns in red using degrees over seconds. (B, C) Angular velocity with slow turns in blue (B) and fast turns in red (C) 92

4 Snout and tail angular velocities across both slow and fast turns. (A) Representative traces of one trial's angular velocities over time for the snout (orange) and tail (purple). The representative turn is a fast turn. The gray lines represent the time of maximum angular velocity for the snout (orange "B") and tail (purple "C"). (B) Snout and tail angular velocities for each trial at the point where snout angular velocity is maximized (first gray line in A). Each point denotes the value for one trial. (C) Snout and tail angular velocities at the point where tail angular velocity is maximized (second gray line in A). Asterisks denote significance between groups. 93

5 Fish bent their bodies to a similar degree in slow and fast turns. (A, C) Body traces of midlines for one individual for one slow (A) and one fast (C) turn. Points along the midlines denote digitized points, where the orange point is the snout and the purple point is the peduncle. Line color in (A) and (C) corresponds to the time course of the turn with lighter gray representing the beginning and darker gray representing the ending. Note the different time scale between fast and slow turns. (B, D) Normalized moment of inertia for slow (B) and fast (D) turns. Time is centered on the time of maximum angular velocity. 94

6 Within each turn speed, bluegill that bent their bodies more generated higher angular velocities. Mean moment of inertia per trial, normalized by the maximum moment of inertia for that trial, plotted against mean snout angular velocity of that trial. Data is shown for both slow (in blue) and fast turns (in red). Linear regressions for slow (light blue) and fast (red) turns are shown as dashed lines. 95

7 Bluegill consistently maximized angular velocity before minimizing moment of inertia. The time at which moment of inertia was minimized during a turn is plotted against the time at which angular velocity was maximized during that turn for both slow (blue) and fast (red) turns. The yellow shaded region is where the fish maximized its angular velocity before minimizing its moment of inertia, while the unshaded region is where the fish minimized its moment of inertia before maximizing its angular velocity. 96

8 Bluegill converted linear to angular momentum in fast turns but not slow ones. (A,B) Linear (A) and angular (B) momentum for slow (blue) turns before the turn, during the first half of the turn, and during the second half of the turn. (C,D) Linear (C) and angular (D) momentum for fast (red) turns before the turn, during the first half of the turn, and during the second half of the turn. Asterisks denote significance between groups. 97

9 Bluegill used their pectoral fins differently at different speeds. Pectoral fin data for slow (blue circles) and fast (red triangles) turns. (A) Total number of pectoral fin beats increases for longer turns. The black line is the linear fit. (B) Fin beat frequency decreased for longer turns with a 1/x model shown by the black line. (C) Fin amplitude for the inside and outside fins in slow and fast turns. (D) Number of backing strokes increased for longer turns. The black line shows the linear fit. Asterisks denote significance between groups. 98

10 Slow and fast turns differed in their timing of maximum torque and minimum moment of inertia. (A) The time at which moment of inertia was minimized during a turn is plotted against the time at which torque was maximized during that turn for both slow (blue) and fast (red) turns. The yellow shaded region is where the fish maximized its torque before minimizing its moment of inertia, while the unshaded region is where the fish minimized its moment of inertia before maximizing its torque. (B) The difference between the time that the bluegill maximized their torque and minimized their moment of inertia is show for both fast (red) and slow (blue) turns. The solid black line represents the theoretical point at which both events would occur at the same time. 100

Introduction

Many fishes, with the possible exception of long distance migrators, often swim unsteadily. Whether they are slowing down (Flammang and Lauder, 2009; Geerlink, 1987; Higham, 2007; Higham et al., 2005; Hu et al., 2007; Jayne et al., 1996), speeding up (Domenici and Blake, 1997; Domenici and Hale, 2019; Webb, 1978; Weihs, 1973), or turning around (Downs et al., 2023; Fricke and Hissmann, 1992; Gray, 1933; Howe and Astley, 2020; Marcoux and Korsmeyer, 2019; Thandiackal and Lauder, 2020), they are usually moving in a non-consistent and unsteady way. In fact, Webb (1991) found that most of a trout's daily life consists of accelerations, decelerations, and turns rather than swimming consistently in a straight line. However, despite how important unsteady swimming is to fishes, research has tended to focus more on steady swimming. In large part, this is because kinematics studies often require a large amount of repeatable data, which can be difficult to collect on maneuvers.

Instead, maneuvers are often elicited with food (Geerlink, 1987; as in Higham, 2007; Higham et al., 2005; Webb, 1984) or by perturbing the fish (Webb, 2004; Webb and Fairchild, 2001). These methods allow for the collection of many trials, but may not result in very consistent behaviors. Marcoux and Korsmeyer (2019) addressed this issue by developing their own physical device that moves in a consistent manner and elicits repeatable behavior from the fishes they tested. Their aim was to understand how reef fishes respond to a wave-like stimulus, but they also documented many intances in which their fish turned around. Inspired by this device, we constructed our own instrument which we used to consistently motivate fish to perform unsteady behaviors. The device, which we call FISHCAR (**F**ostering **I**nformative **S**wimming by **H**arnessing **C**ompensatory **A**ctions **R**epeatably), consists of an 80/20 chassis with an attached acrylic flow-through chamber powered by a servo motor and allows us to ask detailed questions about maneuvering and unsteady behaviors in fishes and answer those questions with large numbers of repeated trials.

While this dissertation first quantifies steady swimming differences between bluegill sunfish (*Lepomis macrochirus*) and pumpkinseed sunfish (*Lepomis gibbosus*), it quickly moves on to characterizing various

features of unsteady swimming. We first present an analysis of how heart rate changes with maneuvering speed, then quantify braking kinematics in bluegill, and finally detail how bluegill handle the physical trade-offs constraining turning. By examining these various forms of unsteady swimming, we hoped to better understand and quantify kinematic behaviors in bluegill during these unsteady maneuvers. While we feel our results are generalizable as many of our hypotheses are grounded in physics, we nonetheless are cautious in making a blanket statement due to the distinct and surprising differeences we found between bluegill and pumpkinseed kinematics, especially given their similar morphologies.

In chapter 1, before quantifying any component of unsteady swimming, we began with a comparison of the steady swimming kinematics of bluegill and pumpkinseed. Initially motivated by preliminary findings that these two species solve the challenge of swimming at higher speeds differently, we sought to further understand the similarities and differences between their morphologies and how those similarities and differences influenced their kinematics. Specifically, we knew the two species look similar and are found in similar environments (Stuber et al., 1982; Tomeček et al., 2007; Tomeček et al., 2007), but differ in terms of their typical diets (Mittelbach, 1981; Mittelbach, 1984; Mittelbach, 1984; Tomeček et al., 2007). To understand how they differ we used morphometrics to compare their body shape before characterizing their tailbeat frequency and amplitude, two quantities critical for how different fish swim (Bainbridge, 1958; Li et al., 2021).

In chapter 2, we measured electrocardiograms (EKGs) in bluegill to explore whether we can use the technique to understand the energetic costs of steady and unsteady swimming. If heart rate indeed changed to reflect brief changes in energy, it would allow the field to better quantify how unsteady behaviors affect energetic expenditure. We quantified how the fish maneuvered during the trials and whether or not their maneuvering caused any changes in heart rate. Since energetics research is often complicated and equipment dependent (Korsmeyer et al., 2002), we hoped to validate a different method for assessing energetic costs in bluegill that are often used in biomechanics research. We were optimistic that our method would allow us to quantify energetic costs on a very small time scale, as evident by changes in heart rate during a trial that correlate to maneuvering on top of flow speed.

In chapter 3, we caused the fish to brake at various speeds using FISHCAR. In doing so, we hoped to identify speed-based differences in kinematics. As previous research has implicated the pectoral (Bainbridge, 1963; Drucker and Lauder, 2002; Drucker and Lauder, 2003; Geerlink, 1987; Gibbs et al., 2024; Harris, 1938; Higham, 2007; Higham, 2007; Higham et al., 2005; Jayne et al., 1996; Videler, 1981; Webb, 1984; Webb,

2002; Webb, 2002), dorsal (Jayne et al., 1996), caudal (Bainbridge, 1963; Flammang and Lauder, 2009), and pelvic fins (Harris, 1938; Standen, 2008) in braking in fishes, we quantified their movements, along with those of the anal fin, and estimated braking forces. As stability is also key to braking (Webb, 1993; Webb, 2002), we explored various ways in which the fish could maintain a stable posture while also slowing down, specifically quantifying lateral fin area and pitch.

In chapter 4, we addressed our most complicated unsteady behavior: turning. During turning, bluegill face a tradeoff: they need to produce enough torque to complete the turn, while simultaneously needing to reduce their momentum of inertia to reduce the resistance to their turn. Since torque scales directly with the associated lever arm and moment of inertia scales inversely with the square of it, the fish must solve the conundrum of keeping their body long to produce sufficient torque while also bending their body to reduce their moment of inertia. Dabiri et al (2020) previously characterized this tradeoff in both jellyfish and zebrafish, but we were interested in whether fish might resolve this tradeoff differently at different speeds. When turning more quickly, fish need to have higher angular acceleration, and as angular acceleration is equal to torque divided by moment of inertia (resulting in an $\frac{r}{r^2}$ relationship with respect to the length of the lever arm), we hypothesized that during fast turns, fish would priotize bending their bodies to minimize moment of inertia, while keeping their bodies long in slow turns to maximize torque. In this chapter, we quantified distinct differences between slow and fast turns and concluded that while the two share similarities, a fast turn is not simply a slow turn sped up, but is kinematically distinct.

Overall, while the topics in this this dissertation stretch from heart rate all the way to turning, the general theme is how kinematics change for behaviors at different speeds. By understanding and quantifying these kinematics, we aim to contribute to the larger body of literature that seeks to understand the life history and physics of these behaviors. We also aim to inspire future researchers to ask similar questions about complicated unsteady behaviors and conduct analyses to quantify the kinematics that underlie them.

References

Bainbridge, R. (1958). The speed of swimming of fish as related to size and to the frequency and amplitude of the tail beat. *Journal of Experimental Biology* **35**, 109–133. doi: 10.1242/jeb.35.1.109.

Bainbridge, R. (1963). Caudal fin and body movement in the propulsion of some fish. *Journal of Experimental Biology* **40**, 23–56. doi: 10.1242/jeb.40.1.23.

Dabiri, J. O., Colin, S. P., Gemmell, B. J., Lucas, K. N., Leftwich, M. C. and Costello, J. H. (2020). Jellyfish and fish solve the challenges of turning dynamics similarly to achieve high maneuverability. *Fluids* **5**, 106. doi: 10.3390/fluids5030106.

Domenici, P. and Blake, R. W. (1997). The kinematics and performance of fish fast-start swimming. *Journal of Experimental Biology* **200**, 1165–1178. doi: 10.1242/jeb.200.8.1165.

Domenici, P. and Hale, M. E. (2019). Escape responses of fish: A review of the diversity in motor control, kinematics and behaviour. *Journal of Experimental Biology* **222**, jeb166009. doi: 10.1242/jeb.166009.

Downs, A. M., Kolpas, A., Block, B. A. and Fish, F. E. (2023). Multiple behaviors for turning performance of Pacific bluefin tuna (*Thunnus orientalis*). *Journal of Experimental Biology* **226**, jeb244144. doi: 10.1242/jeb.244144.

Drucker, E. G. and Lauder, G. V. (2002). Wake dynamics and locomotor function in fishes: Interpreting evolutionary patterns in pectoral fin design. *Integrative and Comparative Biology* **42**, 997–1008. doi: 10.1093/icb/42.5.997.

Drucker, E. G. and Lauder, G. V. (2003). Function of pectoral fins in rainbow trout: Behavioral repertoire and hydrodynamic forces. *Journal of Experimental Biology* **206**, 813–826. doi: 10.1242/jeb.00139.

Flammang, B. E. and Lauder, G. V. (2009). Caudal fin shape modulation and control during acceleration, braking and backing maneuvers in bluegill sunfish, *Lepomis macrochirus*. *Journal of Experimental Biology* **212**, 277–286. doi: 10.1242/jeb.021360.

Fricke, H. and Hissmann, K. (1992). Locomotion, fin coordination and body form of the living coelacanth *Latimeria chalumnae*. *Environmental Biology of Fishes* **34**, 329–356. doi: 10.1007/BF00004739.

Geerlink, P. J. (1987). The role of the pectoral fins in braking of mackerel, cod and saithe. *Netherlands Journal of Zoology* **37**, 81–104. doi: 10.1163/002829687X00053.

Gibbs, B. J., Akanyeti, O. and Liao, J. C. (2024). Kinematics and muscle activity of pectoral fins in rainbow trout (*Oncorhynchus mykiss*) station holding in turbulent flow. *Journal of Experimental Biology*

227, jeb246275. doi: 10.1242/jeb.246275.

Gray, J. (1933). Directional control of fish movement. *Proceedings of the Royal Society B: Biological Sciences* 115–125. doi: 10.1098/rspb.1933.0035.

Harris, J. E. (1938). The role of the fins in the equilibrium of the swimming fish: II. The role of the pelvic fins. *Journal of Experimental Biology* **15**, 32–47. doi: 10.1242/jeb.15.1.32.

Higham, T. E. (2007). Feeding, fins and braking maneuvers: Locomotion during prey capture in centrarchid fishes. *Journal of Experimental Biology* **210**, 107–117. doi: 10.1242/jeb.02634.

Higham, T. E., Malas, B., Jayne, B. C. and Lauder, G. V. (2005). Constraints on starting and stopping: Behavior compensates for reduced pectoral fin area during braking of the bluegill sunfish *Lepomis macrochirus*. *Journal of Experimental Biology* **208**, 4735–4746. doi: 10.1242/jeb.01966.

Howe, S. P. and Astley, H. C. (2020). The control of routine fish maneuvers: Connecting midline kinematics to turn outcomes. *Journal of Experimental Zoology Part A: Ecological and Integrative Physiology* **333**, 579–594. doi: 10.1002/jez.2398.

Hu, W., Tong, B. and Liu, H. (2007). Dynamics of free straight swimming of *Angulla angulla* including forward, braking and backward locomotion. *Journal of Hydrodynamics, Ser. B* **19**, 395–402. doi: 10.1016/S1001-6058(07)60132-2.

Jayne, B. C., Lozada, A. F. and Lauder, G. V. (1996). Function of the dorsal fin in bluegill sunfish: Motor patterns during four distinct locomotor behaviors. *Journal of Morphology* **228**, 307–326. doi: 10.1002/(SICI)1097-4687(199606)228:3<307::AID-JMOR3>3.0.CO;2-Z.

Korsmeyer, K. E., Steffensen, J. F. and Herskin, J. (2002). Energetics of median and paired fin swimming, body and caudal fin swimming, and gait transition in parrotfish (*Scarus schlegeli*) and triggerfish (*Rhinecanthus aculeatus*). *Journal of Experimental Biology* **205**, 1253–1263. doi: 10.1242/jeb.205.9.1253.

Li, G., Liu, H., Müller, U. K., Voesenek, C. J. and van Leeuwen, J. L. (2021). Fishes regulate tail-beat kinematics to minimize speed-specific cost of transport. *Proceedings of the Royal Society B: Biological Sciences* **288**, 20211601. doi: 10.1098/rspb.2021.1601.

Marcoux, T. M. and Korsmeyer, K. E. (2019). Energetics and behavior of coral reef fishes during oscillatory swimming in a simulated wave surge. *Journal of Experimental Biology* **222**, jeb191791. doi: 10.1242/jeb.191791.

Mittelbach, G. G. (1981). Foraging efficiency and body size: A study of optimal diet and habitat use by

bluegills. *Ecology* **62**, 1370–1386. doi: 10.2307/1937300.

Mittelbach, G. G. (1984). Predation and resource partitioning in two sunfishes (Centrarchidae). *Ecology* **65**, 499–513. doi: 10.2307/1941412.

Standen, E. M. (2008). Pelvic fin locomotor function in fishes: Three-dimensional kinematics in rainbow trout (*Oncorhynchus mykiss*). *Journal of Experimental Biology* **211**, 2931–2942. doi: 10.1242/jeb.018572.

Stuber, R. J., Gebhart, G. and Maughan, O. E. (1982). *Habitat Suitability Index Models: Bluegill*. Western Energy and Land Use Team, Office of Biological Services, Fish and Wildlife Service, U.S. Department of the Interior.

Thandiackal, R. and Lauder, G. V. (2020). How zebrafish turn: Analysis of pressure force dynamics and mechanical work. *Journal of Experimental Biology* **223**, jeb223230. doi: 10.1242/jeb.223230.

Tomeček, J., Kováč, V. and Katina, S. (2007). The biological flexibility of the pumpkinseed: A successful colonizer throughout Europe. In *Biological Invaders in Inland Waters: Profiles, Distribution, and Threats* (ed. Gherardi, F.), pp. 307–336. Dordrecht: Springer Netherlands. doi: 10.1007/978-1-4020-6029-8_16.

Videler, J. J. (1981). Swimming movements, body structure and propulsion in cod *Gadus morhua*. *Symposia of the Zoological Society of London* **48**, 1–27.

Webb, P. W. (1978). Fast-start performance and body form in seven species of teleost fish. *Journal of Experimental Biology* **74**, 211–226. doi: 10.1242/jeb.74.1.211.

Webb, P. W. (1984). Form and function in fish swimming. *Scientific American* **251**, 72–83.

Webb, P. W. (1991). Composition and mechanics of routine swimming of rainbow trout, *Oncorhynchus mykiss*. *Canadian Journal of Fisheries and Aquatic Sciences* **48**, 583–590. doi: 10.1139/f91-074.

Webb, P. W. (1993). Is tilting behaviour at low swimming speeds unique to negatively buoyant fish? Observations on steelhead trout, *Oncorhynchus mykiss*, and bluegill, *Lepomis macrochirus*. *Journal of Fish Biology* **43**, 687–694. doi: 10.1111/j.1095-8649.1993.tb01146.x.

Webb, P. W. (2002). Control of posture, depth, and swimming trajectories of fishes. *Integrative and Comparative Biology* **42**, 94–101. doi: 10.1093/icb/42.1.94.

Webb, P. W. (2004). Response latencies to postural disturbances in three species of teleostean fishes. *Journal of Experimental Biology* **207**, 955–961. doi: 10.1242/jeb.00854.

Webb, P. W. and Fairchild, A. G. (2001). Performance and maneuverability of three species of teleostean

fishes. *Canadian Journal of Zoology* **79**, 1866–1877. doi: 10.1139/z01-146.

Weihs, D. (1973). The mechanism of rapid starting of slender fish. *Biorheology* **10**, 343–350. doi: 10.3233/BIR-1973-10308.

Chapter 1: Not a caudal relationship: Form does not fully drive function of the tail in bluegill and pumpkinseed

Co-author: Olivia Hawkins

Introduction

It is easy to assume that that form and function are inextricably linked. We often assess form then hypothesize function, and a lot of work centers around the link between the two. This assumption is deeply ingrained in the scientific literature, tracing back to such works as Lamarck's *Philosophie zoologique* which assumes that commitment to a function will create a heritable form (Mayr, 1972) and Darwin's study on finches that assumes that particular forms are better adapted to specific functions (i.e. specific bird beaks allow finches to access specific types of food) (Sulloway, 1982).

In the field of fish biomechanics, this form and function link manifests in the assumption that body shape and structure correlates with the swimming capabilities of different fish species. Webb (1984b) notably created an heuristic to represent this idea: a functional morphology triangle where he divided fish species up into three categories: cruising specialists like the tuna which has a stiff body and a streamlined shape; accelerating specialists like the pike which has a long, slender, and bendable body; and maneuvering specialists like the banded butterfly fish which has a short and deep body with propulsive fins positioned around its center of mass. But how effective is such a paradigm? Does form partition function in that way?

Satterfield et al (2023) would argue not, finding instead that different forms do not result in different functions. More specifically, Satterfield (2023) tested an array of reef fishes with different morphologies, expecting to see that, in accordance with Webb's (1984b) triangle, different bodies would function differently.

Quantifying swimming kinematics of fish with body shapes ranging around Webb's triangle, Satterfield et al (2023) wanted to see if fish with morphologies similar to those of the specialists described by Webb would perform well in each of the specialized categories (cruising, accelerating, and maneuvering). Satterfield et al (2023) found that the "specialized" forms they analyzed did not align with their hypothesized functions, and that different forms did not have different functions, contradicting the ideas put forward by Webb (1984b).

In this paper, we did the complement to Satterfield et al's (2023) work: we tested whether a similar form had a similar function by quantifying the kinematics of bluegill sunfish (*Lepomis macrochirus*) and pumpkinseed sunfish (*Lepomis gibbosus*), two morphologically similar and closely related fish.

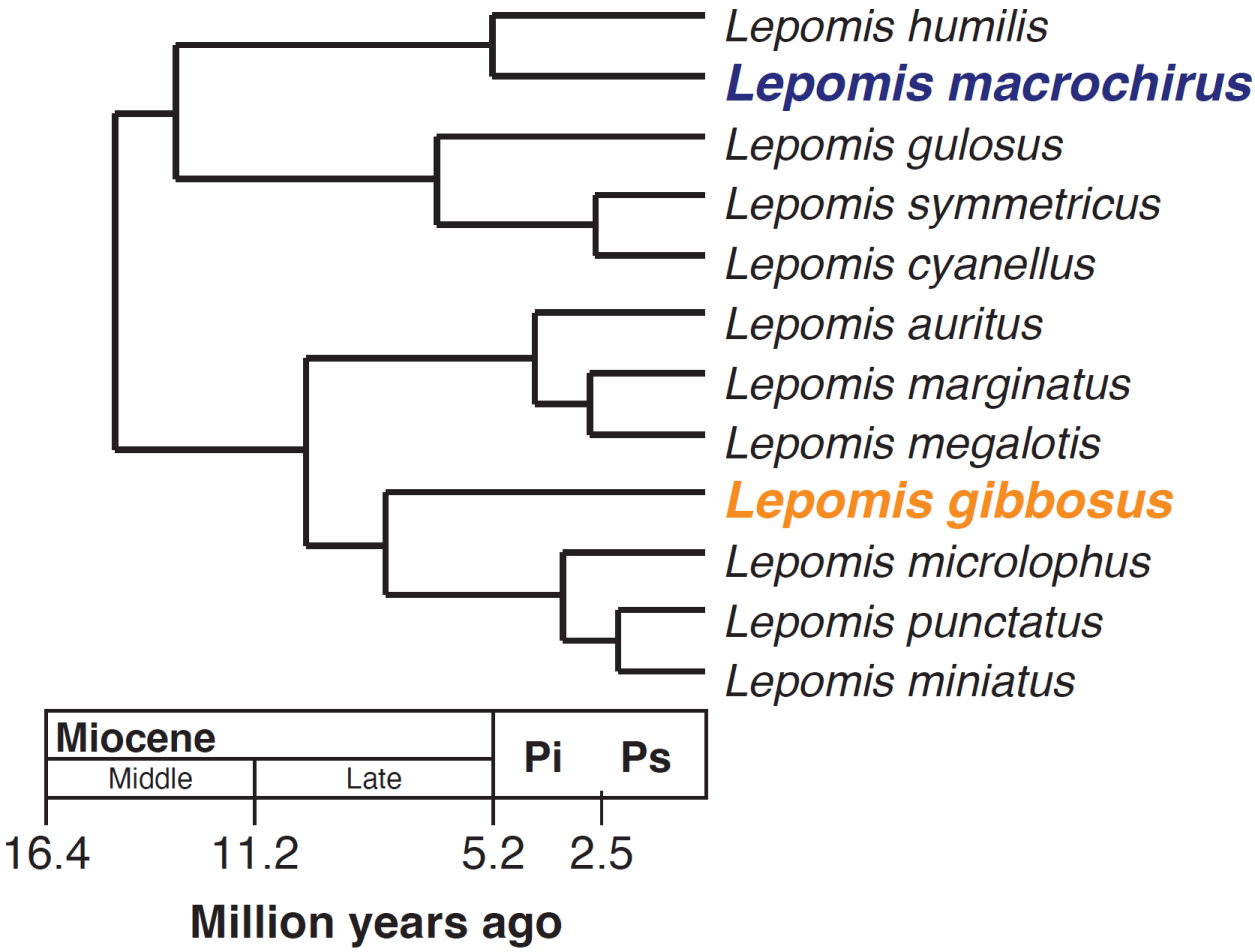

Figure 1: Phylogeny of *Lepomis* modified from Near and Koppelman (2009), Fig. 1.31. Near and Koppelman (2009) generated the phylogeny using a mixed-model Bayesian analysis of mitochondrial and nuclear DNA. They time-calibrated the phylogeny using fossils. It is calibrated against the geological time scale.

While bluegill and pumpkinseed are not each others' most closely related species, they are still closely

related, having diverged about 15My ago (Figure 1). Like all sunfishes in the genus *Lepomis*, bluegill and pumpkinseed share most physical characteristics: they have deep, narrow bodies with prominent pectoral, dorsal, anal, pelvic, and caudal fins. They also tend to occupy similar local environments (lentic areas with vegetation) (Stuber et al., 1982; Tomeček et al., 2007), and even occupy the same niche at the same time (Tomeček et al., 2007), as is the case with the individuals we used in this study as we collected them from the same locations. Additionally, on average, their home ranges are not significantly different, although the maximum size of the home ranges for pumpkinseed may be somewhat larger than in bluegill (Fish and Savitz, 1983). The two species distinguish themselves in terms of diet: bluegill mainly eat zooplankton (Mittelbach, 1984) and other larvae (Mittelbach, 1981), while pumpkinseed prefer mollusks (Mittelbach, 1984), which other fish species ignore (Tomeček et al., 2007). Due to the ecological and behavioral similarities, it follows that bluegill and pumpkinseed swim with similar kinematics.

Many studies have characterized and quantified swimming kinematics in fishes (Liu and Jiang, 2022 for examples; see Sfakiotakis et al., 1999). Bluegill, in particular, have been heavily studied by biomechanists (Flammang and Lauder, 2009; Lauder and Drucker, 2004; Standen and Lauder, 2005 for example), while pumpkinseed have as well, although to a lesser extent (Brett and Sutherland, 1965; but see Lauder, 1982). Here we combined our analyses of the two species to better understand their similarities and differences. Unsurprisingly, in fishes, swimming is often driven by how the fish uses its fins. Bluegill, in particular, rely heavily on their pectoral fins when they swim below 1.5 body lengths per second (L/s), and shift to using their their caudal fins when they swim at speeds above 1.5 L/s (Drucker and Lauder, 1999). The caudal fin is also particularly important in speed control, since speed increases linearly with increases in tailbeat frequency (Bainbridge, 1958). Since changes in frequency are thought to more efficiently increase speed relative to changes in amplitude (Li et al., 2021), it is unsurprising that frequency tends to be the controlled kinematic variable. More specifically, Li et al (2021) found that by keeping tailbeat amplitude set and increasing tailbeat frequency, fish can minimally increase the cost of transport as they swim faster. However, increases in tailbeat amplitude are critical for accelerating (Akanyeti et al., 2017; Wise et al., 2018), and are characteristic during unsteady swimming (Wise et al., 2018), so bluegill and pumpkinseed may increase amplitude instead of frequency.

When considering swimming kinematics, how kinematics rely on morphology, and how similar bluegill and pumpkinseed are morphometrically, it is reasonable to expect that bluegill and pumpkinseed would swim in a similar way. Therefore, we hypothesized that we would see no difference in their kinematics, as they are

similar carangiform swimmers. Specifically, we predicted that they would have similar tailbeat frequencies and tailbeat amplitudes as they occupy similar and overlapping niches. Because we chose to focus on caudal fin swimming instead of pectoral fin swimming, our study centered around these comparisons of frequency and amplitude.

However, preliminary data collected and written up by Michaels (2024) on accelerations in bluegill and pumpkinseed suggests that we may in fact see differences. Specifically, Michaels (2024) compared swimming kinematics in bluegill and pumpkinseed with data from two individuals from each species, and estimated that pumpkinseed had higher body frequencies than bluegill (Figure 2). These results suggest that more experimentation is needed to better quantify the swimming kinematics of bluegill and pumpkinseed.

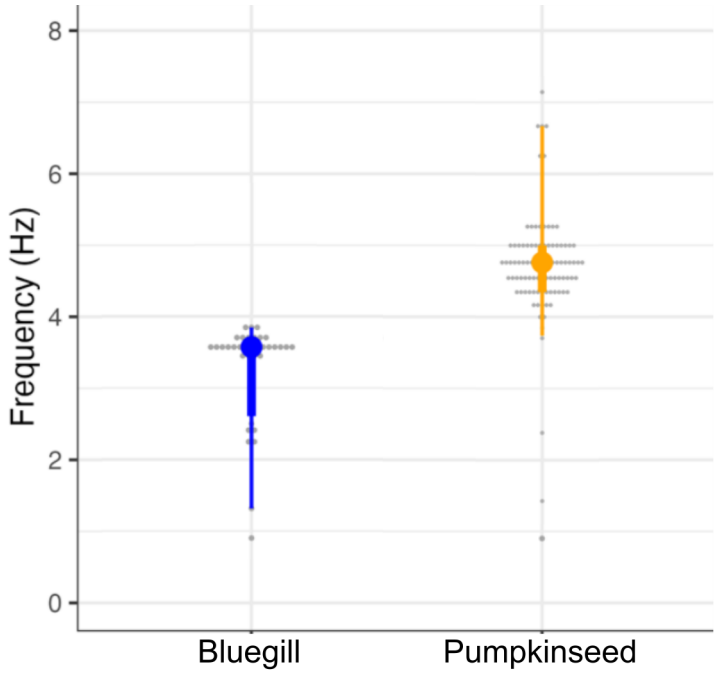

Figure 2: Pumpkinseed swam with a higher body frequency than bluegill. Preliminary data modified from Michaels (2024) shows that across a similar range of steady swimming speeds, pumpkinseed swam with a higher body frequency than bluegill.

Methods

Dataset

We collected all bluegill (*Lepomis macrochirus*) and pumpkinseed (*Lepomis gibbosus*) from either White pond or Walden pond in Concord, MA or from the Mystic Lakes in Medford, MA. We used a seine net along the shores of these ponds to collect the fish before transferring them to an aquaculture facility where they were kept in 10 gallon tanks at a controlled temperature of 20 degrees Celsius until used for experiments. We collected the fish with scientific collection permits 090.22SCF, 146.23SCF, 158.19SCF, and 174.20SCF, and kept them according to protocols M2018-103, M2021-99, and M2024-57.

All experimental procedures and animal handling protocols were approved by the Tufts University Institutional Animal Care and Use Committee.

Morphometrics

For the morphometric dataset, we used a total of 23 previously euthanized individuals, 15 bluegill and 8 pumpkinseeds. See Table 1 for a breakdown of the numbers for each analysis. For each individual, we used calipers to measure each morphological feature and verified the measurements using FIJI (Schindelin et al., 2012) to analyze photos with a ruler in view for scale. We measured body depth, body length from snout to tip of the tail, the dorsal fin position from the snout to the beginning of the spiny dorsal fin, three widths along the body and the dorsal, anal, caudal, and pectoral fin areas (Figure 3).

Table 1: Trial breakdown for morphometric analysis. AR stands for aspect ratio which was the body depth of each individual divided by its length. Numbers represent number of individuals per analysis.

Measurement	Number of bluegill	Number of pumpkinseed
Body AR vs. Dorsal fin position	15	8
Caudal fin area	7	6
Dorsal fin area	9	9
Anal fin area	9	6
Pectoral fin area	13	8

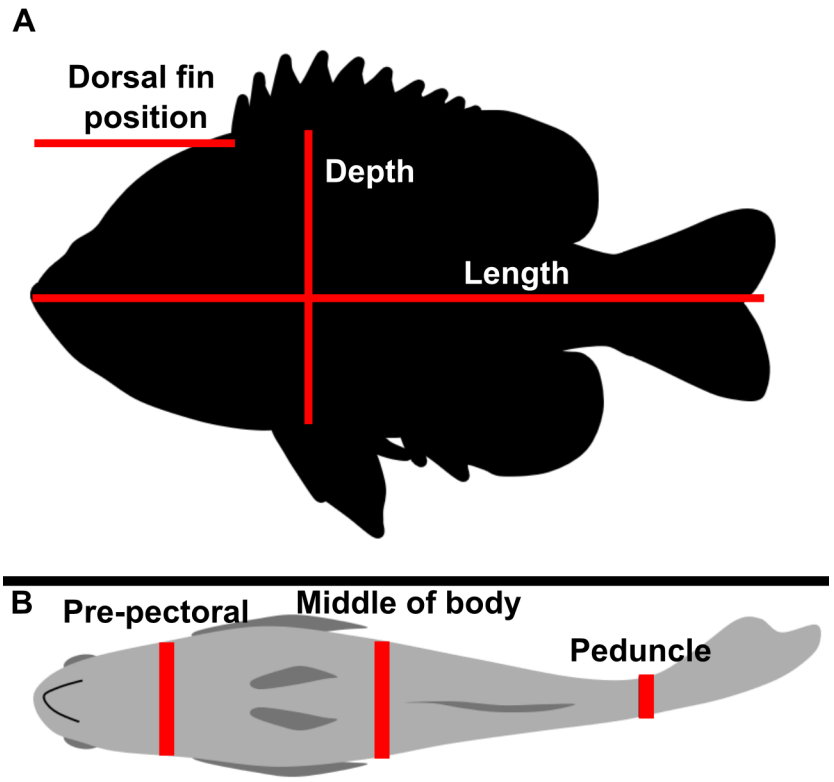

Figure 3: Morphometrics. (A) We measured the depth. length, and dorsal fin position. (B) We also measured three widths along the body. Red lines denote measured distances.

Kinematics

For the kinematics dataset, we swam a total of 3 individuals, 2 bluegill and 1 pumpkinseed. See Table 2 for a breakdown of the numbers of individuals and trials at each swimming speed.

Table 2: Trial breakdown for lateral setup fins analysis. Numbers represent number of trials per flow speed.

Flow speed (L/s)	BG67	BG76	PS6
0.75	2	0	0
1	2	0	0
1.25	2	0	0
1.3	0	2	2
1.4	0	2	2
1.5	2	2	2
1.6	0	2	2
1.7	0	2	2
1.75	2	0	0
1.8	0	2	2
1.9	0	2	2
2	2	2	2
2.1	0	2	2
2.2	0	2	2
2.25	2	0	0
2.3	0	2	2
2.4	0	3	2
2.5	2	2	2
2.6	0	2	2
2.7	0	2	2
2.75	2	0	0
3	2	0	0

Swimming trials

For all trials, we would first set the flow to the desired speed, then give the fish around a minute to acclimate, then record the video when it was swimming steadily. In between trials we set the flow to 1 bodylength per second (L/s). For one bluegill and one pumpkinseed, we ran the flow tank from speeds of 1.3 (L/s) up to 2.7 (L/s), incrementing by 0.1 L/s each time. For one bluegill, we ran the flow tank from 0.75 L/s up to 3 L/s, incrementing by 0.25 L/s. For all individuals, we first ramped up the flow speeds continuously, then upon reaching the maximum speed, randomized the order of the speeds and ran the trials again, resulting in each individual swimming at each speed at least twice.

Filming and digitizing

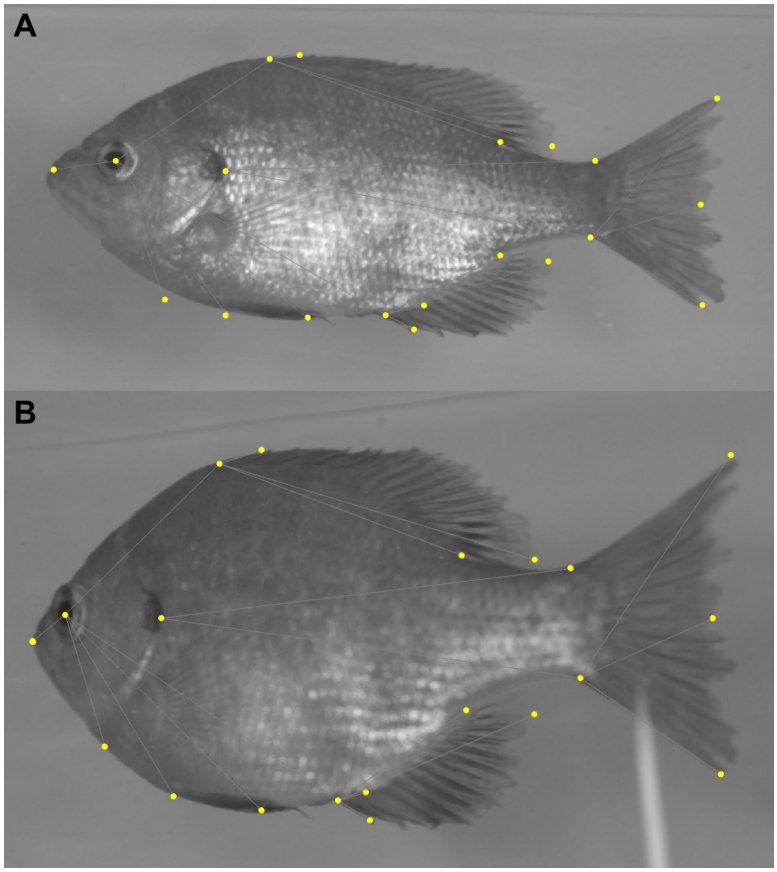

Figure 4: Camera views. (A) Lateral orthogonal view. (B) Lateral off axis view. Yellow points represent SLEAP digitized points

For video recording, we used 2 lateral cameras: A Phantom Miro M120 that was orthogonal to the working section of the flow tank (Figure 1 A), and a Phantom Miro M340 that was at an angle to it and towards the

posterior of the fish (Figure 1 B). For each trial, we captured 601 frames at 120 frames per second. To digitize the videos, we used SLEAP (Pereira et al., 2022) and a ChArUco board (Garrido-Jurado et al., 2014) with the aniposelib package from the Anipose toolkit (Karashchuk et al., 2021) to calibrate the filmed space. We tracked 22 points on the fish (Figure 1). For the analyses, we used the tip of the snout, the dorsal and ventral tips of the peduncle, the dorsal and ventral tips of the caudal fin, and the middle of the caudal fin. For the analysis of caudal fin angle, we estimated a point in the middle of the tip of the peduncle by averaging the positions of the other two peduncle points.

We smoothed all points for each individual trial using a 9th order low pass Butterworth filter with a cut off frequency of 8 Hz.

Analysis

We restricted the analysis to flow speeds at or above 1.5 L/s because this is the point at which pectoral fin swimming transitions into caudal fin swimming for bluegill (Drucker and Lauder, 1999).

Statistics

For all analysis and visualization, we used R version 4.4.1 with Rstudio version 2024.04.2 and the following packages: tidyverse version 2.0.0 (Wickham et al., 2019), lme4 version 1.1.35.5 (Bates et al., 2015), car version 3.1.2 (Fox and Weisberg, 2019), ggspatial version 1.1.9 (Dunnington et al., 2023), ggdist version 3.3.2 (Kay, 2024; Kay and Wiernik, 2024), and beeswarm version 0.4.0 (Eklund and Trimble, 2021).

All means are provided plus or minus one standard deviation, unless otherwise noted.

Morphometrics

For all pairwise comparisons, we ran a student's t-test to assess if the variable of interest is significantly different between species using the t.test function from the stats package. For the analysis of body aspect ratio and dorsal fin position, we ran a MANOVA to assess how aspect ratio and dorsal fin position differ between species. We used the manova function from the stats package to do so.

Kinematics

To avoid pseudoreplication, for the analyses of frequency and amplitude we used every third tailbeat from each trial.

When quantifying the effect of swimming speed on tailbeat amplitude, frequency, tail speed, and tail angular amplitude, we ran a linear model using the lm function from the stats package.

When comparing bluegill and pumpkinseed, we fit a linear mixed model with the interaction between flow speed and species as the fixed effects before using the Anova function from the cars package to assess significance.

Results

We want to begin the results by emphasizing that the analysis of the swimming trials is a preliminary analysis as we only include data from one pumpkinseed individual. We included statistical comparisons

between species for completeness, but focused on the numerical differences even when we did not find any significant differences.

Body morphology was similar

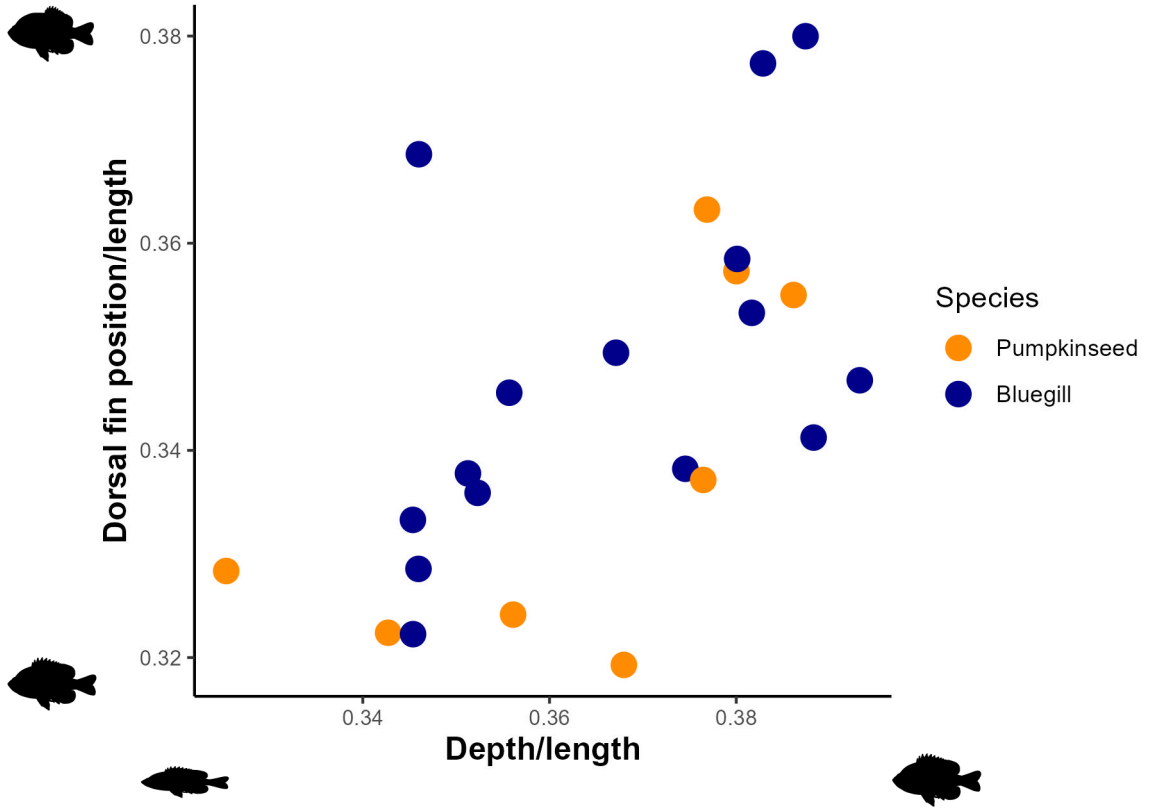

Figure 5: Body shape was similar between the two species. The position of the dorsal fin divided by the total length of the fish as it relates to the aspect ratio (depth/length) of the fish for bluegill (blue) and pumpkinseed (orange). Solid lines denote linear fits. Fish sillouettes illustrate what high and low values signify on each axis.

The correlation between dorsal fin position divided by length and body depth divided by length Figure 5 was not significantly different between bluegill and pumpkinseed (MANOVA, Wilk's lambda = 0.079, p = 0.437).

The body width did not differ significantly at any point for the two species (Figure 6; $p > 0.600$ in all cases).

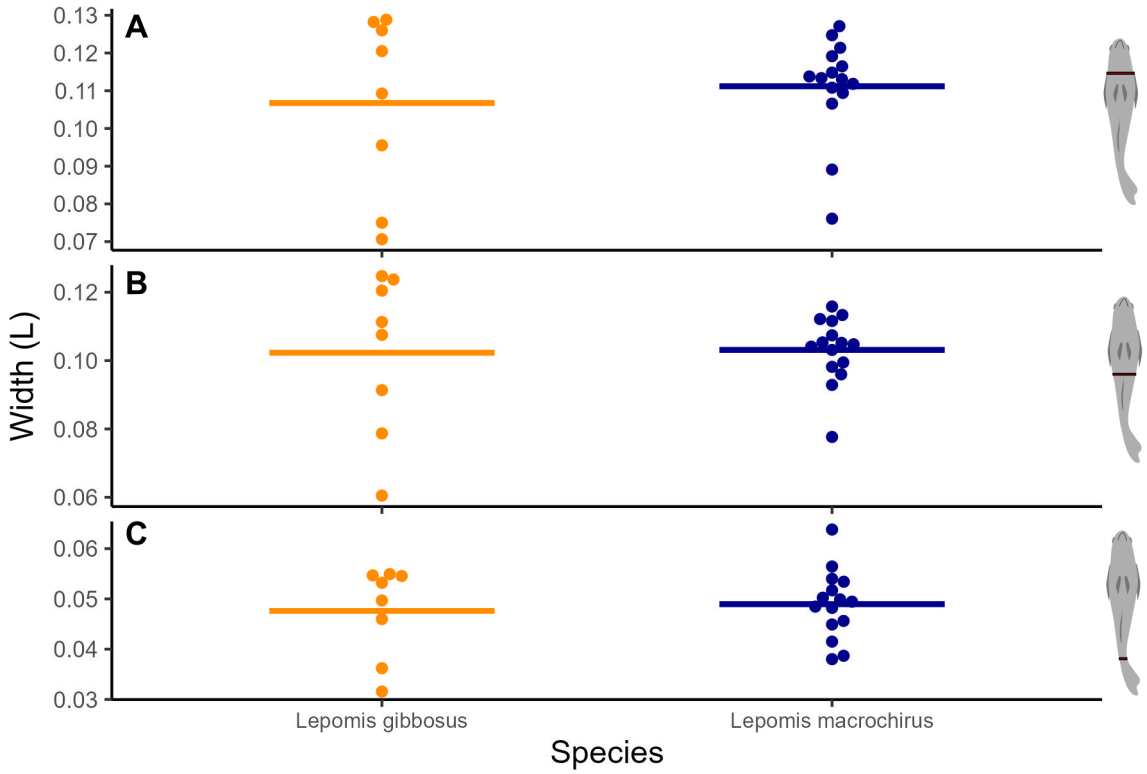

Figure 6: Body width was similar for both species. Widths in bodylengths along the length of the fish for (A) between the pectoral fins, (B) at the middle of the body, and (C) at the peduncle. Solid lines denote means for each group.

Bluegill had larger caudal and anal fins

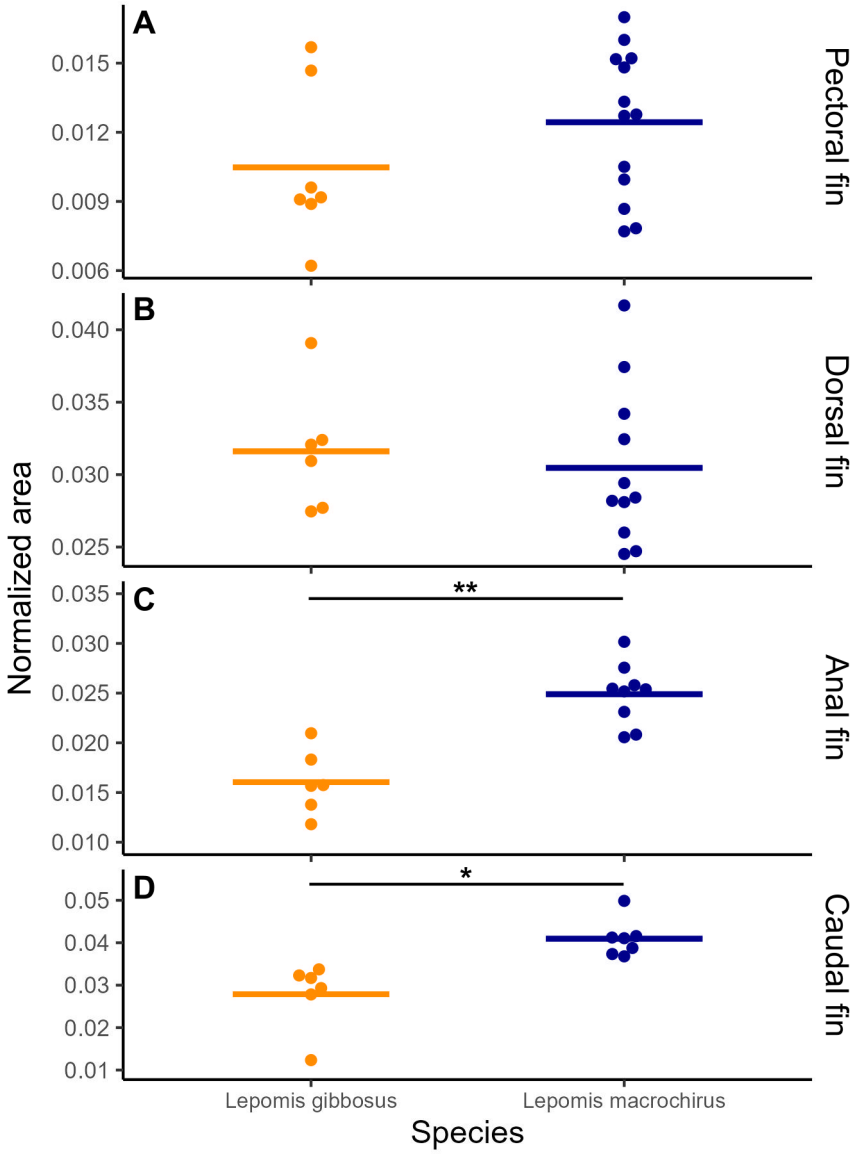

Figure 7: The anal and caudal fins were larger for bluegill than pumpkinseed. Fin area normalized by body length for (A) one pectoral fin, (B) the dorsal fin, (C) the anal fin, and (D) the caudal fin. Solid lines represent each group's mean. Asterisks denote $p < 0.05$ (*) and $p < 0.001$ (**)

Bluegill had 1.5x larger caudal fins ($p = 0.008$) and 1.6x larger anal fins ($p < 0.001$) than pumpkinseed, on average. The pectoral fin and dorsal fin areas were not significantly different ($p = 0.235$ and $p = 0.639$, respectively).

Tailbeat frequency was higher in pumpkinseed, but amplitude was higher in bluegill

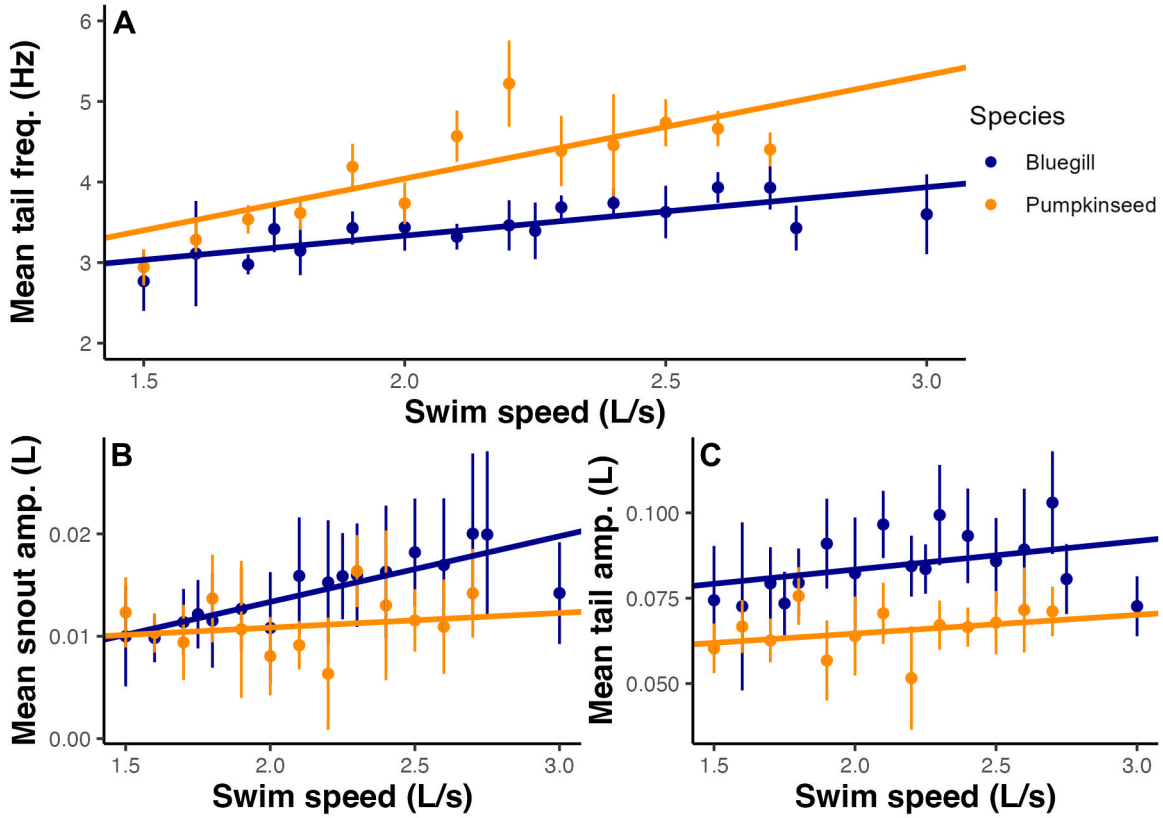

Figure 8: Tailbeat amplitude and frequency were different between the two species. (A) Tailbeat frequency over the range of tested flow speeds in bodylengths per second. (B, C) Amplitudes for both the snout (B) and the tail (C) over the range of flow speeds. Vertical lines represent the standard deviation and the two solid lines show a linear fit.

As both bluegill and the pumpkinseed swam faster, their tailbeat frequency increased significantly ($p < 0.001$). The pumpkinseed increased its frequency at a significantly higher rate than bluegill (slope of 1.3 vs. 0.6, $p < 0.001$) and beat its tail at an overall higher frequency ($p < 0.001$). Bluegill increased their snout amplitude with swimming speed ($p < 0.001$), but the pumpkinseed did not ($p = 0.205$). Bluegill also increased their snout amplitude at a significantly faster rate than the pumpkinseed (slope of 0.007 vs. 0.002, $p = 0.001$) and overall, had a significantly higher snout amplitude than the pumpkinseed ($p < 0.001$). Both bluegill and the pumpkinseed significantly increased their tailbeat amplitude ($p < 0.001$ and $p = 0.031$ respectively). While bluegill increased their tailbeat amplitude at a faster rate than the pumpkinseed (slope of 0.01 vs. 0.005), the difference was not significant ($p = 0.458$). Overall, bluegill beat their tail with a higher amplitude than the pumpkinseed ($p < 0.001$).

But their snout and tail speed were similar

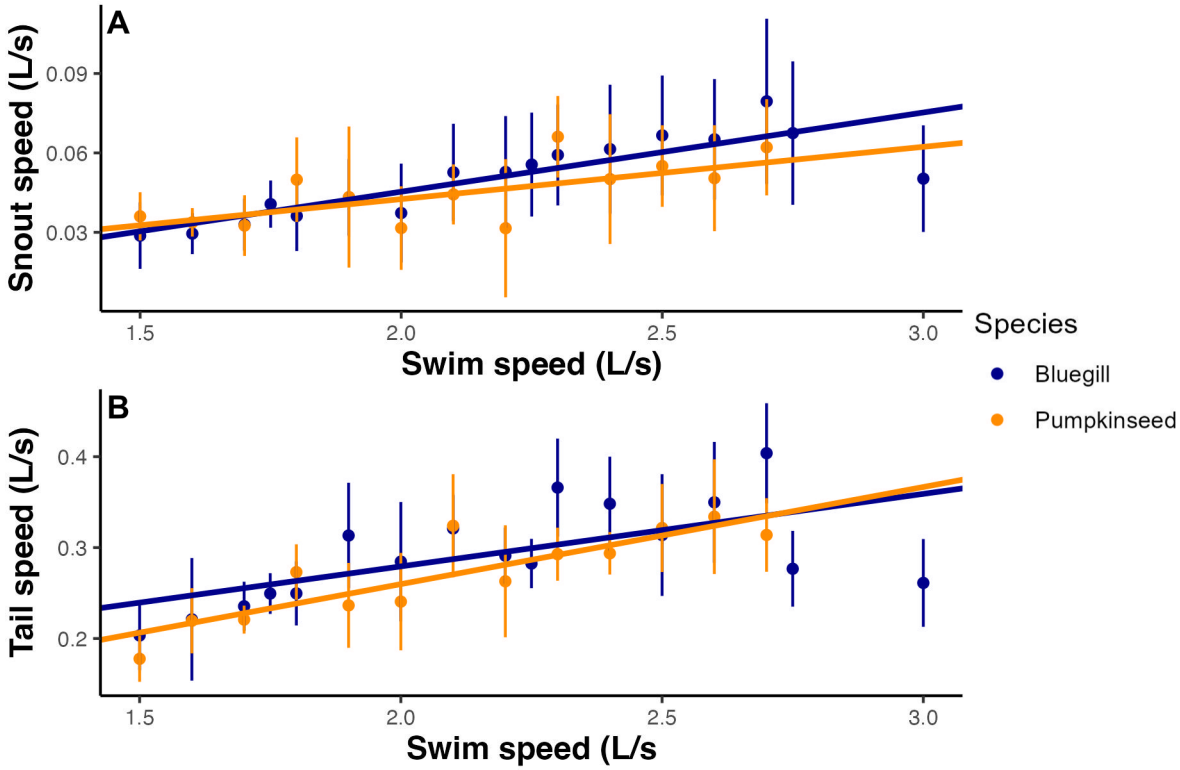

Figure 9: The side-to-side speed of the snout and tail was similar for the two species. Speed of both (A) the snout and (B) the tail over the range of tested flow speeds. Vertical lines represent the standard deviation and the two solid lines show the linear fits.

Both bluegill and pumpkinseed significantly increased their snout velocities with flow speed ($p < 0.001$ for both), and did so with similar slopes (0.03 for bluegill and 0.02 for pumpkinseed). There was no significant difference between the two species in either slope ($p = 0.075$) or overall ($p = 0.052$). They also significantly increased their tail velocities with flow speed (both $p < 0.001$) and again did so with similar slopes (0.09 for bluegill and 0.1 for pumpkinseed) that were not significantly different ($p = 0.093$). Overall, bluegill had a higher tail velocity than pumpkinseed ($p = 0.016$).

Bluegill and pumpkinseed used their caudal fins differently

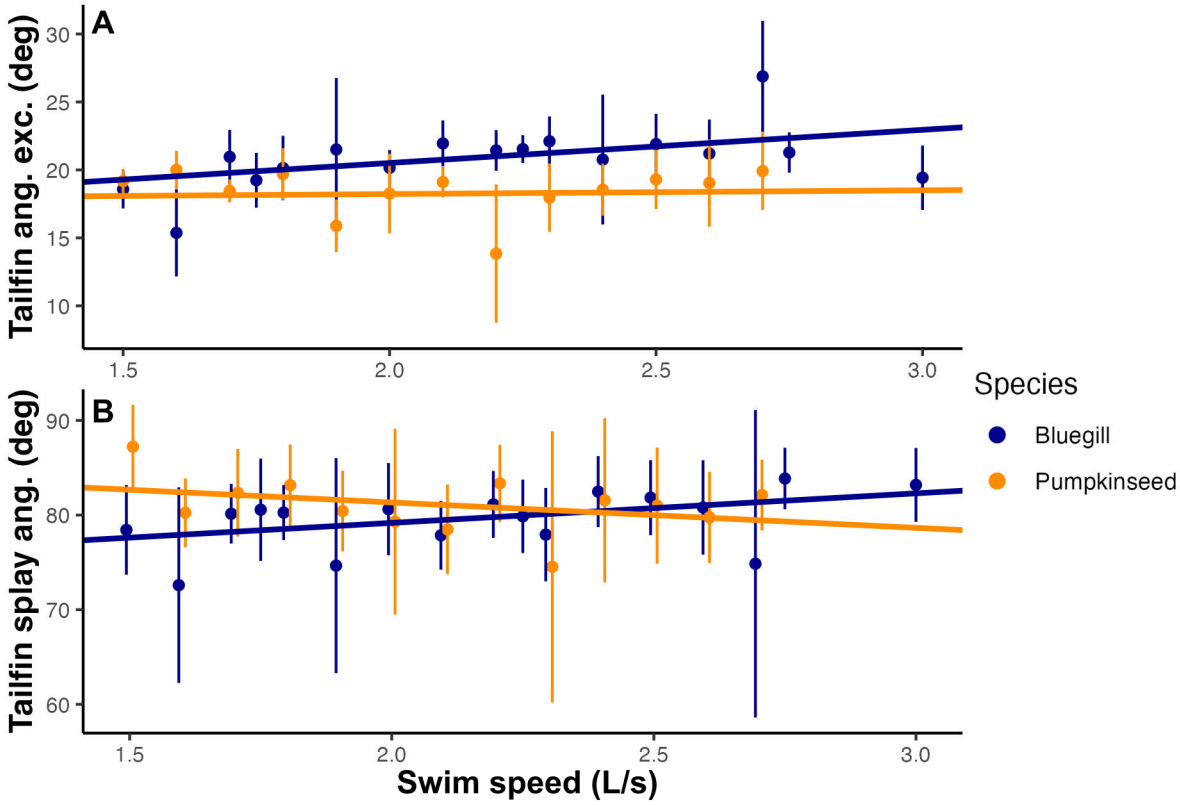

Figure 10: Caudal fin angular excursion and splay angle of the caudal fin was different among the species. (A) Tail fin angular excursion about the flow axis over the range of tested flow speeds. (B) Caudal fin splay angle as defined by the vectors from the middle of the peduncle to the top of the caudal fin and from the middle of the peduncle to the bottom of the caudal fin. Vertical lines represent the standard deviation and the two solid lines represent the linear fits

Both bluegill and pumpkinseed increased their caudal fin angular excursion over time, but the increase was only significant in bluegill ($p < 0.001$) and not in pumpkinseed ($p = 0.683$). Despite increasing their tailfin angular amplitude at a faster rate (slope of 2.6 vs. 0.3, Figure 10), bluegill did not do so significantly differently from pumpkinseed ($p = 0.067$). Bluegill flared their caudal fin more when they swam faster (slope of 2.5, Figure 10 B; $p < 0.001$). Pumpkinseed, however, pinched their caudal fin as speed increased (slope of -2.7) ($p < 0.001$). There was no significant difference between species ($p = 0.794$).

Discussion

Bluegill and pumpkinseed have similarly shaped bodies. All body morphometrics for bluegill overlapped substantially with those for pumpkinseed (Figure 5, Figure 6), and we found no statistical differences except in the anal and caudal fins, which quantitatively establishes that bluegill and pumpkinseed are morphologically similar species. This is unsurprising given how the two species are closely related (Figure 1), and the fact that we collected the individuals from similar locations (by the banks of ponds and lakes), which should further constrain morphology and plasticity (Gillespie and Fox, 2003; Hamel and Crispo, 2016; Vila-Gispert et al., 2007). However, the two species were not identical in fin shape as bluegill had larger anal and caudal fins than pumpkinseed, potentially contributing to functional differences. Additionally, while we quantified fin area, we did not account for overall shape of the fins. In particular, differences in caudal fin shape could drive kinematic differences, and even differences in the pectoral fins could drive kinematic differences at lower swim speeds.

Our preliminary results suggest that the two species differ in their swimming kinematics. Because of the small sample size, only the difference in tailbeat frequency was significant, but overall, bluegill tended to have a higher tailbeat amplitude and a lower tailbeat frequency than pumpkinseed (Figure 8). Based on previous work from Michaels' (2024), which also showed the same pattern, we expect that we will find more significant differences in swimming kinematics of the two species in a larger dataset.

The differences in swimming kinematics, coupled with the finding that bluegill also had a higher caudal fin splay angle (Figure 10 A) suggest that bluegill are not as efficient at swimming as pumpkinseed are, especially at higher speeds. To reach this conclusion, we turned to the work of Li et al (2021) who found that increases in tailbeat frequency result in lower costs of transport than increases in tailbeat amplitude, in large part because larger amplitudes mean more body excursion, which results in higher drag forces. However, bluegill may generally swim more unsteadily with bursts of swimming because of how they increase tailbeat amplitude and how larger amplitudes are associated with unsteady swimming (Wise et al., 2018) and accelerations (Akanyeti et al., 2017; Wise et al., 2018). Additionally, the significant differences in caudal fin area could mean bluegill are even less efficient as their larger caudal fin would encounter more drag per tailbeat as it beats from side to side.

Additionally, while we did not measure body stiffness, we nonetheless expect it to play an important role. Stiffness cannot be inferred or accounted for by morphology (Jimenez et al., 2023). Due to how variable

stiffness can be, both between species and even along the body within species, it is possible that bluegill have different passive stiffnesses than pumpkinseed. Additionally, as stiffness is actively modulated by muscle activation during swimming, it could have contributed to the differences that we are seeing, especially considering how significantly stiffness has been modeled to impact swimming performance (Tytell et al., 2010).

Finally, we did not quantify the type or size of the muscles in bluegill and pumpkinseed. Despite having similar external body dimensions, bluegill and pumpkinseed may have different muscles sizes such that pumpkinseed muscles could be longer and bluegill muscles could have larger cross sectional areas, resulting in diferente performances. Finally, we did not quantify the composition of red and white muscles in bluegill and pumpkinseed, which could further impact their kinematics.

Overall, when considering the broader research surrounding form and function, we believe our work suggests that form and function are more decoupled than we initially thought. Bluegill and pumpkinseed had no significant differences in their body shape with the exceptions of their anal and caudal fins, but our preliminary results suggest that they swim significantly differently. Our results align more with the findings of Satterfield et al (2023) than a more rigid interpretation of Webb (1984b). While Satterfield et al (2023) found that different forms have similar functions, we found that the similar forms have different functions. Along with Satterfield's work, our quantification of kinematic differences between morphometrically similar bluegill and pumpkinseed suggests that form is not a perfect predictor of function, and that function can vary more than we might expect. That being said, Webb's triangle (1984a) still serves as a compelling heuristic that helps inspire future directions.

Future directions

While our analysis captured the role of the caudal fin, we did not quantify the kinematics of the dorsal fin. The dorsal fin, in particular, could account for substantial thrust as Lauder (Lauder and Drucker, 2004) previously found that it accounts for 12% of a bluegill's total thrust. Additionally, while we looked at tailbeat frequency and amplitude, amplitude along the body could provide an important window into the differences. According to Lighthill (1969), for carangiform swimmers, large posterior amplitudes can be generated from small anterior amplitudes. Thus, changes to anterior amplitudes could hinder the efficiency of steady swimming in bluegill and pumpkinseed. This is because the more the body extrudes from side to side, the more drag opposes forward velocity (Li et al., 2021).

We also did not quantify the physical properties of the fishes' morphologies. Specifically, body (Jimenez et al., 2023; Tytell et al., 2010) and fin ray stiffness could play a role as they have previously been found to affect thrust production in robotic models (Esposito et al., 2012). Additionally, a future direction could be measuring the body stiffness of the fish while they are swimming. Such an analysis, combined with EMGs, would let us know the muscular contribution to stiffness, would allow us to determine if either bluegill or pumkpkinseed are doing something differently kinematically to achieve some more optimal stiffness during swimming. We believe such a study might find that stiffness is in fact more important than the tradeoff between frequency and amplitude.

Finally, it would be interesting to collect bluegill and pumpkinseed from different ecological locations. Ecological differences impact morphology in pumpkinseed (Gillespie and Fox, 2003; Hamel and Crispo, 2016; Vila-Gispert et al., 2007) and bluegill (Papadopoulos, 2009) such that body dimensions vary between lakes and rivers (Papadopoulos, 2009) and even between littoral and pelagic zones in the same body of water (Gillespie and Fox, 2003). We expect that fish collected from more pelagic, still bodies of water will have deeper bodies that would swim less efficiently than their river and littoral counterparts, but defining how those morphologies correlate to kinematics within a species would help address the form vs. function debate.

Contributions

For this study, Olivia Hawkins collected the morphometrics data, we both collected the kinematics data, and I analyzed all of the data. Stephen Michaels collected and analyzed the preliminary data that inspired this study.

References

Akanyeti, O., Putney, J., Yanagitsuru, Y. R., Lauder, G. V., Stewart, W. J. and Liao, J. C. (2017). Accelerating fishes increase propulsive efficiency by modulating vortex ring geometry. *Proceedings of the National Academy of Sciences* **114**, 13828–13833. doi: 10.1073/pnas.1705968115.

Bainbridge, R. (1958). The speed of swimming of fish as related to size and to the frequency and amplitude of the tail beat. *Journal of Experimental Biology* **35**, 109–133. doi: 10.1242/jeb.35.1.109.

Bates, D., Mächler, M., Bolker, B. and Walker, S. (2015). Fitting linear mixed-effects models using Lme4. *Journal of Statistical Software* **67**, 1–48. doi: 10.18637/jss.v067.i01.

Brett, J. R. and Sutherland, D. B. (1965). Respiratory metabolism of pumpkinseed (*Lepomis gibbosus*) in relation to swimming speed. *Journal of the Fisheries Research Board of Canada* **22**, 405–409. doi: 10.1139/f65-039.

Drucker, E. G. and Lauder, G. V. (1999). Locomotor forces on a swimming fish: Three-dimensional vortex wake dynamics quantified using digital particle image velocimetry. *Journal of Experimental Biology* **202**, 2393–2412. doi: 10.1242/jeb.202.18.2393.

Dunnington, D., Thorne, B. and Hernangómez, D. (2023). Ggspatial: Spatial data framework for Ggplot2. url: https://cran.r-project.org/web/packages/ggspatial/index.html.

Eklund, A. and Trimble, J. (2021). Beeswarm: The bee swarm plot, an alternative to stripchart. url: https://cran.r-project.org/web/packages/beeswarm/index.html.

Esposito, C. J., Tangorra, J. L., Flammang, B. E. and Lauder, G. V. (2012). A robotic fish caudal fin: Effects of stiffness and motor program on locomotor performance. *Journal of Experimental Biology* **215**, 56–67. doi: 10.1242/jeb.062711.

Fish, P. A. and Savitz, J. (1983). Variations in home ranges of largemouth bass, yellow perch, bluegills, and pumpkinseeds in an Illinois lake. *Transactions of the American Fisheries Society* **112**, 147–153. doi: 10.1577/1548-8659(1983)112<147:VIHROL>2.0.CO;2.

Flammang, B. E. and Lauder, G. V. (2009). Caudal fin shape modulation and control during acceleration, braking and backing maneuvers in bluegill sunfish, *Lepomis macrochirus*. *Journal of Experimental Biology* **212**, 277–286. doi: 10.1242/jeb.021360.

Fox, J. and Weisberg, S. (2019). *An R Companion to Applied Regression*. Third edition. Thousand Oaks CA: Sage.

Garrido-Jurado, S., Muñoz-Salinas, R., Madrid-Cuevas, F. J. and Marín-Jiménez, M. J. (2014). Automatic generation and detection of highly reliable fiducial markers under occlusion. *Pattern Recognition* **47**, 2280–2292. doi: 10.1016/j.patcog.2014.01.005.

Gillespie, G. J. and Fox, M. G. (2003). Morphological and life-history differentiation between littoral and pelagic forms of pumpkinseed. *Journal of Fish Biology* **62**, 1099–1115. doi: 10.1046/j.1095-8649.2003.00100.x.

Hamel, C. I. and Crispo, E. (2016). Morphology of pumpkinseed sunfish (*Lepomis gibbosus*) is related to water body size. *BIOS* **87**, 56–66. doi: 10.1893/BIOS-D-14-00029.1.

Jimenez, Y. E., Lucas, K. N., Long, J. H., Jr and Tytell, E. D. (2023). Flexibility is a hidden axis of biomechanical diversity in fishes. *Journal of Experimental Biology* **226**, jeb245308. doi: 10.1242/jeb.245308.

Karashchuk, P., Rupp, K. L., Dickinson, E. S., Walling-Bell, S., Sanders, E., Azim, E., Brunton, B. W. and Tuthill, J. C. (2021). Anipose: A toolkit for robust markerless 3D pose estimation. *Cell Reports* **36**, 109730. doi: 10.1016/j.celrep.2021.109730.

Kay, M. (2024). Ggdist: Visualizations of distributions and uncertainty in the grammar of graphics. *IEEE Transactions on Visualization and Computer Graphics* **30**, 414–424. doi: 10.1109/TVCG.2023.3327195.

Kay, M. and Wiernik, B. M. (2024). Ggdist: Visualizations of distributions and uncertainty. url: https://cloud.r-project.org/web/packages/ggdist/index.html.

Lauder, G. V. (1982). Structure and function in the tail of the Pumpkinseed sunfish (*Lepomis gibbosus*). *Journal of Zoology* **197**, 483–495. doi: 10.1111/jzo.1982.197.4.483.

Lauder, G. V. and Drucker, E. G. (2004). Morphology and experimental hydrodynamics of fish fin control surfaces. *IEEE Journal of Oceanic Engineering* **29**, 556–571. doi: 10.1109/JOE.2004.833219.

Li, G., Liu, H., Müller, U. K., Voesenek, C. J. and van Leeuwen, J. L. (2021). Fishes regulate tail-beat kinematics to minimize speed-specific cost of transport. *Proceedings of the Royal Society B: Biological Sciences* **288**, 20211601. doi: 10.1098/rspb.2021.1601.

Lighthill, M. J. (1969). Hydromechanics of aquatic animal propulsion. *Annual Review of Fluid Mechanics* **1**, 413–446. doi: 10.1146/annurev.fl.01.010169.002213.

Liu, Y. and Jiang, H. (2022). Research development on fish swimming. *Chinese Journal of Mechanical Engineering* **35**, 114. doi: 10.1186/s10033-022-00791-4.

Mayr, E. (1972). Lamarck revisited. *Journal of the History of Biology* **5**, 55–94. url: https://www.jstor.org/stable/4330569.

Michaels, S. (2024). Evaluating kinematic differences in the acceleration of two centrarchid species.

Mittelbach, G. G. (1981). Foraging efficiency and body size: A study of optimal diet and habitat use by bluegills. *Ecology* **62**, 1370–1386. doi: 10.2307/1937300.

Mittelbach, G. G. (1984). Predation and resource partitioning in two sunfishes (Centrarchidae). *Ecology* **65**, 499–513. doi: 10.2307/1941412.

Near, T. J. and Koppelman, J. B. (2009). Species Diversity, Phylogeny and Phylogeography of Centrarchidae. In *Centrarchid Fishes*, pp. 1–38. John Wiley & Sons, Ltd. doi: 10.1002/9781444316032.ch1.

Papadopoulos, A. (2009). An ecophysiological framework for the morphological evolution of bluegill sunfish. url: https://hdl.handle.net/1969.1/ETD-TAMU-1393.

Pereira, T. D., Tabris, N., Matsliah, A., Turner, D. M., Li, J., Ravindranath, S., Papadoyannis, E. S., Normand, E., Deutsch, D. S., Wang, Z. Y., et al. (2022). SLEAP: A deep learning system for multi-animal pose tracking. *Nature Methods* **19**, 486–495. doi: 10.1038/s41592-022-01426-1.

Satterfield, D. R., Claverie, T. and Wainwright, P. C. (2023). Body shape and mode of propulsion do not constrain routine swimming in coral reef fishes. *Functional Ecology* **37**, 343–357. doi: 10.1111/1365-2435.14227.

Schindelin, J., Arganda-Carreras, I., Frise, E., Kaynig, V., Longair, M., Pietzsch, T., Preibisch, S., Rueden, C., Saalfeld, S., Schmid, B., et al. (2012). Fiji: An open-source platform for biological-image analysis. *Nature Methods* **9**, 676–682. doi: 10.1038/nmeth.2019.

Sfakiotakis, M., Lane, D. M. and Davies, J. B. C. (1999). Review of fish swimming modes for aquatic locomotion. *IEEE Journal of Oceanic Engineering* **24**, 237–252. doi: 10.1109/48.757275.

Standen, E. M. and Lauder, G. V. (2005). Dorsal and anal fin function in bluegill sunfish *Lepomis macrochirus*: Three-dimensional kinematics during propulsion and maneuvering. *Journal of Experimental Biology* **208**, 2753–2763. doi: 10.1242/jeb.01706.

Stuber, R. J., Gebhart, G. and Maughan, O. E. (1982). *Habitat Suitability Index Models: Bluegill*. Western Energy and Land Use Team, Office of Biological Services, Fish and Wildlife Service, U.S. Department of the Interior.

Sulloway, F. J. (1982). Darwin and his finches: The evolution of a legend. *Journal of the History of Biology* **15**, 1–53. doi: 10.1007/BF00132004.

Tomeček, J., Kováč, V. and Katina, S. (2007). The biological flexibility of the pumpkinseed: A successful colonizer throughout Europe. In *Biological Invaders in Inland Waters: Profiles, Distribution, and*

Threats (ed. Gherardi, F.), pp. 307–336. Dordrecht: Springer Netherlands. doi: 10.1007/978-1-4020-6029-8_16.

Tytell, E. D., Hsu, C.-Y., Williams, T. L., Cohen, A. H. and Fauci, L. J. (2010). Interactions between internal forces, body stiffness, and fluid environment in a neuromechanical model of lamprey swimming. *Proceedings of the National Academy of Sciences* **107**, 19832–19837. doi: 10.1073/pnas.1011564107.

Vila-Gispert, A., Fox, M. G., Zamora, L. and Moreno-Amich, R. (2007). Morphological variation in pumpkinseed *Lepomis gibbosus* introduced into Iberian lakes and reservoirs; adaptations to habitat type and diet? *Journal of Fish Biology* **71**, 163–181. doi: 10.1111/j.1095-8649.2007.01483.x.

Webb, P. W. (1984a). Form and function in fish swimming. *Scientific American* **251**, 72–83.

Webb, P. W. (1984b). Body and fin form and strike tactics of four teleost predators attacking fathead minnow (*Pimephales promelas*). *Canadian Journal of Fisheries and Aquatic Sciences* **41**, 157–165. doi: 10.1139/f84-016.

Wickham, H., Averick, M., Bryan, J., Chang, W., McGowan, L. D., François, R., Grolemund, G., Hayes, A., Henry, L., Hester, J., et al. (2019). Welcome to the Tidyverse. *Journal of Open Source Software* **4**, 1686. doi: 10.21105/joss.01686.

Wise, T. N., Schwalbe, M. A. B. and Tytell, E. D. (2018). Hydrodynamics of linear acceleration in bluegill sunfish, *Lepomis macrochirus*. *Journal of Experimental Biology* **221**, jeb190892. doi: 10.1242/jeb.190892.

Chapter 2: Bluegill increase their heart rate with swimming speed

Co-author: Brendan Kelleher

Introduction

Arguably the most important behavior in a animal's daily life is locomotion, but it comes with a metabolic cost (Bennett, 2013). Due to how important movement is and how critical metabolism is to to an animal's survival, a lot of research has focused on locomotion, metabolism, and the link between the two. Our understanding of this biological process comes from research that ranges from humans (McAllister et al., 2025) to insects (Full et al., 1990) to fishes (Moves and West, 1995) and beyond. There are many ways in which we can study it, starting with direct calorimetry. Direct calorimetry measures temperature changes to quantify calories used (Lavoisier, 1865; translated by West, 2013), but such data is often challenging to obtain. Instead, indirect calorimetry in the form of measuring oxygen consumption provides a much easier alternate research route. In heterotrophs, the metabolic rate is equal to the rate of respiration because oxygen is needed for the respiration reaction to occur with carbon dioxide produced as a byproduct (Brown et al., 2004). There are also anaerobic metabolic costs that are not typically accounted for by measuring changes in oxygen concentration, however these can be quantified by measuring changes in post exercise oxygen saturation or lactic acid (Zhang and Lauder, 2024).

Despite respiration being an imperfect measure of calorimetry, most research on fishes relies on it for a handful of reasons. First off, while there are several approaches to directly quantify energy consumption in fishes, they often fall short due to individual differences, resulting in the need for large sample sizes and terminal protocols (Nelson, 2016). Additionally, while we could quantify changes in body temperature to

quantify energy expenditure, water is a massive heat sink and would obscure our results (Nelson, 2016). As a result, measuring dissolved gasses like oxygen and carbon dioxide tends to be the best approach to analyzing metabolism in fishes (Nelson, 2016). However, measuring carbon dioxide is not quite feasible as it can change due to many factors besides respiration (Nelson, 2016), so the most reliable way to quantify fish metabolism is by looking at changes in dissolved oxygen. However, quantifying changes in dissolved oxygen concentration in water can fall short from direct calorimetry because it does not account for anaerobic activity (Nelson, 2016). Finally, while dissolved oxygen has proved a useful tool, it may not be the optimal one and may fall out of favor in the future due to its inability to track metabolic pathways that do not depend on oxygen uptake (Nelson, 2016). However, anaerobic changes can be measured by quantifying post exercise oxygen uptake (Zhang and Lauder, 2024), or by measuring changes in the concentration of lactic acid in the blood so future studies may incorporate such methods.

Additionally, for researchers to measure changes in dissolved oxygen, those changes must be large enough in the surrounding medium to be measured. If, for example, a small fish swims in a large tank, it could result in inaccurate or insufficient measurements on a short time scale (Korsmeyer et al., 2002). In particular, if one needs a long time to measure changes in oxygen concentration, then it is difficult to assess intermittent behaviors as they occur on a much smaller timescale (as with Korsmeyer et al., 2002). For our purposes, this means we are unable to use this method to quantify behaviors that occur on the matter of seconds to minutes. As a result, it was important to find other ways to measure energetic costs in fishes, which was what we were hoping to do with this study. Specifically we wanted to find and validate a method that would indirectly give us a sense of metabolic costs with a more rapid response than dissolved oxygen allows. Having this finer time resolution for energetic measurements would be valuable for the field of biomechanics which often tries to link energetics with movement (Biewener and Wilson, 2025), as well as for commercial fish farms who are always looking for the best and most direct way to understand how their fish are expending energy and how they can optimally care for them (Li, 1987).

Because it is hard to use dissolved oxygen to assess energetic costs on a small time scale, we instead turned to their total cardiac output. It is not enough for an animal to go through a metabolic reaction; it also needs to distribute the energy throughout the body. This involves moving oxygen from wherever it is collected to where it is needed to facilitate localized reactions and the production of ATP (Nelson, 2016). In fish, this involves moving blood over the gills and pulling the oxygen that it takes up from the water throughout the rest of the body (Randall, 1982). For this reason, we turned to the heart rate as a potential

way to quantify energetic cost, in part because of how increases in cardiac output link with increases in oxygen uptake (Randall, 1982).

But before we go into detail on how to measure heart rate in fish, it is important to understand the structure of the fish heart. Whereas human hearts have two atria and two ventricles, fish hearts only have one atrium and one ventricle (Evans and Claiborne, 2005). In addition to those two chambers, they have two more: the sinus venosus and the conus arteriosus (Evans and Claiborne, 2005). A heartbeat begins in the pacemaker cells of the sinus venosus, before spreading throughout the heart (Evans and Claiborne, 2005). This heart rate can then be measured by amplifying its signal, a procedure called an electrocardiogram (EKG) (Pardee, 1914). The fish heart has a similar EKG to that of the mammalian heart (Evans and Claiborne, 2005), where the p-wave signals atrial depolarization, the QRS complex signals the ventricle depolarization, and the T-wave signals ventrical repolarization (see Figure 1 C for an example).

While fish and human hearts are similar in many important ways, fish use different methods to modulate total cardiac output. Cardiac output is the product of the stroke volume (total volume of blood expelled per heart beat) multiplied by the number of heart beats per unit time. Thus it is the total volume of blood pumped by the heart in a unit of time, and is therefore a good heart-related measure of metabolism in organisms. In humans, we tend to modulate cardiac output using both heart rate, the number of beats per minute and stroke volume, how much blood is pumped per heartbeat (Bezucha et al., 1982). This allows us to more rapidly transfer blood throughout our bodies to where it is needed. Similarly, fish can also increase heart rate (as in the case of tuna where they can increase it up to 6 times baseline (Clark et al., 2008)), and they can increase their stroke volume (sometimes up to 300 percent as with trout (Shiels et al., 2006)).

As it is easier to measure, especially in smaller fish, we chose to quantify heart rate. For our experiment, we chose to use bluegill sunfish (*Lepomis macrochirus*), which are commonly used in biomechanics research. By using bluegill we hoped to validate our method in a species that is often used to assess kinematics, thereby providing researchers another avenue to assess how their fish are behaving and why they are behaving in that way. We hypothesized that small scale kinematics changes are supported by changes in heart rate in bluegill. Specifically, we predicted that as bluegill swim at higher speeds and as they maneuver around more, they will increase their heart rate so they can send more blood to the areas that need it. Some work on bluegill already exists, such as a study by Marvin and Heath (1968) and Spitzer et al (1969), who found that bluegill have lower heart rates the more hypoxic the surrounding water is.

Methods

Dataset

We collected 3 bluegill (*Lepomis macrochirus*) (of lengths 10cm, 11cm, and 14cm) from either White pond or Walden pond in Concord, MA. We used a seine net along the shores of these ponds to collect the fish before transferring them to an aquaculture facility where they were kept in 10 gallon tanks at a controlled temperature of 20 degrees Celsius until used for experiments. We collected the fish with scientific collection permits 090.22SCF, 146.23SCF, 158.19SCF, and 174.20SCF, and kept them according to protocols M2018-103, M2021-99, and M2024-57.

All experimental procedures and animal handling protocols were approved by the Tufts University Institutional Animal Care and Use Committee.

EKG and surgical preparation

We used a single electrode, created with two 2-meter-long portions of stainless-steel wire (127 µm diameter uninsulated) that we glued together. Tips of the electrodes were offset, and insulation shaved off (2 mm) from each respective tip (Figure 1 B).

Before performing the surgery, we anesthetized the fish in buffered MS222 at 0.02% concentration. Once the fish was anesthetized, we transferred it to the surgical tray with 50% diluted MS222 and intubated it using a peristaltic pump to ensure proper oxygenation for the duration of the surgery. An aquarium bubbler was also added to the surgical tray to increase oxygen concentration in the water. The electrode wires were attached to a head stage for a Dagan EX4-400 quad differential amplifier. We used LabChart (AD instruments) and a PowerLab 16/32 data acquisition system to continuously collect data.

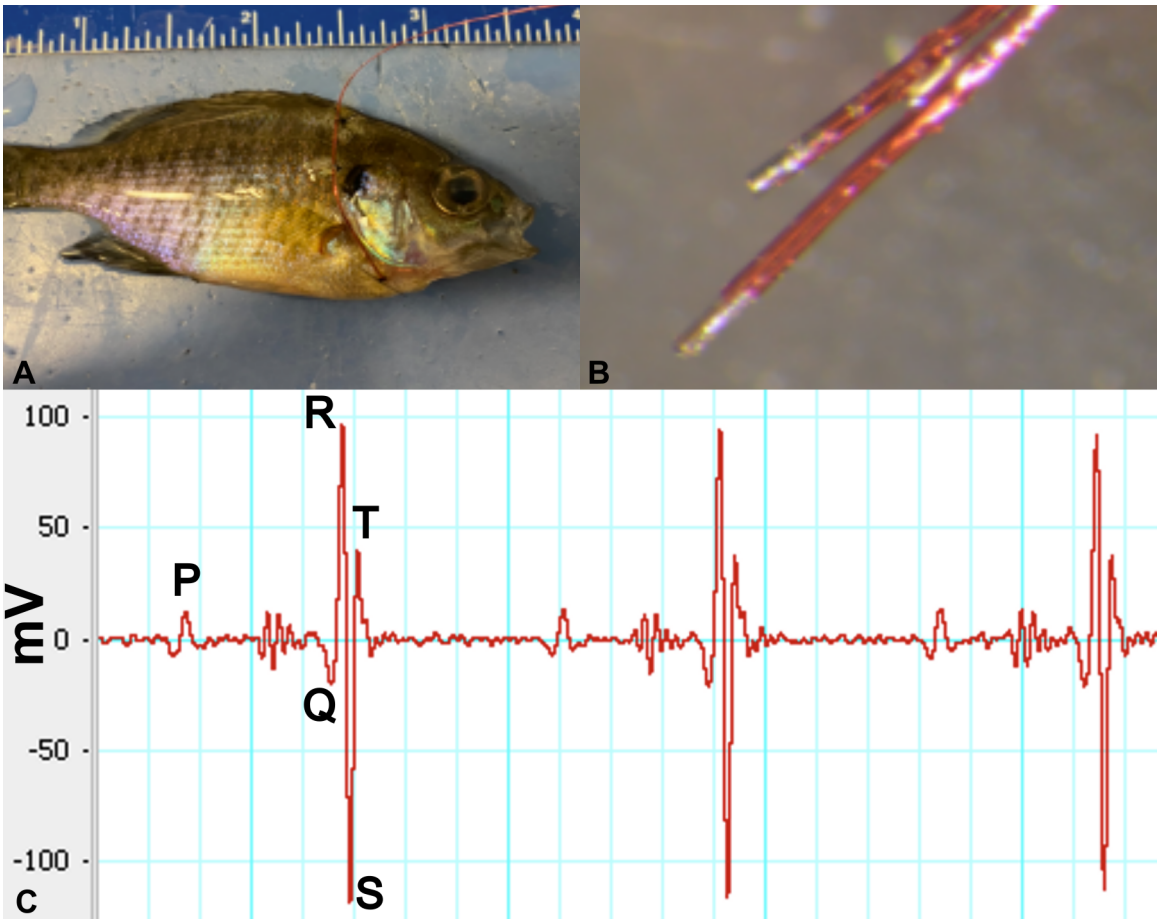

Figure 1: EKG setup. (A) Individual with the electrodes inserted into its pericardial cavity. (B) The electrodes we used with the tips shaved off. (C) Representative trace of a heart beat recorded from an individual during an experiment. Relevant peaks are labeled on the trace of the first beat where P is atrial depolarization, the QRS complex is ventricle depolarization, and T is ventricle repolarization.

Surgical procedure

We first injected bupivacaine (1 mg/kg) in the dorsal musculature near the dorsal fin and then again with the same dosage at the site of insertion. We then removed a small number of ventral scales, and made an entry hole using a sterile 27.5-gauge needle. We then removed the needle and inserted the electrode directly into pericardial cavity through the hole. We inserted it to an estimated depth of about 1cm before making slight adjustments after insertion to maximize the quality of EKG signals visualized on LabChart.

We filtered the EKGs signals with a bandpass filter (10 – 60 Hz). After ensuring we were recording strong EKG signals, we sutured the electrode in 3 locations: directly at the site of insertion, just above the pectoral fin, and on the dorsal edge of the fish, just in front of the dorsal fin Figure 1. We then transferred the fish to a recovery tank where we allowed it to awaken from the anesthesia until it had reoriented dorsal side up. We then transferred the fish to a flow tank with a 25×26×150 cm working section (height x width x length) and allowed it approximately 5-10 minutes to acclimate to its surroundings. The flow tank was oxygenated with an aquarium bubbler in between experiments, but the bubbler was removed during the course of the experiments. Following experimentation, we euthanized the fish, and dissected out the electrodes to ensure proper placement near the heart in the pericardial cavity.

For 1 individual, we followed the same surgical procedures as with the other fish, but gave it a full 8 hours to acclimate in the flow tank at a flow speed of 1 L/s before running any experiments. We refer to this individual as the “day-long acclimation” individual.

Swim speeds

We swam all fish over a range of swimming speeds. For one individual (identified with green points on all figures), we started the flow speed at 0.5 L/s, increasing the speed by 0.5 L/s every 4 minutes up to 1.5 L/s and recording video in the middle of each 4 minute period. For another individual (identified with purple points on all figures), we first swam it at speeds of 0.5 and 1 L/s before ramping up from 1.5 L/s to 2.5 L/s. Unfortunately, that individual did not swim consistently at lower speeds so we only analyzed swimming speeds of 1.5 L/s and higher.

We swam the day-long acclimation individual at speeds from 0.5 to 2 L/s, first starting at 0.5 Ls/, then ramping up to 2 L/s, then ramping down to 0.5 L/s. Each trial lasted 5 minutes and we captured video for the middle 78 seconds of that 5 minute period so that we could be confident the flow speed had steadied.

Heart rate and heart rate variability

To measure heart rate, we used LabChart to identify R peaks by running a cyclic measurement function on the raw EKG traces. Each heart rate is the heart rate estimated at its respective R peak. To estimate heart rate variability, we followed the methods of Jerem and Romero (2023) and divided the standard deviation of heart rate over its mean for a 3 second sliding window for the duration of the trial.

Filming and digitizing

We used a Phantom Miro M340 high speed camera that was positioned ventrally and orthogonally to the working section of the flow tank. We captured around 2000 frames of video at 30 frames per second for the first individual, 100 frames per second for the second individual, and 60 frames per second for the day-long acclimation trial individual. We used the image of a ruler along with FIJI (Schindelin et al., 2012) to convert pixels to centimeters. We used DLTdv8a (Hedrick, 2008) to digitize the videos. To quantify maneuvering, we tracked one point on the body for each trial. We used either the left eye, right eye, or tip of the snout, depending on what was best visible throughout the trial. We synced the physical trigger we used to capture videos with LabChart by attaching it as an input and recording it on a channel so we could link the videos with the LabChart data files.

Maneuvering speed

When we mention maneuvering speed, we refer to the speed at which an individual moves in the reference frame of our ventral camera (movement separate from that induced by the oncoming flow). To estimate maneuvering speed, we first smoothed the x and y positions from the videos with a 9th order Butterworth filter with a low pass cutoff frequency of 10 Hz, then numerically differentiated the position with respect to time by estimating the central difference between points (Smith, 1985). In this way, we estimated the maneuvering speed of each individual separately from the oncoming flow.

Data filtering

We removed outliers that fell more than 2 standard deviations outside of the mean standardized values. To do so, we first standardized both heart rate and maneuvering speed by subtracting each individual's mean from all points, then dividing by each individual's standard deviation. We then used these mean standard-

ized values to select only heart rates and maneuvering speeds that fell within 2 standard deviations of each individual's mean.

Statistics

For all analysis and visualization, we used R version 4.3.3 with Rstudio version 2023.12.1.402 and the following packages: tidyverse version 2.0.0 (Wickham et al., 2019), lme4 version 1.1.35.1 (Bates et al., 2015), car version 3.1.2 (Fox and Weisberg, 2019), ggspatial version 1.1.9 (Dunnington et al., 2023), ggdist version 3.3.2 (Kay, 2024; Kay and Wiernik, 2024), arrow version 19.0.1 (Richardson et al., 2025), and parquetize version 0.5.7 [dotta2024].

For the two individuals that did not have a full day to acclimate, we assessed significance of heart rate, heart rate variability, and maneuvering speed with respect to oncoming flow speed by running a linear model for each individual with either heart rate, heart rate variability, or maneuvering speed as the dependent variable and flow speed as the independent variable. We then used the Anova function from the car package to estimate the p values. For the day-long acclimation individual, we used the same linear model, but ran it on separately on the ramp up and ramp down portions. Additionally, when we statistically compared heart rate and heart rate variability between the ramp up and ramp down, we also used the same linear model, but with ramp direction as the fixed effect and flow speed as the random effect.

For the non-acclimation individuals, when we modeled linear fits comparing heart rate and heart rate variability to maneuvering speed, we used the lm function to run a linear model for each individual with maneuvering speed and flow speed as fixed effects. For the day-long acclimation individual, we ran the same linear model, but also added ramp direction as a fixed effect. For plotting purposes, for both the day-long acclimation individual and the non-acclimation individuals, we show a linear model from the lm function with either heart rate or heart rate variability regressed onto maneuvering speed with no additional fixed or random effects.

All means are provided plus or minus one standard deviation, unless otherwise noted.

Results

Individuals with no acclimation

Individuals changed heart rate and heart rate variability differently with increasing flow speed

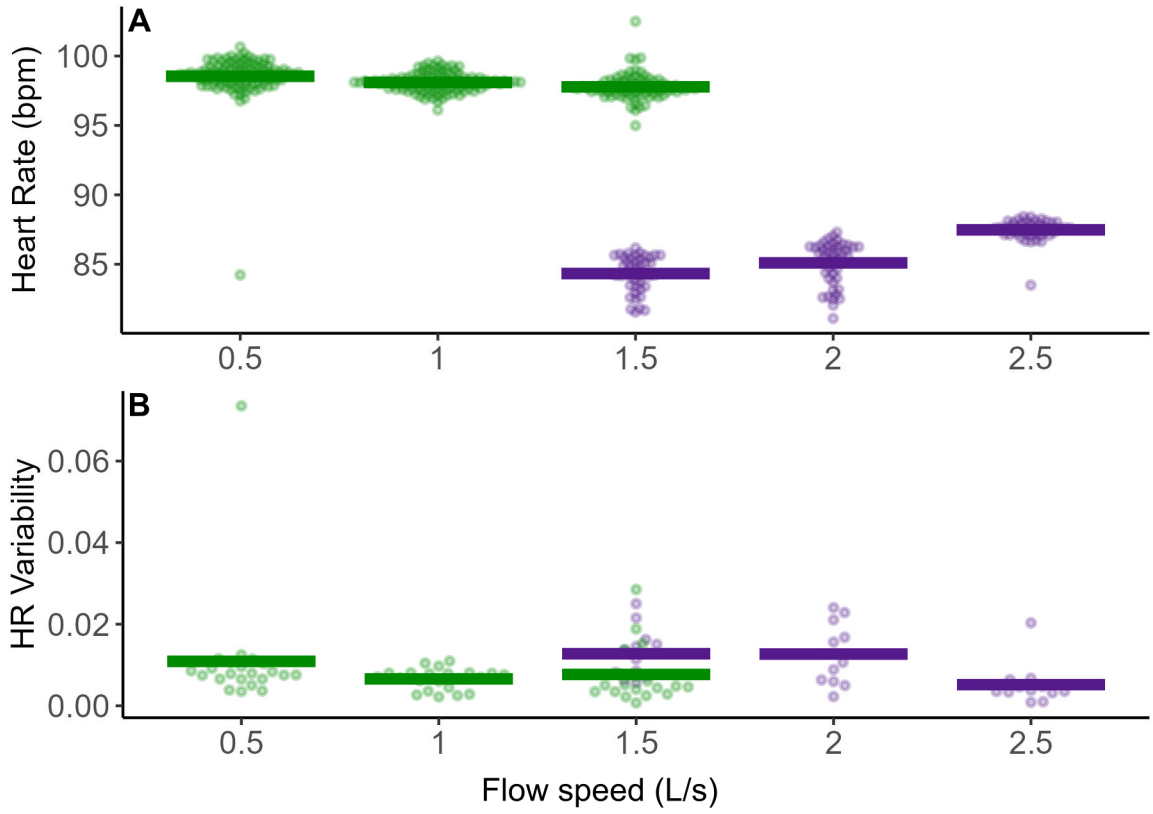

Figure 2: Each individual changed their heart rate (A) and heart rate variability (B) differently with flow speed. Color denotes individual. Lines represent means within groups.

The two individuals changed their heart rate differently as flow speed increased (Figure 2). The individual coded with purple points significantly increased their heart rate (84.3 $\pm$ 1.3bpm to 87.5 $\pm$ 0.8bpm, $p < 0.001$) while the individual coded with green points significantly decreased their heart rate (98.5 $\pm$ 1.6bpm to 97.8 $\pm$ 0.9bpm), but the difference was less than 1bpm on average so there was no functional change in heart rate at each speed. The individual coded with purple points significantly decreased their heart rate variability as flow speed increased ($p = 0.007$) (Figure 2), while the individual coded with green points did not significantly change their heart rate variability with flow speed ($p = 0.254$).

Bluegill swam more unsteadily as flow speed increased

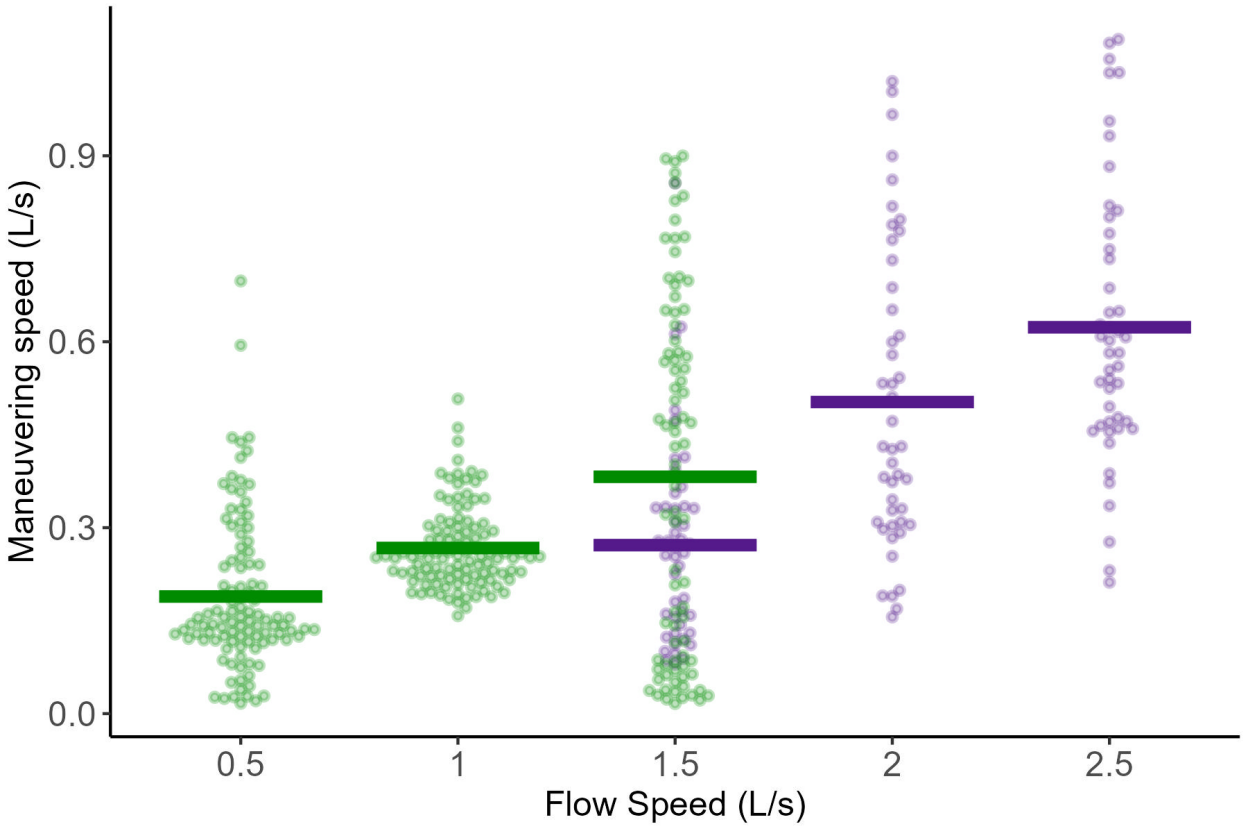

Figure 3: Maneuvering speed increased with flow speed. Color denotes individual. Lines represent means within groups.

As flow speed increased, maneuvering speed also increased significantly (both $p < 0.001$) (Figure 3).

Heart rate and heart rate variability did not change much as bluegill swam more unsteadily

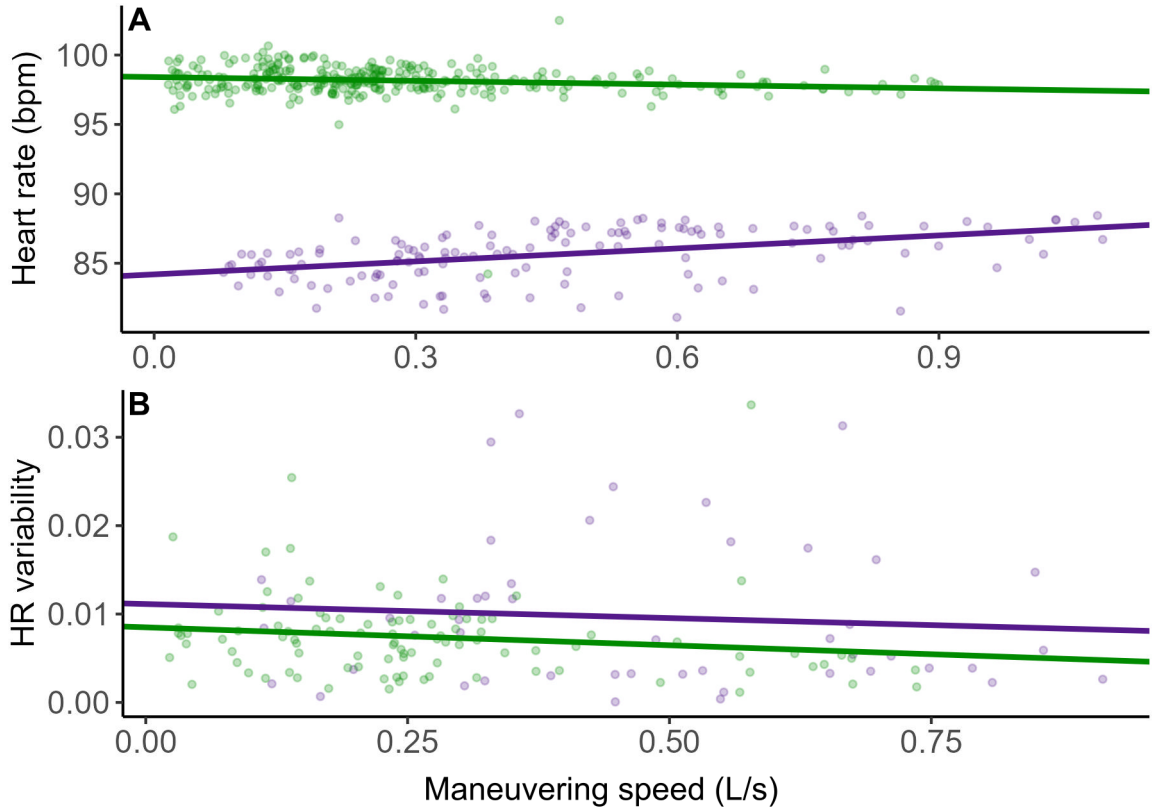

Figure 4: Heart rate (A) and heart rate variability (B) did not significantly change with flow speed. Color denotes individual. Lines represent linear fits of the regression of heart rate or heart rate variability on maneuvering speed.

Neither individual significantly changed their heart rate with swimming speed ($p = 0.426$ for the individual coded with purple points and $p = 0.430$ for the individual coded with green points), nor did they significantly change their heart rate variability with maneuvering speed ($p = 0.577$ for the individual coded with purple points and $p = 0.098$ for the individual coded with green points) (Figure 7).

Day long acclimation

As flow speed increased, heart rate increased while heart rate variability stayed the same

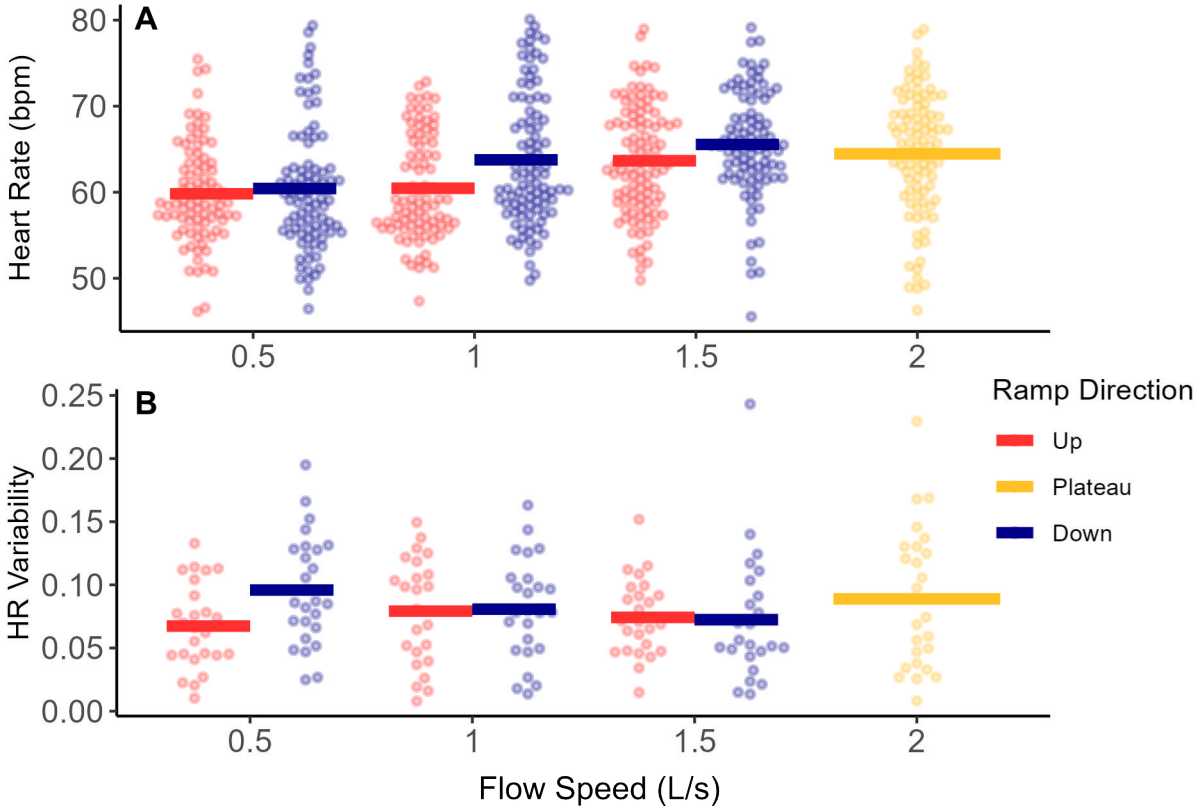

Figure 5: (A) Heart rate increased with flow speed during the ramp up (in red) and decreased with flow speed during the ramp down (in blue). (B) Heart rate variability did not change much with flow speed. Color denotes ramp direction. Lines represent means within groups. The 2.0 speed is shown in both panels because it is the plateau speed.

As the bluegill swam at higher flow speeds on the ramp up, its heart rate increased significantly, from 59.8 $\pm$ 5.7bpm to 64.5 $\pm$ 7.1bpm ($p < 0.001$) (Figure 5). On the ramp down, the bluegill significantly decreased its heart rate, going from 64.5 $\pm$ 7.1bpm to 60.4 $\pm$ 7.3bpm ($p < 0.001$). The bluegill did not change its heart rate variability on either the ramp up ($p = 0.591$), or the ramp down ($p = 0.454$) (Figure 5). Additionally, the bluegill had a significantly higher heart rate on the ramp down compared to the ramp up ($p < 0.001$), but did not have a significantly different heart rate variability between the two ramp directions ($p = 0.871$).

The bluegill swam more unsteadily as flow speed increases

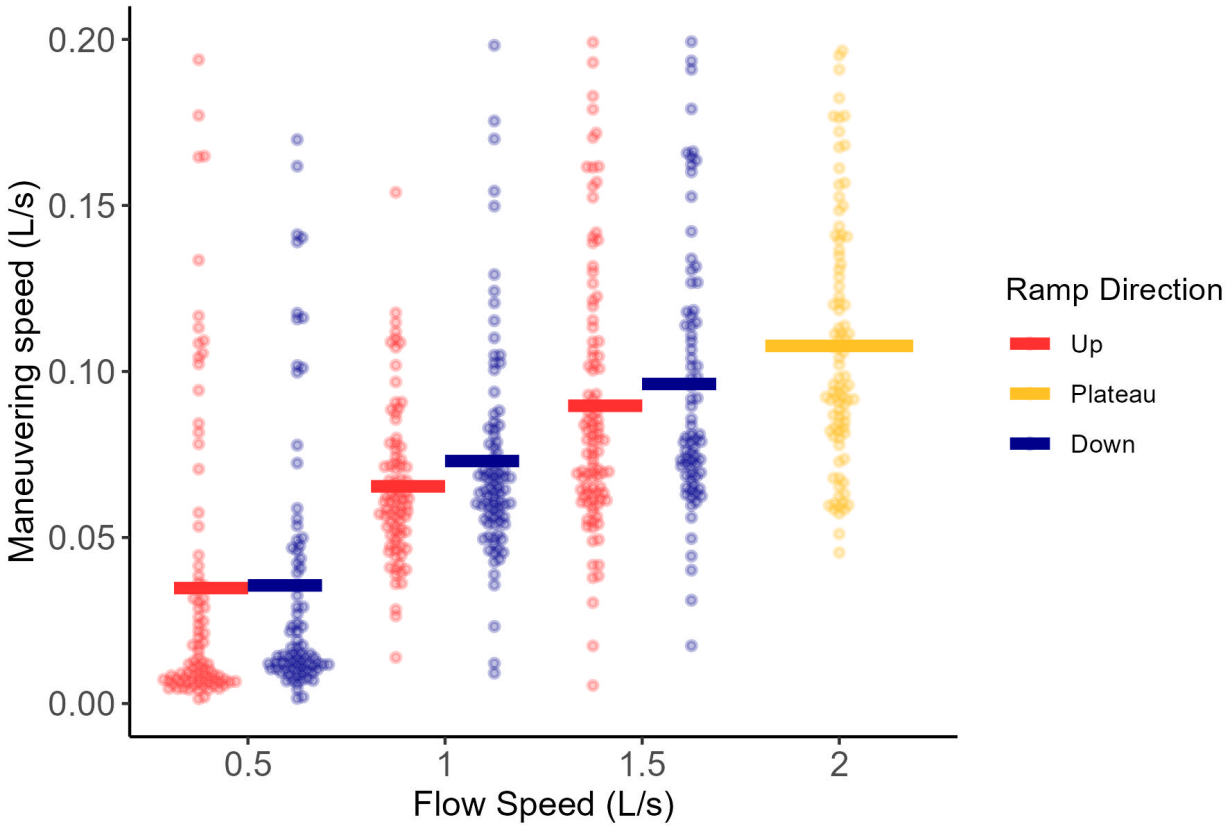

Figure 6: Maneuvering speed increased with flow speed. Color denotes ramp direction. Lines represent means within groups.

The bluegill maneuvered significantly faster as flow speed ramped up and significantly slower as flow speed ramped down (both $p < 0.001$) (Figure 6).

But neither heart rate nor heart rate variability changed as the bluegill swam more unsteadily

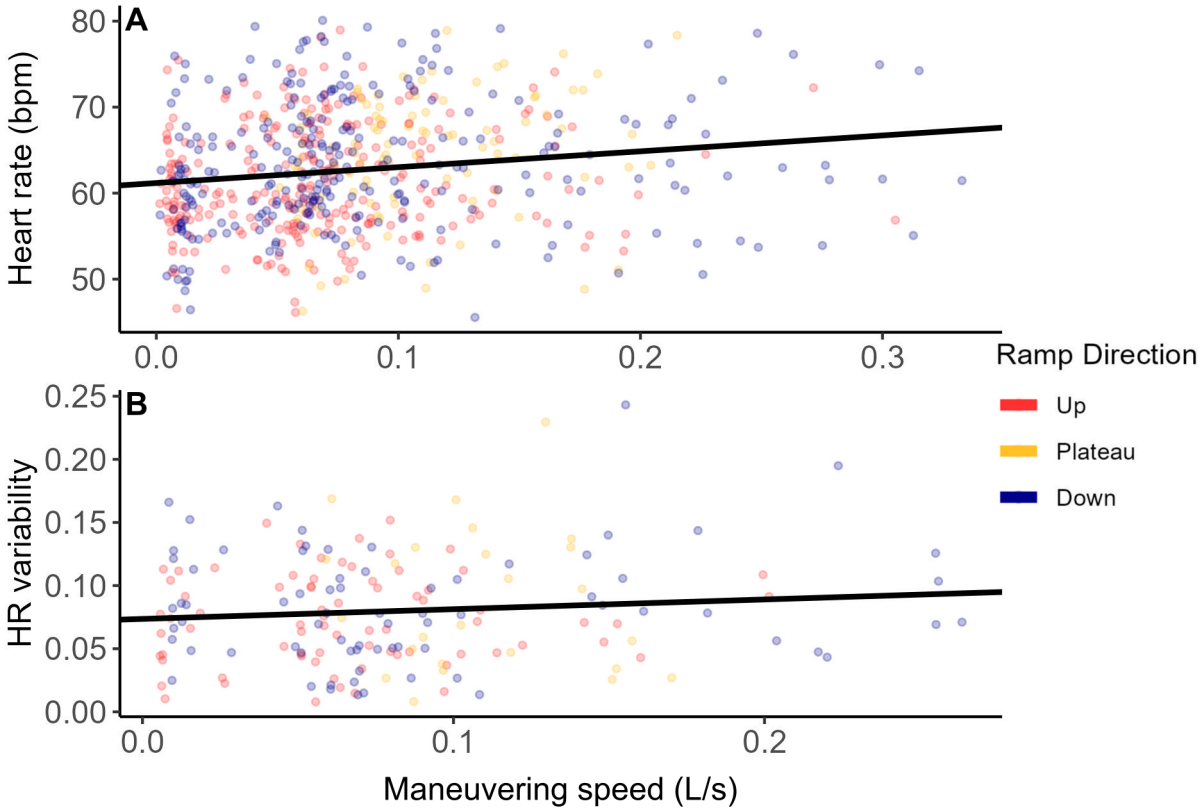

Figure 7: (A) Heart rate remained constant as maneuvering speed increased. (B) Heart rate variability also remaind constant as maneuvering speed increased. Color denotes individual. The lines represent linear fits of the regression of heart rate or heart rate variability on maneuvering speed.

The bluegill did not significantly change its heart rate with maneuvering speed ($p = 0.598$), nor did it significantly change its heart rate variability ($p = 0.127$) (Figure 7).

Discussion

Stress impacted the results

Overall, while we measured a consistent increase in heart rate with swimming speed after a day-long acclimation, we did not record a clear pattern from the other two individuals that had a much shorter acclimation period. Specifically, the two individuals without a long acclimation period had different results (Figure 2 A). In contrast, the day-long acclimation individual consistently increased heart rate at higher swimming speeds on the ramp up and consistently decreased heart rate at lower swimming speeds on the ramp down (Figure 5). This was consistent with our hypothesis. This may be because the non-acclimated fish had elevated heart rates at all speeds, likely from the stress of the surgery. In fact, the highest mean heart rate from the day-long acclimation individual occurred at the 2 L/s plateau, and was still less than 77% of the rate of the non-acclimated individuals' lowest mean heart rates. Furthermore, one of the individuals had a high mean heart rate that was only about 30 BPM below those of tuna, who are notorious for increasing their heart rate during fast bouts of swimming (Clark et al., 2008). We believe that because the fish had such elevated heart rates, they were near their maximum rates, reducing any chance for variation due to swimming speed.

The elevated heart rate in the non-acclimated individuals was likely driven by the sympathetic nervous systems dominating their parasympathetic ones, elevating their heart rate. Previous work has found that with invasive techniques, fish heart rate can double (Evans and Claiborne, 2005) and their heart rate variability decreases. Our results seem to show a similar effect. Furthermore, we hypothesize that the sympathetic nervous system was the driver because heart rate variability was so low (Jerem and Romero, 2023). This point is supported by the heart rate variability. Heart rate variability did not vary significantly with swim speed for any of the trials. However, the day-long acclimated individual had much higher heart rate variability than either of the no-acclimation individuals (about five times as high). As low heart rate variability has previously been shown to be a hallmark of stress in animals, we further take this to be evidence that the observed lack of changes in heart rate at higher speeds was due to an elevated heart rate caused by stress and mediated by the sympathetic nervous system.

When we gave the fish time to acclimate post-surgery, we observed heart rate changing as we predicted

Focusing on the day-long acclimation trial, we observed that heart rate could indeed play an important role in quantifying the energetics of bluegill on a smaller time scale. In less than half an hour, the bluegill significantly increased and then significantly decreased its heart rate according with swim speed, with each of the 7 flow speeds needing just a few minutes to produce usable data. This avoided the challenge of accurately measuring metabolic rate through dissolved oxygen concentration in the water column as less time is needed (Korsmeyer et al., 2002). This suggests that if we want to understand kinematics and metabolic costs on a smaller time scale, we can measure heart rate for bluegill.

However, it may still take several minutes for heart rate to reflect swimming energetics. We hoped that heart rate might increase and decrease to reflect even short-term variability in swimming speed, which we called maneuvering speed. However, we did not observe any significant links between maneuvering speed and heart rate. While this was disappointing because it showed that we cannot quantify the kinematics of these maneuvering events on the small time scale in which they occur, it could indicate that these events were indeed too small and too irregular for the heart to have the time and ability to respond to. Measurements of lactic acid concentration or of post exercise oxygen uptake could help us understand if this was indeed the case.

Future Directions

We do have data from the day-long acclimation trial that seems to show the effect that we had predicted. However, we still only have data from one fish, making it difficult to definitively answer our initial question. Therefore, an obvious future direction would be to add more individuals specifically a the day-long acclimation period to give them time to recover from the stress of their surgery.

Additionally, while we used heart rate as a proxy for energetic expenditure, we would need to simultaneously measure dissolved oxygen and heart rate to statistically connect the two. This would enable us to calibrate the changes in heart rate relative to changes in energetics.

Finally, while we found that heart rate is linked to swimming speed in bluegill, we were not able to quantify the other component of cardiac output: stroke volume. In the day-long acclimation trial, we observed that changes in heart rate corresponded to changes in swimming speed, however it may still be important to

quantify changes in stroke volume. Stroke volume is difficult to quantify as it involves the implantation of various instruments that were not available for use in our experiments. For example, Graham and Cooke (2008) implanted a flow probe into largemouth bass (*Micropterus salmoides* at the time) who were 27cm in length on average, more than double the average length of the fish we tested.

Contributions

For this study, Brendan Kelleher performed the surgery while I assisted, we both collected the kinematics data, and I analyzed all of the data.

References

Bates, D., Mächler, M., Bolker, B. and Walker, S. (2015). Fitting linear mixed-effects models using Lme4. *Journal of Statistical Software* **67**, 1–48. doi: 10.18637/jss.v067.i01.

Bennett, A. F. (2013). Chapter 10. Energetics and Locomotion. In *Functional Vertebrate Morphology*, pp. 173–184. Harvard University Press.

Bezucha, G. R., Lenser, M. C., Hanson, P. G. and Nagle, F. J. (1982). Comparison of hemodynamic responses to static and dynamic exercise. *Journal of Applied Physiology* **53**, 1589–1593. doi: 10.1152/jappl.1982.53.6.1589.

Biewener, A. A. and Wilson, A. M. (2025). Integrating biomechanics, energetics and ecology perspectives in locomotion. *Journal of Experimental Biology* **228**, jeb249585. doi: 10.1242/jeb.249585.

Brown, J. H., Gillooly, J. F., Allen, A. P., Savage, V. M. and West, G. B. (2004). Toward a metabolic theory of ecology. *Ecology* **85**, 1771–1789. doi: 10.1890/03-9000.

Clark, T. D., Taylor, B. D., Seymour, R. S., Ellis, D., Buchanan, J., Fitzgibbon, Q. P. and Frappell, P. B. (2008). Moving with the beat: Heart rate and visceral temperature of free-swimming and feeding bluefin tuna. *Proceedings of the Royal Society B: Biological Sciences* **275**, 2841–2850. doi: 10.1098/rspb.2008.0743.

Dunnington, D., Thorne, B. and Hernangómez, D. (2023). Ggspatial: Spatial data framework for Ggplot2. url: https://cran.r-project.org/web/packages/ggspatial/index.html.

Evans, D. H. and Claiborne, J. B. (2005). *The Physiology of Fishes, Third Edition*. CRC Press. url: https://books.google.com?id=lBltoKDaBVEC.

Fox, J. and Weisberg, S. (2019). *An R Companion to Applied Regression*. Third edition. Thousand Oaks CA: Sage.

Full, R. J., Zuccarello, D. A. and Tullis, A. (1990). Effect of variation in form on the cost of terrestrial locomotion. *Journal of Experimental Biology* **150**, 233–246. doi: 10.1242/jeb.150.1.233.

Graham, A. L. and Cooke, S. J. (2008). The effects of noise disturbance from various recreational boating activities common to inland waters on the cardiac physiology of a freshwater fish, the largemouth bass (*Micropterus salmoides*). *Aquatic Conservation: Marine and Freshwater Ecosystems* **18**, 1315–1324. doi: 10.1002/aqc.941.

Hedrick, T. L. (2008). Software techniques for two- and three-dimensional kinematic measurements

of biological and biomimetic systems. *Bioinspiration & Biomimetics* **3**, 034001. doi: 10.1088/1748-3182/3/3/034001.

Jerem, P. and Romero, L. M. (2023). It's cool to be stressed: Body surface temperatures track sympathetic nervous system activation during acute stress. *Journal of Experimental Biology* **226**, jeb246552. doi: 10.1242/jeb.246552.

Kay, M. (2024). Ggdist: Visualizations of distributions and uncertainty in the grammar of graphics. *IEEE Transactions on Visualization and Computer Graphics* **30**, 414–424. doi: 10.1109/TVCG.2023.3327195.

Kay, M. and Wiernik, B. M. (2024). Ggdist: Visualizations of distributions and uncertainty. url: https://cloud.r-project.org/web/packages/ggdist/index.html.

Korsmeyer, K. E., Steffensen, J. F. and Herskin, J. (2002). Energetics of median and paired fin swimming, body and caudal fin swimming, and gait transition in parrotfish (*Scarus schlegeli*) and triggerfish (*Rhinecanthus aculeatus*). *Journal of Experimental Biology* **205**, 1253–1263. doi: 10.1242/jeb.205.9.1253.

Lavoisier, A.-L. de (1865). *Oeuvres de Lavoisier*. Imprimerie Impériale. url: https://books.google.com?id=5jYkK58_eMwC.

Li, S. (1987). Energy structure and efficiency of a typical Chinese integrated fish farm. *Aquaculture* **65**, 105–118. doi: 10.1016/0044-8486(87)90255-9.

Marvin, D. E. and Heath, A. G. (1968). Cardiac and respiratory responses to gradual hypoxia in three ecologically distinct species of fresh-water fish. *Comparative Biochemistry and Physiology* **27**, 349–355. doi: 10.1016/0010-406X(68)90777-9.

McAllister, M. J., Chen, A. and Selinger, J. C. (2025). Behavioural energetics in human locomotion: How energy use influences how we move. *Journal of Experimental Biology* **228**, jeb248125. doi: 10.1242/jeb.248125.

Moves, C. D. and West, T. G. (1995). Chapter 16: Exercise Metabolism of Fish. In *Biochemistry and Molecular Biology of Fishes* (ed. Hochachka, P. W. and Mommsen, T. P.), pp. 367–392. Elsevier. doi: 10.1016/S1873-0140(06)80019-6.

Nelson, J. A. (2016). Oxygen consumption rate v. Rate of energy utilization of fishes: A comparison and brief history of the two measurements. *Journal of Fish Biology* **88**, 10–25. doi: 10.1111/jfb.12824.

Pardee, H. E. B. (1914). Form of the electrocardiogram: Diagnostic significance of its variations. *Journal of the American Medical Association* **LXII**, 1311–1317. doi: 10.1001/jama.1914.02560420017009.

Randall, D. (1982). The control of respiration and circulation in fish during exercise and hypoxia. *Journal of Experimental Biology* **100**, 275–288. doi: 10.1242/jeb.100.1.275.

Richardson, N., Cook, I., Crane, N., Dunnington, D., François, R., Keane, J., Moldovan-Grünfeld, D., Ooms, J., Wujciak-Jens, J. and Apache Arrow (2025). Arrow: Integration to 'Apache' 'Arrow'. url: https://CRAN.R-project.org/package=arrow.

Schindelin, J., Arganda-Carreras, I., Frise, E., Kaynig, V., Longair, M., Pietzsch, T., Preibisch, S., Rueden, C., Saalfeld, S., Schmid, B., et al. (2012). Fiji: An open-source platform for biological-image analysis. *Nature Methods* **9**, 676–682. doi: 10.1038/nmeth.2019.

Shiels, H. A., Calaghan, S. C. and White, E. (2006). The cellular basis for enhanced volume-modulated cardiac output in fish hearts. *The Journal of General Physiology* **128**, 37–44. doi: 10.1085/jgp.200609543.

Smith, G. D. (1985). *Numerical Solution of Partial Differential Equations: Finite Difference Methods*. Clarendon Press.

Spitzer, K. W., Marvin, D. E. and Heath, A. G. (1969). The effect of temperature on the respiratory and cardiac response of the bluegill sunfish to hypoxia. *Comparative Biochemistry and Physiology* **30**, 83–90. doi: 10.1016/0010-406X(69)91299-7.

West, J. B. (2013). The collaboration of Antoine and Marie-Anne Lavoisier and the first measurements of human oxygen consumption. *American Journal of Physiology-Lung Cellular and Molecular Physiology* **305**, L775–L785. doi: 10.1152/ajplung.00228.2013.

Wickham, H., Averick, M., Bryan, J., Chang, W., McGowan, L. D., François, R., Grolemund, G., Hayes, A., Henry, L., Hester, J., et al. (2019). Welcome to the Tidyverse. *Journal of Open Source Software* **4**, 1686. doi: 10.21105/joss.01686.

Zhang, Y. and Lauder, G. V. (2024). Energy conservation by collective movement in schooling fish. *eLife* **12**, RP90352. doi: 10.7554/eLife.90352.

Chapter 3: Braking is about balance in addition to drag

Introduction

While a lot of research has focused on steady swimming in fishes, fishes regularly speed up, slow down, and maneuver during everyday life. Researchers have carefully documented accelerations during C start turns (Domenici and Hale, 2019), and have conducted some research on rapid deceleration (Flammang and Lauder, 2009; Geerlink, 1987; Higham, 2007; Higham et al., 2005; Hu et al., 2007; Jayne et al., 1996) and turning (Dabiri et al., 2020; Downs et al., 2023; Porter et al., 2009), but work still remains to quantify unsteady behaviors. In particular, relatively little is known about more routine decelerations and, overall, how fish modulate their speed. This led me to ask the question: how do fish slow down sub-maximally and how do they change their kinematics with the speed of the slowdown? To answer this question, I designed an experiment that motivates bluegill sunfish (*Lepomis macrochirus*) to slow down at a controlled rate, allowing me to quantify the kinematics for decelerations of different rates.

Much of what we know about braking in fishes comes from research on predator-prey interactions, during which precise changes in speed can prove critical to a successful strike on prey or food (Geerlink, 1987 for examples; see Higham, 2007; Higham et al., 2005; Webb, 1984). During feeding strikes, bluegill in particular heavily rely on their pectoral fins, rapidly extending them to slow themselves down (Drucker and Lauder, 2002; Harris, 1938; Higham, 2007; Higham et al., 2005; Jayne et al., 1996). Other species also use their pectoral fins during braking, including trout (Drucker and Lauder, 2002; Drucker and Lauder, 2003; Gibbs et al., 2024; Webb, 1984), bass (Higham, 2007; Webb, 1984), goldfish (Bainbridge, 1963; Webb, 2002), silver dollars (Webb, 2002), cod (Geerlink, 1987; Videler, 1981), tiger musky (Webb, 1984), mackerel (Geerlink, 1987), and saithe (Geerlink, 1987). In addition to using their pectoral fins, bluegill also use their caudal

fins to brake, modulating the shape and area of the fin during maneuvers (Flammang and Lauder, 2009). Specifically, bluegill will form an "S" shape with their tails while pushing away their dorsal and ventral edges in opposite directions to produce additional drag (Flammang and Lauder, 2009). Goldfish, on the other hand, will move their caudal fin such that it is transverse to the direction of motion (Bainbridge, 1963). Other fins are also known to contribute to braking and maneuvering. Specifically, in bluegill, the dorsal fin actively extends to one side during a brake, adding to the total drag and helping the fish slow down (Jayne et al., 1996). Additionally, the dorsal fin is active during turning maneuvers, as observed by Drucker and Lauder (2001; 2005), Lauder and Drucker (2004), and Standen and Lauder (2005; 2007). The dorsal fin can produce high forces during steady swimming (Tytell, 2006), which makes it seem likely that it might be involved in deceleration as well. The pelvic fins may also contribute to deceleration, but their contributions are less well understood. Harris (1938) found that pelvic fins may work in concert with pectoral fins to help fish brake, and Standen (2008) found that pelvic fins are used by maneuvering trout, but their overall function is more uncertain.

However, many of these results came from experiments on predator-prey interactions which may not reflect the strategies that fish use for more gradual gliding deceleration. Gliding decelerations, in which a fish stops swimming and coasts, have been studied as part of kick-and-glide behavior, where fish will kick and propel themselves forwards before gliding and losing speed over a short time window (Flammang and Lauder, 2009; Jayne et al., 1996; Videler, 1981; Webb and Fairchild, 2001). Videler (1981) also explicitly studied gliding separate from maximal braking, finding that cod extend their pectoral fins and flare their dorsal and anal fins to slow themselves down.

My study focused on intermediate decelerations – stronger than gliding decelerations but weaker than rapid braking during feeding strikes – where fish must actively change their swimming behavior to slow down. This allowed me to ask: how do fish brake at high speeds and how does that change at lower speeds?

To quantify fin use, I used a modified equation to quantify the component of the drag forces on each fin (D_f). This is similar to Vogel (1996):

$$D_f = \frac{1}{2}\rho C_D S_f (U_f + U_w)^2 \tag{0.1}$$

where ρ is the density of water (1 g cm^{-3}), C_D is the drag coefficient, S_f is the surface area in the frontal plane for each fin, U_f is the mean velocity in the forward direction of all points bounding that fin, and U_w

is the velocity of the oncoming flow. There is not a good way to estimate the drag coefficient for moving deforming panels like fins, so I left it out in my estimations. Furthermore, since density does not vary, I also left out that quantity. Because the fish were of different lengths, I finally controlled for length and was left with

$$F_f = \frac{1}{2} S_{fn} (U_{fn} + U_{wn})^2 \tag{0.2}$$

where F_f is fin force, S_{fn} is the fin surface area normalized by dividing by bodylength squared, U_{fn} is the normalized fin velocity in L/s, and U_{wn} is the normalized flow speed in L/s. This gave me the units of $\frac{L^4}{s^2}$.

In addition to quantifying fin force in this manner, my experiments characterized braking behavior at a range of speeds. I hypothesized that fin use would vary with brake speed, predicting that at lowest speeds, fish would not employ many of their fins, while at medium speeds, they would start to use their pectoral and caudal fins, before employing their dorsal, anal, and pelvic fins at the highest speeds because the pectoral fins alone are not sufficient to brake rapidly.

Methods

Setup

For a complete description of the experimental setup, see Chapter 4 (currently in review for publication). Briefly, I used a device consisting of a Teknic ClearPath-SDSK servo motor (part number CPM-SDSK-2310S-EQN) mounted to an 80/20 chassis with an attached acrylic flow-through chamber that is 20.3cm wide by 30.5cm long and 7.6cm tall. An Arduino Uno sent signals to the servo motor to drive the device forwards and backwards at varying programmable speeds. For this experiment I programmed the motion such that the car drove in a sinusoid with its peak speed occurring at the middle of its progress along the track.

For all trials, I ran the flow tank with a constant speed of 1.5 Ls^{-1}, with the device running on top of the tank with a peak speed, in addition to that of the flow tank, of either 1 body length per second (Ls^{-1}; referred to as "slow"), 2 Ls^{-1} (medium), or 3 Ls^{-1} (fast) for each individual. With the flow speed, the slow, medium, and fast trials thus caused fish to swim at a peak speed of 2.5 BL s^{-1}, 3.5 Ls^{-1}, and 4.5 Ls^{-1}, respectively,

decelerating in all cases to 1.5 Ls^{-1} Some individuals were unable to swim at the highest peak speed, so for them, I collected data only at slow and medium speeds.

Filming and digitizing

I collected kinematic data with two Phantom Miro M340 high-speed cameras and one Phantom Miro M120 high-speed camera. All videos were filmed at 100 frames per second. To best quantify the behavior of all fins associated with braking, I used two different camera setups: one with two lateral cameras and one ventral camera (two lateral setup), and one with two ventral cameras and one lateral camera (two ventral setup). For the analyses, I used either the two lateral setup with only the two lateral cameras or the two ventral setup with only the two ventral cameras. Most of the analyses were conducted using the two lateral camera setup, except that I used the two ventral setup to quantify the behavior of the pectoral fins.

I used the corners of the device to define the axes which I digitized using DLTdv (Hedrick, 2008). I defined the planes such that the X vector points directly against oncoming flow, the Y vector points laterally to the fish's left out of the tank, and the Z vector points directly up. The YZ and XZ planes are important since the YZ plane is the plane that is directly orthogonal to flow and the XZ plane is the vertical plane in line with the flow. To digitize the videos, I used SLEAP (Pereira et al., 2022) to identify points and a ChArUco board (Garrido-Jurado et al., 2014) with the aniposelib package from the Anipose toolkit (Karashchuk et al., 2021) along with custom code to calibrate the filmed space.

Camera setup

The two lateral setup featured one lateral camera orthogonal to the viewing pane and one lateral camera that was off axis and towards the rear of the fish. I digitized 25 points on the fish in each view (Figure 1) A, C, including the snout; the left eye; the bases of soft dorsal fin; three points along the soft dorsal fin; the bases of the anal fin; three points along the anal fin; the base of the left pelvic fin; the tip of the left pelvic fin; the most dorsal point of the left pelvic fin; the top, middle, and bottom of the border between the peduncle and the caudal fin; and 5 points along the edge of the caudal fin.

For the second setup, I used one ventral camera orthogonal to the bottom of the flow tank and one ventral camera off axis to the first camera and positioned towards the snout of the fish (Figure 1) B, D. For this setup, because the pectoral fins are difficult to see, I used SLEAP to predict automatically before manually

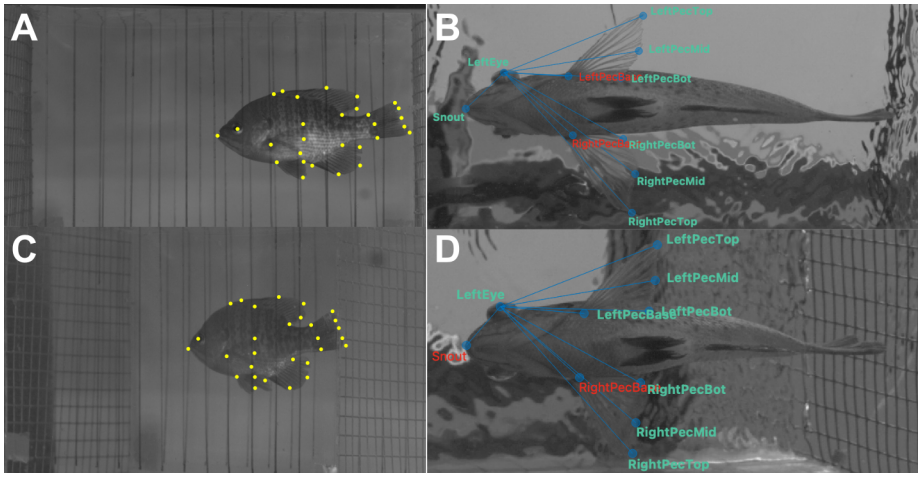

Figure 1: (A, C) Stills from videos collected using the two lateral setup using a (A) lateral orthogonal and (C) lateral off axis camera. (B, D) Stills from videos collected using the two ventral setup using a (B) ventral orthogonal and (D) ventral off axis camera. Yellow points in A and C are SLEAP predicted points. Blue points in B and D are SLEAP predicted points with blue lines denoting the skeleton used during training. Point names in red are automatically predicted points, while point names in light blue are manually digitized points

correcting every relevant point. For 5 individuals, I used all frames leading up to the point at which it appeared that the fish had stopped swimming forwards, only digitizing frames in which I could see the pectoral fins (i.e. when they were not pressed against the body).

Data smoothing and selection

For the lateral setup, I smoothed the x, y, and z locations of all digitized points individually using a 9th order low pass Butterworth filter with a cut off frequency of 5 Hz. For the ventral setup, since I only digitized frames in which the fish was using its pectoral fins, I smoothed the x, y, and z locations of all points individually with a 9th order low pass Butterworth filter with a cut off frequency of 10 Hz, filling in the gaps between pectoral fin strokes with a linear interpolation. Interpolated values were only used to prevent edge effects in the filter and were removed after smoothing.

To select the relevant portion of each trial, I then estimated snout velocity by numerically differentiating the position with respect to time using the central difference (Smith, 1985). I then only analyzed portions of each trial bounded by its maximum velocity, and the point at which it reaches a velocity of zero in the laboratory frame of reference (the full brake).

For much of the analysis, I then divided each trial into five segments with equal duration and took either

the mean or sum during each segment. To account for individual differences in size, I divided distance or its derivatives by each individual's maximum length (L).

Overall deceleration

I estimated each trial's average deceleration (α_{tot}) as

$$\alpha_{tot} = \frac{v_{max} - v_{min}}{t_{max} - t_{min}} \tag{0.3}$$

where v_{max} and v_{min} are the maximum and minimum velocity the fish reached and t_{max} and $tmin$ are the time where the fish reached its maximum and minimum velocities. I then used these estimates to redistribute the behaviors into slow, medium, and fast categories, dividing them into thirds. With this method, the slow brakes had an overall deceleration ranging from -0.2 to -0.5 Ls^{-2}, the medium brakes had an overall deceleration ranging from -0.5 to -1.1 Ls^{-2}, and the fast brakes had an overall deceleration ranging from -1.1 to -2 Ls^{-2}.

Dataset

Data are from 6 bluegill (*Lepomis macrochirus*) collected from either White Pond or Walden Pond in Concord, Massachusetts. I used a seine net along the shores of these ponds to collect the fish before transferring them to an aquaculture facility where they were kept in 10 gallon tanks at a controlled temperature of 20 degrees Celsius until used for experiments. I collected the fish with scientific collection permits 090.22SCF, 146.23SCF, 158.19SCF, and 174.20SCF, and kept them according to protocols M2018-103, M2021-99, and M2024-57.

All experimental procedures and animal handling protocols were approved by the Tufts University Institutional Animal Care and Use Committee.

Table 1: Trial breakdown for lateral setup fins analysis. Numbers represent number of trials per car speed.

Individual	Slow	Medium	Fast
BG63	9	4	0
BG64	8	10	0
BG65	9	9	9
BG81	0	8	8
BG82	0	6	1

For each individual I tested them at speeds as high as the fish could maintain, with the goal of testing each fish at peak speeds of 2.5, 3.5, and 4.5 Ls^{-1} (individual speed + flow speed). Not all individuals could swim and produce usable data at all speeds (see Table 1), but I still included all of them in the analysis.

Table 2: Trial breakdown for lateral setup fins analysis. Numbers represent number of trials per brake speed as defined by each trial's overall deceleration.

Individual	Slow	Medium	Fast
BG63	6	4	3
BG64	8	2	8
BG65	13	10	4
BG81	0	6	10
BG82	0	5	2

After redefining each brake according to its overall deceleration, I ended up with a dataset where each brake speed had 27 trials, but not all individuals were represented in all brake speeds because some individuals consistently had higher overall decelerations than others (see Table 2).

The ventral setup was digitized by hand for 5 individuals at every speed they were able to reach. Only one trial was used per individual per speed. Again, not all individuals were able to swim at all speeds, with two individuals being unable to reach the fastest speed of 4.5 Ls^{-1}.

Fins

For the analysis of fin area, I used the "polyarea" function from the pracma R package (Borchers, 2023) to estimate surface area projected onto the plane of interest, as defined by the polygon bounded by each fin's digitized points (see Figure 1 for specific points). I normalized fin area according to body length by dividing by the body length squared (L^2) in all cases. Finally, I estimated how much the fish abducted their caudal fins to increase dorsal-ventral height (flared) or adducted their caudal fins to decrease dorsal-ventral height (pinched) by summing the distance between each pair of points along its trailing edge, and then normalized relative to the maximum value measured for each individual.

I then used Equation 0.2 to estimate the forces contributed by each fin and estimate cumulative fin force by taking the cumulative integral of fin force over time using the "cumtrapz" function from the pracma package.

Body angle

To estimate body angle over time, I used methods similar to Fath and Tytell (2023). I used "atan2" to estimate the angle relative to the horizontal of the line defined by the snout point and the point on where the peduncle inserts into the main body of the fish.

Statistics

For all analysis and visualization, I used R version 4.4.1 with Rstudio version 2024.04.2 and the following packages: tidyverse version 2.0.0 (Wickham et al., 2019), lme4 version 1.1.35.5 (Bates et al., 2015), car version 3.1.2 (Fox and Weisberg, 2019), ggspatial version 1.1.9 (Dunnington et al., 2023), ggdist version 3.3.2 (Kay, 2024; Kay and Wiernik, 2024), and beeswarm version 0.4.0 (Eklund and Trimble, 2021).

When testing the effects of the "slow," "medium," and "fast" speed groups on the various variables, I used the "lmer" function from the lme4 package to run an ANOVA on a linear mixed-effects model with individual as a random effect and the speed group as the fixed effect. I then used "emmeans" (Lenth et al., 2025) to run pairwise comparisons to assess significance.

All means are provided plus or minus one standard deviation, unless otherwise noted.

Results

Brake Speeds

Overall, as the car caused fish to swim faster, it also caused them to brake more rapidly (Figure 2 A). Regardless of the brake speed category, as bluegill swam faster, they needed larger distances to stop (Figure 2 C; $p < 0.001$).

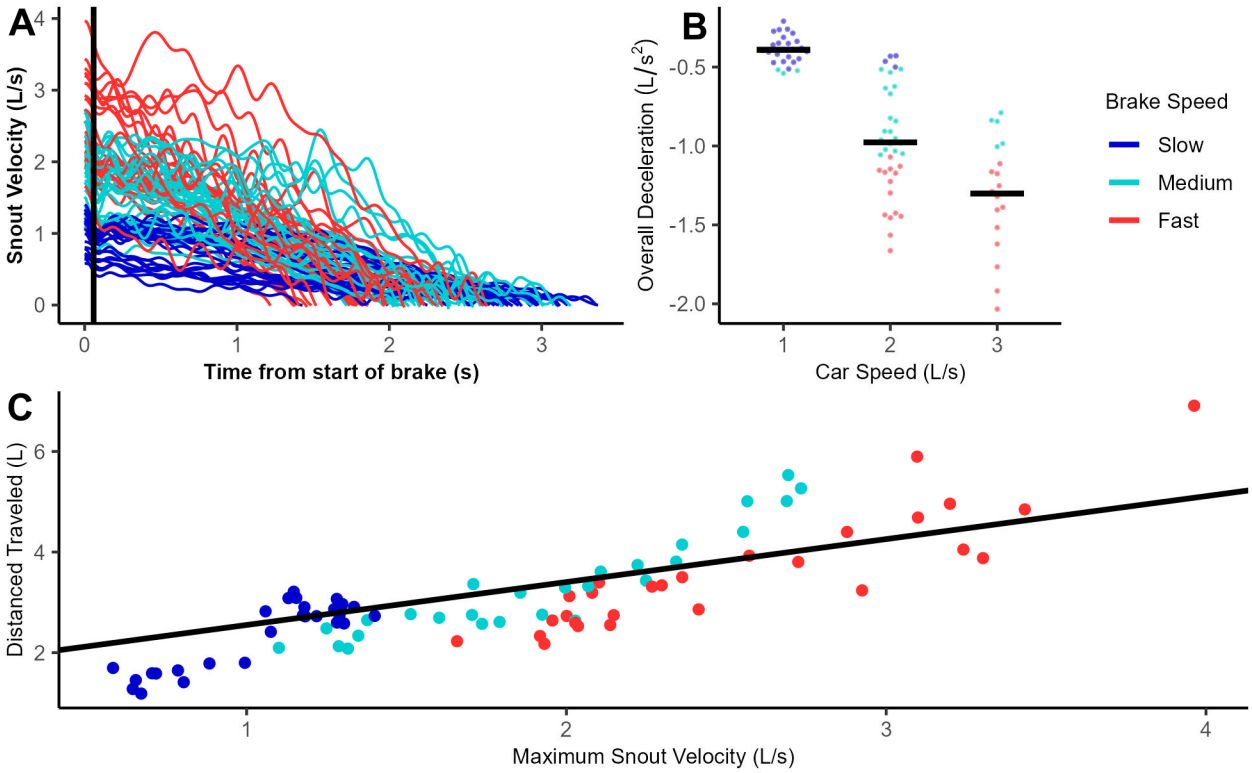

Figure 2: (A) Snout velocity normalized by bodylength over the course of the trial. The vertical black line represents the mean total braking time after prey capture reported by Flammang and Lauder in their study (Flammang and Lauder (2009)) (B) The overall deceleration during each trial as elicted by its respective brake speed. The black lines represent the means. (C) The maximum velocity reached compared with how much distance the fish needed to stop. In all cases, dark blue is slow brakes, light turquoise is medium brakes, and red is fast brakes.

Most of the braking force and differences in braking force came from the pectoral fins

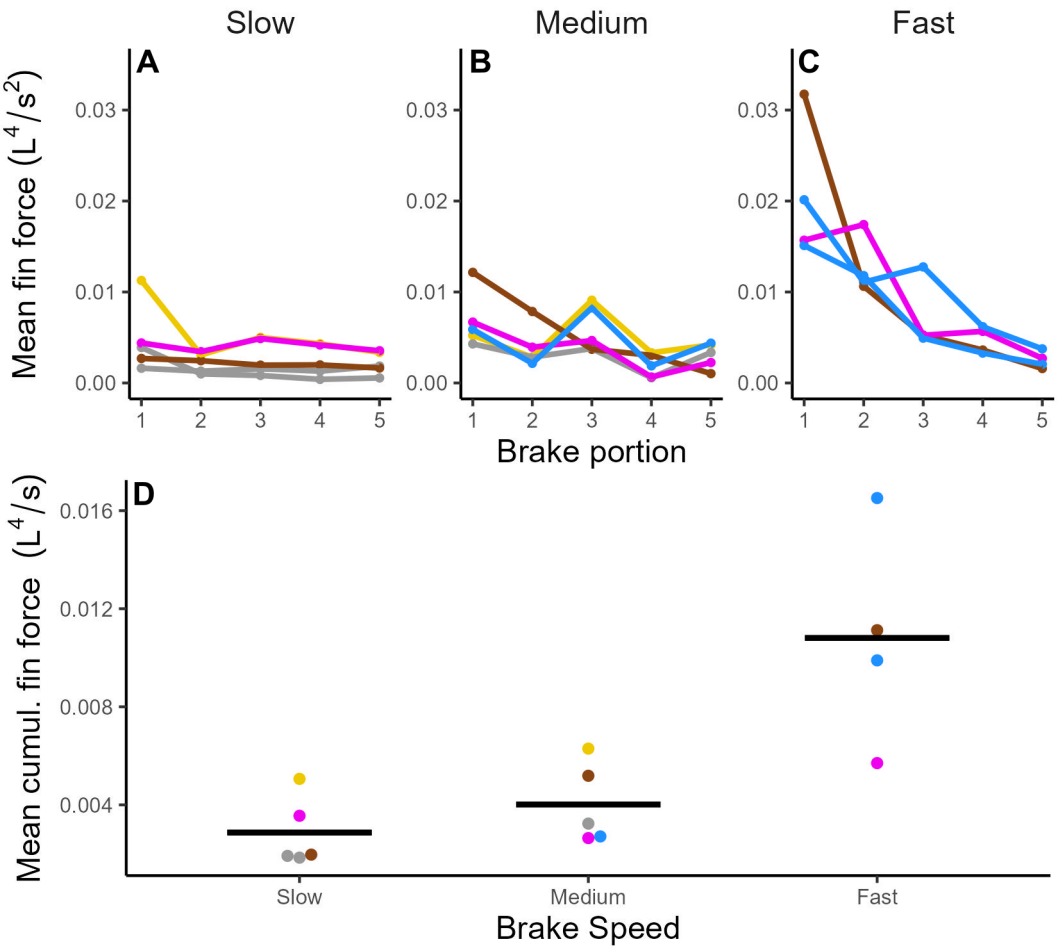

Figure 3: Fin forces from the pectoral fins. Body length normalized fin forces from both pectoral fins over time for slow (A), medium (B), and fast (C) brakes. (D) Total normalized fin force from both pectoral fins over time for slow, medium, and fast brakes. Colors denote individual and lines connect points from the same trial. Black lines in (C) are the means of each speed.

During braking, bluegill flared their pectoral fins (Figure 3 A, B, C). On average, they produced the most fin force at the beginning of each brake (brake portion 1) before decreasing their fin force production over time (Figure 3 A, B, C). During brake portion 1, the pectoral fins produced the least amount of force during slow brakes, more during medium brakes (1.4 times slow brakes), and the most during fast brakes (4.3 times slow brakes). All groups were significantly different from each other in terms of mean fin force with all $p < 0.001$.

Bluegill also generated more total fin force the faster they braked, generating the least during slow brakes, more during medium brakes (1.4 times slow brakes), and the most during fast brakes (3.8 times slow brakes).

They did not significantly increase total fin force between slow and medium brakes ($p = 0.728$), but did between slow and fast ($p < 0.001$) and medium and fast ($p < 0.001$) brakes.

Bluegill used their dorsal, anal, and pelvic fins more at higher speeds

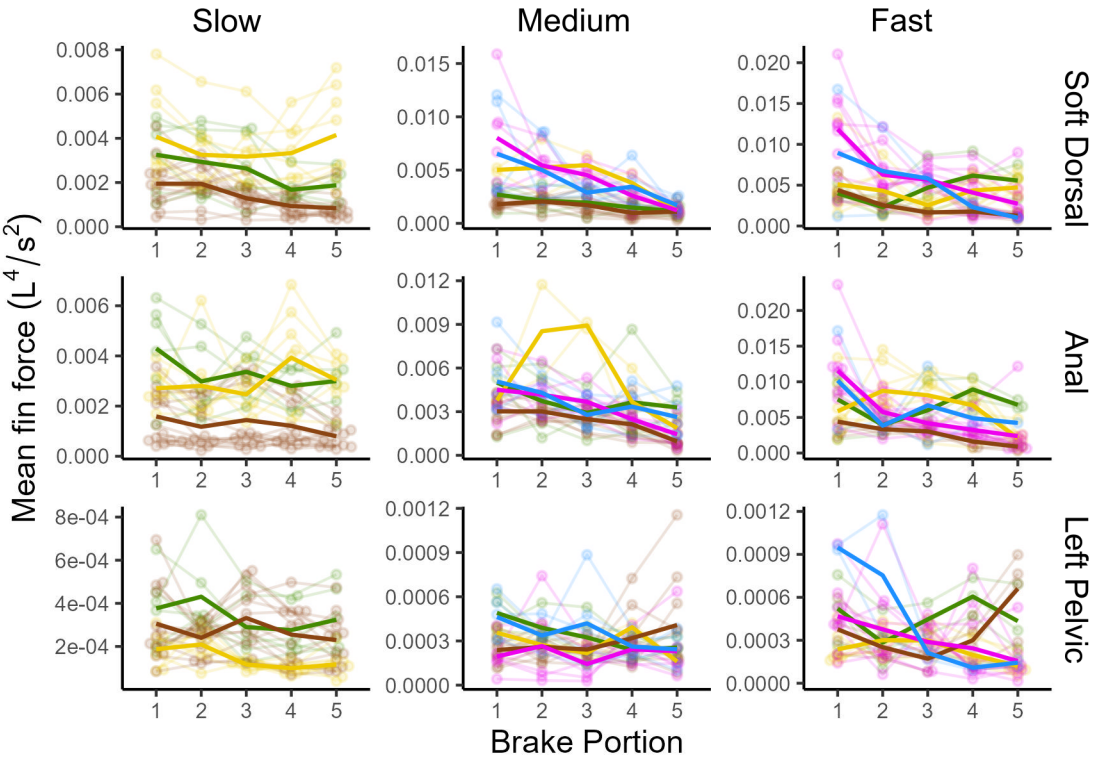

Figure 4: Forces from the dorsal, anal, and left pelvic fins over the time course of the brake for slow, medium, and fast brakes. Color represents individual with thin lines connecting trials and thick lines connecting individual means. Note the different y axis scales.

Bluegill produced the highest mean dorsal fin force in brake portion 1 at all speeds. The mean dorsal fin force in brake portion 1 was lowest in slow brakes, higher in medium brakes (1.5 times higher than in slow brakes), and highest in fast brakes (2.7 times higher than in slow brakes). Bluegill did not significantly increase their dorsal fin force between slow and medium brakes ($p = 0.963$), but did significantly increase fin force between medium and fast ($p = 0.001$) and slow and fast ($p < 0.001$) brakes.

Bluegill also produced the highest mean anal fin force in brake portion 1 at all speeds. The mean anal fin force in brake portion 1 was lowest in slow brakes, higher in medium brakes (1.6 times higher than in slow brakes), and highest in fast brakes (3.3 times higher than in slow brakes). Bluegill significantly increased their anal fin force between all speeds: between slow and medium brakes ($p = 0.009$), medium and fast brakes ($p < 0.001$), and slow and fast ($p < 0.001$) brakes.

Bluegill also produced the highest mean pelvic fin force in brake portion 1 at all speeds. The mean pelvic fin force in brake portion 1 was approximately equal in slow and medium brakes (fin force during medium

brakes was 1.1 times what it was during slow brakes), and was 1.5 times higher in fast brakes. Bluegill did not significantly increase their pelvic fin force between slow and medium brakes ($p = 0.486$), but did significantly increase fin force between medium and fast ($p = 0.011$) and slow and fast ($p < 0.001$) brakes.

Additionally, while bluegill produced comparable fin forces with their dorsal and anal fins, the fin forces they produced with their pelvic fins were about an order of magnitude lower.

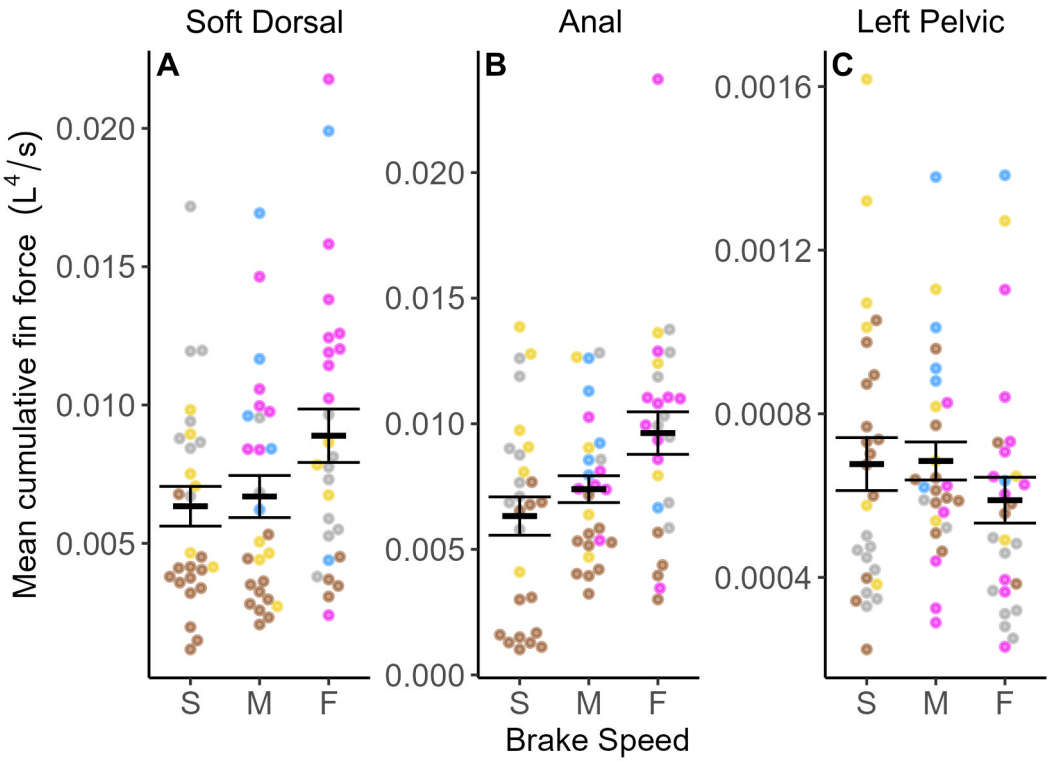

Figure 5: Total normalized impulse from the dorsal (A), anal (B), and left pelvic fins (C) for slow, medium, and fast brakes. Color represents individual with the black lines representing the means and standard deviations. Note the different y axis scales.

Bluegill did not significantly increase their total fin force between any speeds for either their dorsal fins ($p = 0.158$), anal fins ($p = 0.110$), or pelvic fins ($p = 0.460$), however, they tended to produce more total impulse with at higher brake speeds with their dorsal and anal fins. With their dorsal fins, bluegill produced the least amount of total impulse during slow brakes, more during medium brakes (1.1 times slow brakes), and more during fast brakes (1.4 times slow brakes). With their anal fins, they also produced the least amount of total impulse during slow brakes, more during medium brakes (1.2 times slow brakes), and the most during fast brakes (1.5 times slow brakes). With their pelvic fins, they produced similar total impulses during slow and medium brakes with medium brakes, and less impulse during fast brakes (0.9 times slow brakes.)

Bluegill flared their fins in the lateral plane over time

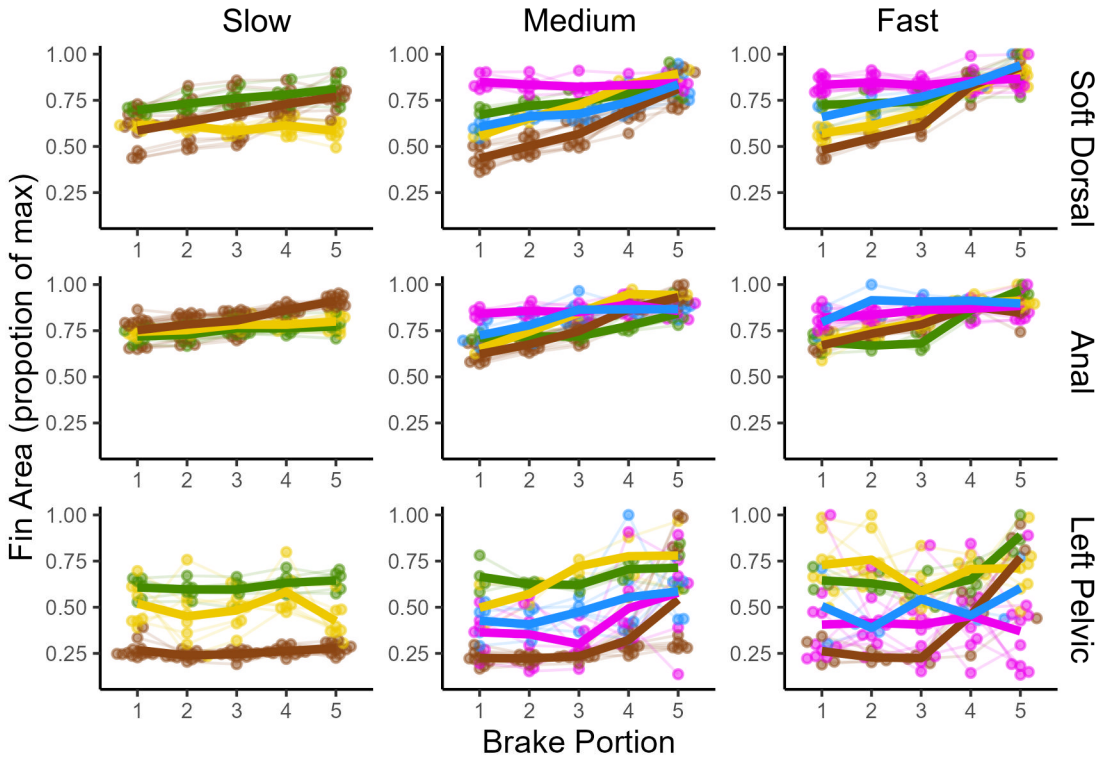

Figure 6: Normalized lateral surface area over the time course of the brake for slow, medium, and fast brakes. Color represents individual with thin lines connecting trials and thick lines connecting individual means.

For all speeds, bluegill tended to flare all their fins the most at the end of the brake (brake portion 5), with the exception of their pelvic fins during slow brakes, which did not change across all brake portions.

In brake portion 5, they flared their dorsal fins the least during slow brakes, more during medium brakes (1.2 times slow brakes), and the most during fast brakes (1.2 times slow brakes). They did not flare their dorsal fins significantly differently in medium brakes compared to slow brakes (0.738), but did flare their dorsal fins significantly more during fast brakes compared with medium brakes ($p = 0.0104$) and fast brakes compared with slow brakes ($p < 0.001$).

In brake portion 5, bluegill flared their anal fins similarly during all brakes, with the lowest being during slow brakes, followed by medium brakes (1.2 times slow brakes), followed by fast brakes (1.06 times slow brakes). They did not flare their dorsal fins significantly more or less across brake speeds ($p = 0.165$).

In brake portion 5, bluegill flared their pelvic fins the least during slow brakes, and similarly during medium and fast brakes (both of which are 1.5 times slow brakes). They flared their pelvic fins significantly

more during medium brakes than during slow brakes ($p < 0.001$) and during fast brakes than during slow brakes ($p < 0.001$), but did not flare their pelvic fins any differently between medium and fast brakes ($p = 0.120$).

Bluegill pinched their caudal fins, but individuals behaved differently

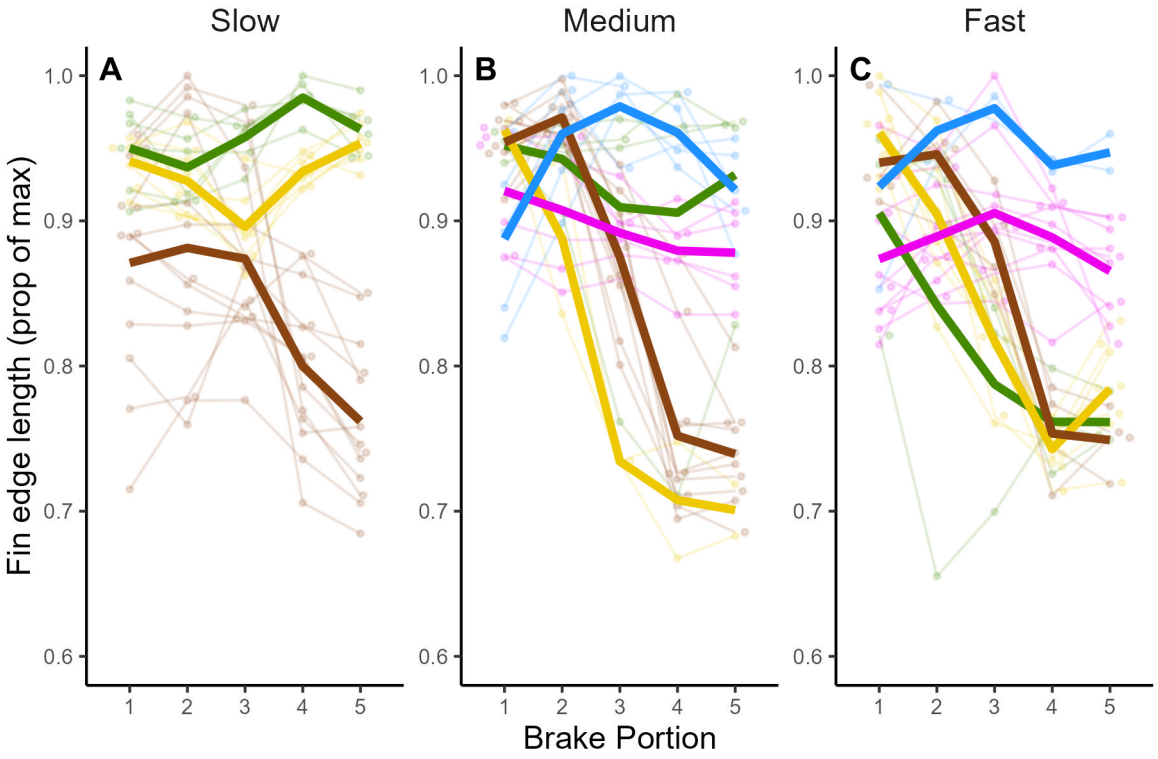

Figure 7: The length of the trailing edge of the caudal fin for slow, medium, and fast brakes. Data are presented as means during the course of the brake broken up into five temporally equal portions. Color represents individual and the black lines show the means.

Overall, bluegill pinched their caudal fin during slow brakes (caudal edge length was 1.05 times longer at the start of the brake), and during medium and fast brakes (caudal edge length was 1.1 times longer at the start of the brake for both). Their tail was significantly more pinched during medium brakes compared to during slow brakes ($p = 0.044$), and was significantly more pinched during fast brakes than during medium ($p = 0.016$) and slow ($p < 0.001$) brakes. Individuals behaved differently, with one pinching its caudal fin during all brakes, one pinching its tail during medium and fast brakes but not during slow brakes, and one only pinching its tail during fast brakes.

However, individuals behave differently. Two individuals did not change how flared their caudal fin was across any speeds. Individuals that pinched their caudal fins were overall larger than individuals that did not (mean span of 18.8cm compared to mean of 8.3cm).

Bluegill pitched down

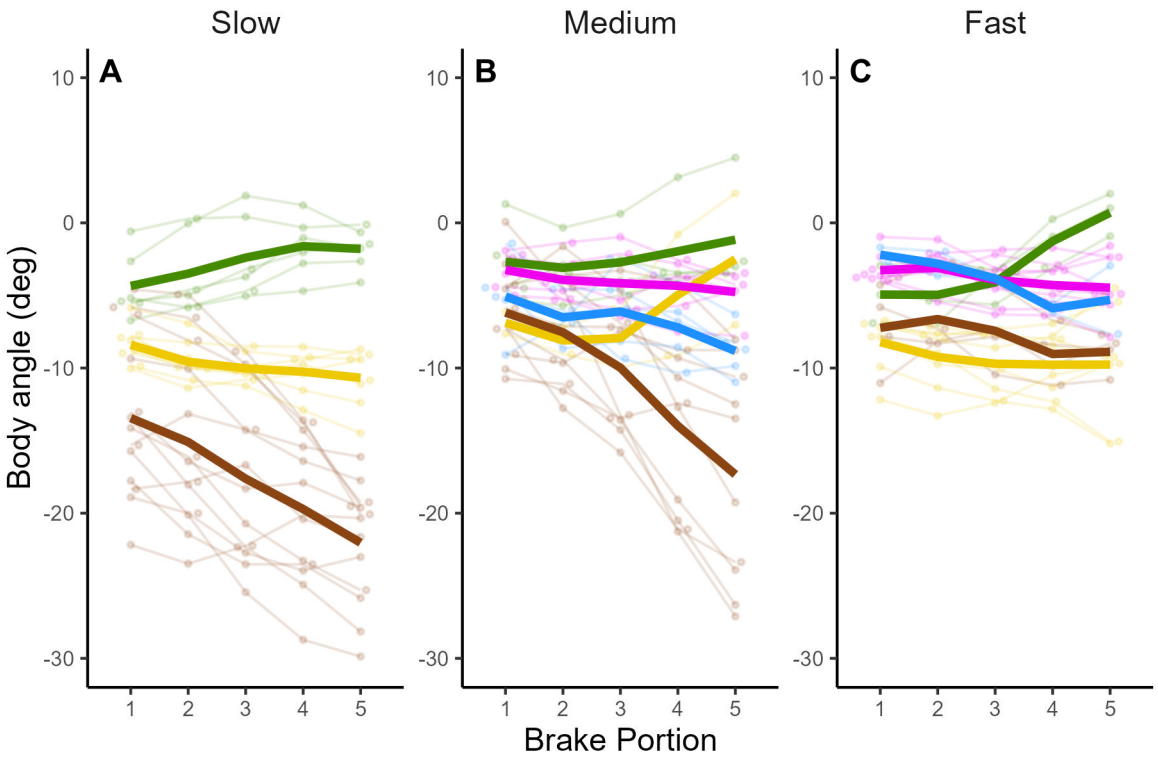

Figure 8: Body angle in degrees relative to the horizontal over the time course of the brake for slow, medium, and fast brakes. Negative values indicate the bluegill is pitched down while positive values indicate it is pitched up. Color represents individual with thin lines connecting trials and thick lines connecting individual means.

Overall, bluegill pitched head down over the course of the brake (Figure 8), going from -10 $\pm$ 5 deg to -14 $\pm$ 9 deg during slow brakes, from -5 $\pm$ 3 deg to -9 $\pm$ 8 deg during medium brakes, and from -5 $\pm$ 3 deg to -6 $\pm$ 4 degrees during fast brakes. There were significant differences between slow and medium ($p < 0.001$) and slow and fast brakes ($p < 0.001$), but no significant differences between medium and fast brakes ($p = 0.999$).

However, individuals behaved differently as some pitched up, some pitched down, and some did not pitch much at all.

Discussion

Bluegill primarily used their pectoral fins to slow down, but recruited other fins more for higher speed decelerations

In line with my hypothesis, bluegill produced the most instantaneous frontal braking force with their pectoral fins, and increased how much force they produce the faster they needed to brake (Figure 3). This was consistent with the previously documented importance of these fins in bluegill (Drucker and Lauder, 2002; Geerlink, 1987; Harris, 1938; Higham, 2007; Higham et al., 2005; Jayne et al., 1996) and other fish species (Drucker and Lauder, 2002; Drucker and Lauder, 2003; Geerlink, 1987; Gibbs et al., 2024; Higham, 2007; Videler, 1981; Webb, 1984; Webb, 2002). Additionally, they also produced more instantaneous frontal braking force with their other fins as speed increased (Figure 4), meaning that all of their fins were important when it comes to producing forces necessary to brake.

The story became more complicated when I looked at total impulse. Unlike with instantaneous braking forces, at each speed, bluegill produced about the same total impulse with their pectoral fins as they did with their dorsal fin and their anal fin (Figure 4 and Figure 9). Since total impulse was similar for the pectoral, dorsal, and anal fins, I concluded that each fin was equally important over the full time course of the brake, however, since the pectoral fins produced much higher instantaneous fin force which changes with brake speed, I conclude that much of the differences between higher brake speeds came down to the instantaneous use of the pectoral fins. However, when considering the consistency in the trends for all fins, cumulatively, total impulse increased. For this reason, I highlight the importance of the dorsal and anal fins, which are relatively infrequently focused on in the literature (however see Jayne et al. (1996); Drucker and Lauder (2005); Lauder and Drucker (2004); Standen and Lauder (2005); Standen and Lauder (2007); Tytell (2006); Tytell and Lauder (2008); for the dorsal fin; Videler (1981); Webb and Fairchild (2001); Standen and Lauder (2005); Tytell (2006); Tytell and Lauder (2008); Standen and Lauder (2007) for the anal fin).

Some fins were threshold dependent

While bluegill used their pectoral fins and anal fins more instantaneously at all speeds as evidenced by significantly higher fin forces (Figure 4 and Figure 3), they did not start using their dorsal and pelvic fins any differently until they crossed from medium brakes into fast brakes. This suggests there is a threshold during braking, under which bluegill tend not to use their dorsal and pelvic fins as much as they may not be needed.

In this way, braking in bluegill is somewhat like braking with a bike: when you need to slow down, you apply your back brake, after which you apply your front brake if you are still unable to slow down quickly enough.

Bluegill may have used their dorsal, anal, and pelvic fins for stability during braking

When considering how fin area changes in the lateral plane, I believe that bluegill flared their dorsal and anal fins specifically to prevent rolling during braking. Of all the perturbations, rolling has been posited to be the most catastrophic for fish, as found by Webb (2004) who perturbed fish with water jets and found that they would sometimes ignore yawing and pitching instabilities, but would always correct rolling perturbations. Lateral fin expansion provides stability in the roll axis, thereby counteracting the most detrimental destabilizing force. Thus, in addition to providing critical braking forces, the dorsal and anal fins are likely also used to stabilize the fish.

While I did not directly measure how these fins contributed to stability, I nonetheless believe that their flaring in the lateral plane contributed to active stabilization. I believe by doing so, these fins were creating surfaces that actively resisted destabilizing forces. This concept is not novel, as early work written about by Breder (1926) showed that when one removes a pectoral fin from a bluegill, they use their dorsal fin to compensate for the instability, a pattern also seen in pumpkinseed sunfish and pinfish (Breder, 1926). Indeed, an absence of the dorsal and anal fins results in a large amount of rolling during swimming (Breder, 1926; Harris, 1938). This pattern is conserved across species as trout have previously been found to produced counteracting rolling torques with their dorsal and anal fins to help them stay balanced (Standen and Lauder, 2007).

While it is clear that the dorsal and anal fins were important in providing roll stability, it is less clear that the pelvic fins were important. Previous work has found that removing the pelvic fins sometimes results in rolling, but this is not always the case (Breder, 1926). Some work even asserts that they are primarily used to control pitch and yaw rather than roll (Standen, 2010). Interestingly, Harris (1938) asserted that the pelvic fins can induce rolling moments, while at the same time saying that their role in rolling is negligible. Overall, based on my results I do feel that the pelvic fins could be important stabilizers, but I am unsure of exactly what role they may play.

There may be a tradeoff between speed and stability

My results further suggest that there is an important tradeoff between producing braking and staying stable. Specifically, as instantaneous fin forces decreased (Figure 3 and Figure 4), lateral surface area increased in the dorsal, anal, and pelvic fins (Figure 6). This resulted in less stopping force and more stabilizing force. In this way, I return to my bike analogy and assert that braking is somewhat like riding a bike, where bluegill are more stable when they are moving fast, but as they slow down, they become less stable, and need to find a way to stay upright. This relationship between speed and stability has previously been found in a handful of studies (Webb, 2002).

Most notably, Webb (1993) found that as bluegill swim at a lower speed, they pitch more head down than at higher speeds. Webb went on to propose that this, coupled with extending control surfaces, contributes to stability. My experiment seems to share this pattern, both with the changes in body angle over time as bluegill pitched more head down at lower speeds (Figure 8), and with the lateral flaring of the dorsal, anal, and pelvic fins as time goes on and speed decreased (Figure 6). The contribution of the head down pitching in some individuals further lines up with results found by Fath and Tytell (2023) who found that a fish's unstable equilibrium is at 53 degrees head down, and that at night, bluegill rest around 10 degrees head down.

The brakes were sub-maximal

Unexpectedly, bluegill did not use their caudal fin to actively brake in the range of intermediate decelerations that I studied. This contrasts with findings by Flammang and Lauder (Flammang and Lauder, 2009) that showed the caudal fin curving into a "S" shape to actively push against the water to help them rapidly slow down. It also contrasts work by Jayne et al (1996) that found the caudal fin to be active in braking and work done by Webb (2004) that found that fish flare their caudal fin for added stability. In contrast, the bluegill seem to be using their caudal fins like they would during a glide where they pinch the tips together (Flammang and Lauder, 2009). This may be because I studied intermediate decelerations, not the strong braking maneuvers that Flammang and Lauder (2009) examined. The braking times reflected this as each brake took much longer than the mean brake (0.058s) that Flammang and Lauder studied (Figure 2). In other words, the caudal fin behavior of the bluegill suggests that I have indeed managed to record brakes at sub-maximal speeds.

The fact that the bluegill braked sub-maximally could also account for the individual differences that I observed. Specifically, because the constraints were lower (they do not need to stop as rapidly), the bluegill I tested did not need to exhibit as stereotyped behavior as they would have needed to at higher speeds. As a result, they did not heavily constrain how much they pitch (Figure 8) or how much they flared their caudal fin (Figure 7), however these kinematics could be more important at higher speeds.

Future directions

My study was about how bluegill brake, with a focus on how they are physically using their fins to slow themselves down. However, fish fins are not simply control surfaces they use to swim. In fact, fins contain many sensory nerve fibers that allow the fish to sense bending of the fin rays and potentially the flow over the fin (Aiello et al., 2018). This sensory component has previously been examined (Aiello et al., 2018), but more work still remains. Specifically in bluegill, the pectoral fins are innervated and have been found to be proprioceptive, responding differently to different deflections and rates of deflection (Williams IV et al., 2013). This proprioception is important to the fish, as transecting the fin ray nerves in the pectoral fins changes how bluegill use them during hovering (Williams IV and Hale, 2015). Some work has also been done to show that the dorsal fins in rockling fish are innervated and provide a lot of sensory information (Kotrschal et al., 1984). Additionally, the adipose fins in trout are innvervated (Buckland-Nicks, 2016; Buckland-Nicks et al., 2011) and in catfish have been found to act as flow sensors that respond to lateral deflections (Aiello et al., 2016). Thus, I feel further examination and quantification of the innervation and sensory responses of dorsal and anal fins could provide an important window into braking mechanics, in large part because sensing the surrounding flow could help bluegill better respond to it and inform them of how best they can remain stable. If, for example, they experience a rolling force and sense it with their fins, they can respond by flaring or beating their dorsal and anal fins to stay upright and level.

To this end, the pelvic fins may also be a critical sensor that helps the bluegill stay oriented and respond to oncoming flow, which would account for their relatively small fin force during braking. The pelvic fins flared in the lateral plane, suggesting that they operate as roll stabilizers, but based on the innervation and relevance of innervation in pectoral and dorsal fins, I feel that a close examination of the pelvic fins in bluegill could yield relevant results for interpreting my study. Specifically, if the pelvic fins are actively sensing the oncoming flow, based on their positioning near the bluegill's center of mass, they could help the bluegill understand how it is rolling and inform it as to how to flare its fins to stay upright.

Finally, while I estimated fin forces and postulate about drag, more direct comparisons could be made using a more direct approach to quantify shed vortices and estimate drag directly. Specifically, an understanding of the exact physical forces produced by each fin could help me parse apart drag from stability, and better understand each fin's contribution to braking. I expect such quantification would further emphasize the importance of the pectoral fins during braking, as it would not be complicated by the incredible deformability of the fins. It would also help me understand if bluegill are actively producing lateral vortices with their dorsal and anal fins to remain upright and properly oriented.

Competing Interests

The authors declare no competing interests.

Funding

I received funding from NSF IOS 1652582, NSF IOS 2422535, and ARO W911NF-17-1-0234.

References

Aiello, B. R., Stewart, T. A. and Hale, M. E. (2016). Mechanosensation in an adipose fin. *Proceedings of the Royal Society B: Biological Sciences* **283**, 20152794. doi: 10.1098/rspb.2015.2794.

Aiello, B. R., Hardy, A. R., Westneat, M. W. and Hale, M. E. (2018). Fins as mechanosensors for movement and touch-related behaviors. *Integrative and Comparative Biology* **58**, 844–859. doi: 10.1093/icb/icy065.

Bainbridge, R. (1963). Caudal fin and body movement in the propulsion of some fish. *Journal of Experimental Biology* **40**, 23–56. doi: 10.1242/jeb.40.1.23.

Bates, D., Mächler, M., Bolker, B. and Walker, S. (2015). Fitting linear mixed-effects models using Lme4. *Journal of Statistical Software* **67**, 1–48. doi: 10.18637/jss.v067.i01.

Borchers, H. W. (2023). Pracma: Practical numerical math functions. url: https://cran.r-project.org/web/packages/pracma/index.html.

Breder, C. M. (1926). The locomotion of fishes. *Zoologica* **4**, 159–297. doi: 10.5962/p.203769.

Buckland-Nicks, J. A. (2016). New details of the neural architecture of the salmonid adipose fin. *Journal of Fish Biology* **89**, 1991–2003. doi: 10.1111/jfb.13098.

Buckland-Nicks, J. A., Gillis, M. and Reimchen, T. E. (2011). Neural network detected in a presumed vestigial trait: Ultrastructure of the salmonid adipose fin. *Proceedings of the Royal Society B: Biological Sciences* **279**, 553–563. doi: 10.1098/rspb.2011.1009.

Dabiri, J. O., Colin, S. P., Gemmell, B. J., Lucas, K. N., Leftwich, M. C. and Costello, J. H. (2020). Jellyfish and fish solve the challenges of turning dynamics similarly to achieve high maneuverability. *Fluids* **5**, 106. doi: 10.3390/fluids5030106.

Domenici, P. and Hale, M. E. (2019). Escape responses of fish: A review of the diversity in motor control, kinematics and behaviour. *Journal of Experimental Biology* **222**, jeb166009. doi: 10.1242/jeb.166009.

Downs, A. M., Kolpas, A., Block, B. A. and Fish, F. E. (2023). Multiple behaviors for turning performance of Pacific bluefin tuna (*Thunnus orientalis*). *Journal of Experimental Biology* **226**, jeb244144. doi: 10.1242/jeb.244144.

Drucker, E. G. and Lauder, G. V. (2001). Locomotor function of the dorsal fin in teleost fishes: Experimental analysis of wake forces in sunfish. *Journal of Experimental Biology* **204**, 2943–2958. doi: 10.1242/jeb.204.17.2943.

Drucker, E. G. and Lauder, G. V. (2002). Wake dynamics and locomotor function in fishes: Interpreting evolutionary patterns in pectoral fin design. *Integrative and Comparative Biology* **42**, 997–1008. doi: 10.1093/icb/42.5.997.

Drucker, E. G. and Lauder, G. V. (2003). Function of pectoral fins in rainbow trout: Behavioral repertoire and hydrodynamic forces. *Journal of Experimental Biology* **206**, 813–826. doi: 10.1242/jeb.00139.

Drucker, E. G. and Lauder, G. V. (2005). Locomotor function of the dorsal fin in rainbow trout: Kinematic patterns and hydrodynamic forces. *Journal of Experimental Biology* **208**, 4479–4494. doi: 10.1242/jeb.01922.

Dunnington, D., Thorne, B. and Hernangómez, D. (2023). Ggspatial: Spatial data framework for Ggplot2. url: https://cran.r-project.org/web/packages/ggspatial/index.html.

Eklund, A. and Trimble, J. (2021). Beeswarm: The bee swarm plot, an alternative to stripchart. url: https://cran.r-project.org/web/packages/beeswarm/index.html.

Fath, M. and Tytell, E. D. (2023). Day and night posture of the bluegill sunfish (*Lepomis macrochirus*). 2023.07.13.548884. doi: 10.1101/2023.07.13.548884.

Flammang, B. E. and Lauder, G. V. (2009). Caudal fin shape modulation and control during acceleration, braking and backing maneuvers in bluegill sunfish, *Lepomis macrochirus*. *Journal of Experimental Biology* **212**, 277–286. doi: 10.1242/jeb.021360.

Fox, J. and Weisberg, S. (2019). *An R Companion to Applied Regression*. Third edition. Thousand Oaks CA: Sage.

Garrido-Jurado, S., Muñoz-Salinas, R., Madrid-Cuevas, F. J. and Marín-Jiménez, M. J. (2014). Automatic generation and detection of highly reliable fiducial markers under occlusion. *Pattern Recognition* **47**, 2280–2292. doi: 10.1016/j.patcog.2014.01.005.

Geerlink, P. J. (1987). The role of the pectoral fins in braking of mackerel, cod and saithe. *Netherlands Journal of Zoology* **37**, 81–104. doi: 10.1163/002829687X00053.

Gibbs, B. J., Akanyeti, O. and Liao, J. C. (2024). Kinematics and muscle activity of pectoral fins in rainbow trout (*Oncorhynchus mykiss*) station holding in turbulent flow. *Journal of Experimental Biology* **227**, jeb246275. doi: 10.1242/jeb.246275.

Harris, J. E. (1938). The role of the fins in the equilibrium of the swimming fish: II. The role of the pelvic fins. *Journal of Experimental Biology* **15**, 32–47. doi: 10.1242/jeb.15.1.32.

Hedrick, T. L. (2008). Software techniques for two- and three-dimensional kinematic measurements

of biological and biomimetic systems. *Bioinspiration & Biomimetics* **3**, 034001. doi: 10.1088/1748-3182/3/3/034001.

Higham, T. E. (2007). Feeding, fins and braking maneuvers: Locomotion during prey capture in centrarchid fishes. *Journal of Experimental Biology* **210**, 107–117. doi: 10.1242/jeb.02634.

Higham, T. E., Malas, B., Jayne, B. C. and Lauder, G. V. (2005). Constraints on starting and stopping: Behavior compensates for reduced pectoral fin area during braking of the bluegill sunfish *Lepomis macrochirus*. *Journal of Experimental Biology* **208**, 4735–4746. doi: 10.1242/jeb.01966.

Hu, W., Tong, B. and Liu, H. (2007). Dynamics of free straight swimming of *Angulla angulla* including forward, braking and backward locomotion. *Journal of Hydrodynamics, Ser. B* **19**, 395–402. doi: 10.1016/S1001-6058(07)60132-2.

Jayne, B. C., Lozada, A. F. and Lauder, G. V. (1996). Function of the dorsal fin in bluegill sunfish: Motor patterns during four distinct locomotor behaviors. *Journal of Morphology* **228**, 307–326. doi: 10.1002/(SICI)1097-4687(199606)228:3<307::AID-JMOR3>3.0.CO;2-Z.

Karashchuk, P., Rupp, K. L., Dickinson, E. S., Walling-Bell, S., Sanders, E., Azim, E., Brunton, B. W. and Tuthill, J. C. (2021). Anipose: A toolkit for robust markerless 3D pose estimation. *Cell Reports* **36**, 109730. doi: 10.1016/j.celrep.2021.109730.

Kay, M. (2024). Ggdist: Visualizations of distributions and uncertainty in the grammar of graphics. *IEEE Transactions on Visualization and Computer Graphics* **30**, 414–424. doi: 10.1109/TVCG.2023.3327195.

Kay, M. and Wiernik, B. M. (2024). Ggdist: Visualizations of distributions and uncertainty. url: https://cloud.r-project.org/web/packages/ggdist/index.html.

Kotrschal, K., Whitear, M. and Adam, H. (1984). Morphology and histology of the anterior dorsal fin of *Gaidropsarus mediterraneus* (Pisces Teleostei), a specialized sensory organ. *Zoomorphology* **104**, 365–372. doi: 10.1007/BF00312187.

Lauder, G. V. and Drucker, E. G. (2004). Morphology and experimental hydrodynamics of fish fin control surfaces. *IEEE Journal of Oceanic Engineering* **29**, 556–571. doi: 10.1109/JOE.2004.833219.

Lenth, R. V., Banfai, B., Bolker, B., Buerkner, P., Giné-Vázquez, I., Herve, M., Jung, M., Love, J., Miguez, F., Piaskowski, J., et al. (2025). Emmeans: Estimated marginal means, aka least-squares means. url: https://cran.r-project.org/web/packages/emmeans/index.html.

Pereira, T. D., Tabris, N., Matsliah, A., Turner, D. M., Li, J., Ravindranath, S., Papadoyannis, E. S., Normand, E., Deutsch, D. S., Wang, Z. Y., et al. (2022). SLEAP: A deep learning system for

multi-animal pose tracking. *Nature Methods* **19**, 486–495. doi: 10.1038/s41592-022-01426-1.

Porter, M. E., Roque, C. M. and Long Jr., J. H. (2009). Turning maneuvers in sharks: Predicting body curvature from axial morphology. *Journal of Morphology* **270**, 954–965. doi: 10.1002/jmor.10732.

Smith, G. D. (1985). *Numerical Solution of Partial Differential Equations: Finite Difference Methods*. Clarendon Press.

Standen, E. M. (2008). Pelvic fin locomotor function in fishes: Three-dimensional kinematics in rainbow trout (*Oncorhynchus mykiss*). *Journal of Experimental Biology* **211**, 2931–2942. doi: 10.1242/jeb.018572.

Standen, E. M. (2010). Muscle activity and hydrodynamic function of pelvic fins in trout (*Oncorhynchus mykiss*). *Journal of Experimental Biology* **213**, 831–841. doi: 10.1242/jeb.033084.

Standen, E. M. and Lauder, G. V. (2005). Dorsal and anal fin function in bluegill sunfish *Lepomis macrochirus*: Three-dimensional kinematics during propulsion and maneuvering. *Journal of Experimental Biology* **208**, 2753–2763. doi: 10.1242/jeb.01706.

Standen, E. M. and Lauder, G. V. (2007). Hydrodynamic function of dorsal and anal fins in brook trout (*Salvelinus fontinalis*). *Journal of Experimental Biology* **210**, 325–339. doi: 10.1242/jeb.02661.

Tytell, E. D. (2006). Median fin function in bluegill sunfish *Lepomis macrochirus*: Streamwise vortex structure during steady swimming. *Journal of Experimental Biology* **209**, 1516–1534. doi: 10.1242/jeb.02154.

Tytell, E. D. and Lauder, G. V. (2008). Hydrodynamics of the escape response in bluegill sunfish, *Lepomis macrochirus*. *Journal of Experimental Biology* **211**, 3359–3369. doi: 10.1242/jeb.020917.

Videler, J. J. (1981). Swimming movements, body structure and propulsion in cod *Gadus morhua*. *Symposia of the Zoological Society of London* **48**, 1–27.

Vogel, S. (1996). *Life in Moving Fluids: The Physical Biology of Flow*. Princeton University Press.

Webb, P. W. (1984). Form and function in fish swimming. *Scientific American* **251**, 72–83.

Webb, P. W. (1993). Is tilting behaviour at low swimming speeds unique to negatively buoyant fish? Observations on steelhead trout, *Oncorhynchus mykiss*, and bluegill, *Lepomis macrochirus*. *Journal of Fish Biology* **43**, 687–694. doi: 10.1111/j.1095-8649.1993.tb01146.x.

Webb, P. W. (2002). Control of posture, depth, and swimming trajectories of fishes. *Integrative and Comparative Biology* **42**, 94–101. doi: 10.1093/icb/42.1.94.

Webb, P. W. (2004). Response latencies to postural disturbances in three species of teleostean fishes. *Jour-*

nal of Experimental Biology **207**, 955–961. doi: 10.1242/jeb.00854.

Webb, P. W. and Fairchild, A. G. (2001). Performance and maneuverability of three species of teleostean fishes. *Canadian Journal of Zoology* **79**, 1866–1877. doi: 10.1139/z01-146.

Wickham, H., Averick, M., Bryan, J., Chang, W., McGowan, L. D., François, R., Grolemund, G., Hayes, A., Henry, L., Hester, J., et al. (2019). Welcome to the Tidyverse. *Journal of Open Source Software* **4**, 1686. doi: 10.21105/joss.01686.

Williams IV, R. and Hale, M. E. (2015). Fin ray sensation participates in the generation of normal fin movement in the hovering behavior of the bluegill sunfish (*Lepomis macrochirus*). *Journal of Experimental Biology* **218**, 3435–3447. doi: 10.1242/jeb.123638.

Williams IV, R., Neubarth, N. and Hale, M. E. (2013). The function of fin rays as proprioceptive sensors in fish. *Nature Communications* **4**, 1729. doi: 10.1038/ncomms2751.

Chapter 4: Fast turns are not sped up slow turns: How bluegill sunfish change their kinematics with turn speed

Introduction

Steady swimming in fishes has been studied extensively, but for many fish species, unsteady swimming comprises a large part of everyday locomotion. For example, trout spend most of their time accelerating, decelerating, and turning rather than swimming steadily (Webb, 1991). Similarly, both zebrafish and tuna, despite their large difference in size, swim unsteadily, turning regularly during normal swimming bouts (Fuiman and Webb, 1988; Howe and Astley, 2020; Thandiackal and Lauder, 2020; and Downs et al., 2023). Unsteady swimming becomes particularly important during predator-prey interactions, where both predator and prey accelerate, decelerate, and turn during encounters (Higham, 2007; see Webb, 1983; Webb, 1984a; Webb, 1986; and Hitchcock et al., 2015 for examples). Fish also swim unsteadily during territory defense (e.g., Feldmeth, 1983). Finally, sharks swim unsteadily in social situations such that individuals lower in the hierarchy maneuver to keep out of the way of their superiors (Weihs et al., 1981) and will regularly turn facilitated by dramatic body bends (Porter et al., 2009; Porter et al., 2011).

All of these behaviors depend on an organism's maneuverability and agility, both of which vary dramatically depending on the organism. Maneuverability is an individual's ability to turn in a set space and is the radius of its turn divided by its body length (Fish, 2020). Agility is how quickly an individual can turn; in other words, its angular velocity (Fish, 2020). These quantities vary depending on the organism, all the way from boxfish which possess very rigid bodies that are able to slowly turn (max. turn rate = 200.50deg/s) in a very tight radius (min. radius = 0.0005L) (Walker, 2000) to the smallmouth bass which has a more flexible

body and can quickly turn (max. turn rate = 5009.61deg/s) in a larger radius (min. radius = 0.11L) (Webb, 1983). These two quantities further contribute to the interpretation of unsteady swimming as they help define the limits of different organisms.

Understanding unsteady swimming is also important to understanding the energy budget for fishes as they swim. On one side, muscles in some fish species fatigue less over time when they are used intermittently than when they are used continuously Coughlin and Dutterer (2024). In contrast, modeling of swimming states in rummy nose tetras suggests that burst and coast swimming uses more energy than continuous swimming (Ashraf et al., 2020) and *in vivo* studies in salmon show that they incur metabolic costs 40 times greater during burst swimming than during sustained swimming (Puckett and Dill, 1984), further highlighting the need to better understand the mechanics underlying unsteady swimming.

One unsteady behavior that has been studied extensively is the C-start (Domenici and Hale, 2019). Importantly, the C-start is often a strong response, and is straightforward to elicit with strong-enough stimuli. C-starts consist of three stages: the preparatory, propulsive, and variable stage (Weihs, 1973). The first stage involves a rapid whole body bend into a "C" shape while the second stage is characterized by the return flip of the tail and subsequent acceleration Domenici and Blake (1997). C-starts have high angular velocities and occur in short time periods, often occurring in less than one fifth of a second (Domenici and Blake, 1997).

While C-starts are important for survival, routine turning is a much more common behavior – but has been studied much less. From the current body of literature, we know that some fish initiate turning with an anterior bend while "planting" their tail in the water to use it is a fulcrum during the maneuver (Gray, 1933), an idea further supported by the finding that the anterior and posterior regions of the body generate large amounts of positive work at the initiation of turning in zebrafish (Thandiackal and Lauder, 2020). We also know that tuna can turn in one of three ways: with a gliding turn where they use their caudal fin as a rudder, with a powered turn where they keep beating their caudal fin symmetrically, and with a ratchet turn where they asymmetrically beat their caudal fin to one side of their body (Downs et al., 2023). Such asymmetry has also been reported in turning coelacanths (Fricke and Hissmann, 1992). Additionally, body caudal fin swimmers turn around when exposed to an oscillatory stimulus while median-paired fin swimmers do not (Marcoux and Korsmeyer, 2019). Finally, there have been some quantification of various physical quantities such as centripetal acceleration during turning(Howe and Astley, 2020).

Of particular note, Dabiri et al (2020) identified a mechanism that they proposed underlies routine turning across many species. They quantified physical quantities such as torque and moment of inertia as fish turned,

concluding that timing is conserved across species so that animals keep their bodies long to maximize torque before bending their bodies to minimize moment of inertia and accelerate through the turn.

In this study, I examined the mechanism proposed by Dabiri et al (2020) to test whether it holds for turns at different speeds. Inspired by the system built by Marcoux and Korsmeyer (2019), I developed a system that allows me to repeatably elicit 180 degree turning behavior at controlled speeds. The system consists of a flow-through chamber attached to a movable platform that is mounted on top of a flow tank. Fish placed in the chamber reliably turn as the chamber changes direction. Using this system, I worked with bluegill sunfish (*Lepomis macrochirus*) to answer the question: are fast turns simply sped up slow turns, or are there distinct kinematic patterns that differentiate them?

When turning, fish face a tradeoff: they need to produce torque to propel themselves through the turn, but they can also reduce their moment of inertia to speed up the turn. In other words, by keeping their body straight, they generate larger amounts of torque using their tail because their lever arm is long, but they also have a larger rotational moment of inertia (Dabiri et al., 2020). Alternatively, by bending their body, they reduce their moment of inertia, but also reduce the lever arm for generating torque.

Dabiri et al. (2020) observed one solution for this tradeoff. They found that both zebrafish and jellyfish initially keep their bodies straight to produce large amounts of torque before bending their bodies to reduce moment of inertia, thus increasing their angular acceleration through the turn. Here, I explore whether these conclusions might change depending on the speed of the turn. In other words, do fish handle these tradeoffs differently when they need to turn quickly rather than when they have time to slowly turn around? I hypothesized that the tradeoffs would be handled differently: that a fast turn is not simply a sped up slow turn.

I ground this hypothesis in the equation for angular acceleration (α)

$$\alpha = \frac{\tau}{I} \tag{0.1}$$

and the moment of inertia I for a body consisting of many segments is

$$I = \sum_{i=1}^{n} m_i r_i^2 \tag{0.2}$$

with i as the segment number, m_i as the mass of the segment at a point, and r_i^2 as the distance from that

mass to the center of rotation. Torque τ is

$$\tau = r f_{\perp} \tag{0.3}$$

where r is the distance from the center of rotation to the propulsor and $f_{\perp}$ is the force the propulsor produces that is perpendicular to r.

Based on (Equation 0.1), to have a higher angular acceleration, the fish can either increase torque or decrease moment of inertia. Both the torque and moment of inertia depend on r, but while torque scales with r, moment of inertia scales with r^2 (Equation 0.2 and Equation 0.3). Therefore, by bending its body, the fish linearly decreases torque, but quadratically decreases moment of inertia. Since angular acceleration needs to be higher during faster turns, I thus hypothesized that fish would prioritize body bending in fast turns to reduce moment of inertia, but would prioritize high torque by keeping the body straight at the beginning during slow turns, similar to what Dabiri et al (2020) observed.

Additionally, I quantified linear and angular momentum of the body during the turn to examine how fish exchange linear and angular momentum, and whether this exchange might differ depending on speed. Finally, I examined pectoral fin movements during the turns. Bluegill use their pectoral fins regularly for maneuvering and stability Drucker and Lauder (2001). I expected that turns at different speeds might have different stability or control requirements, and this would be reflected in differences in pectoral fin use.

Methods

Dataset

I collected 5 bluegill (*Lepomis macrochirus*) (of lengths 12.5cm, 13cm, 14.5cm, 19cm, 19cm) from either White pond or Walden pond in Concord, MA. I used a seine net along the shores of these ponds to collect the fish before transferring them to an aquaculture facility where they were kept in 10 gallon tanks at a controlled temperature of 20 degrees Celsius until used for experiments. I collected the fish with scientific collection permits 090.22SCF, 146.23SCF, 158.19SCF, and 174.20SCF, and kept them according to protocols M2018-103, M2021-99, and M2024-57. Each individual contributed at least 15 slow and 15 fast turns to the dataset.

All experimental procedures and animal handling protocols were approved by the Tufts University Institutional Animal Care and Use Committee.

Setup

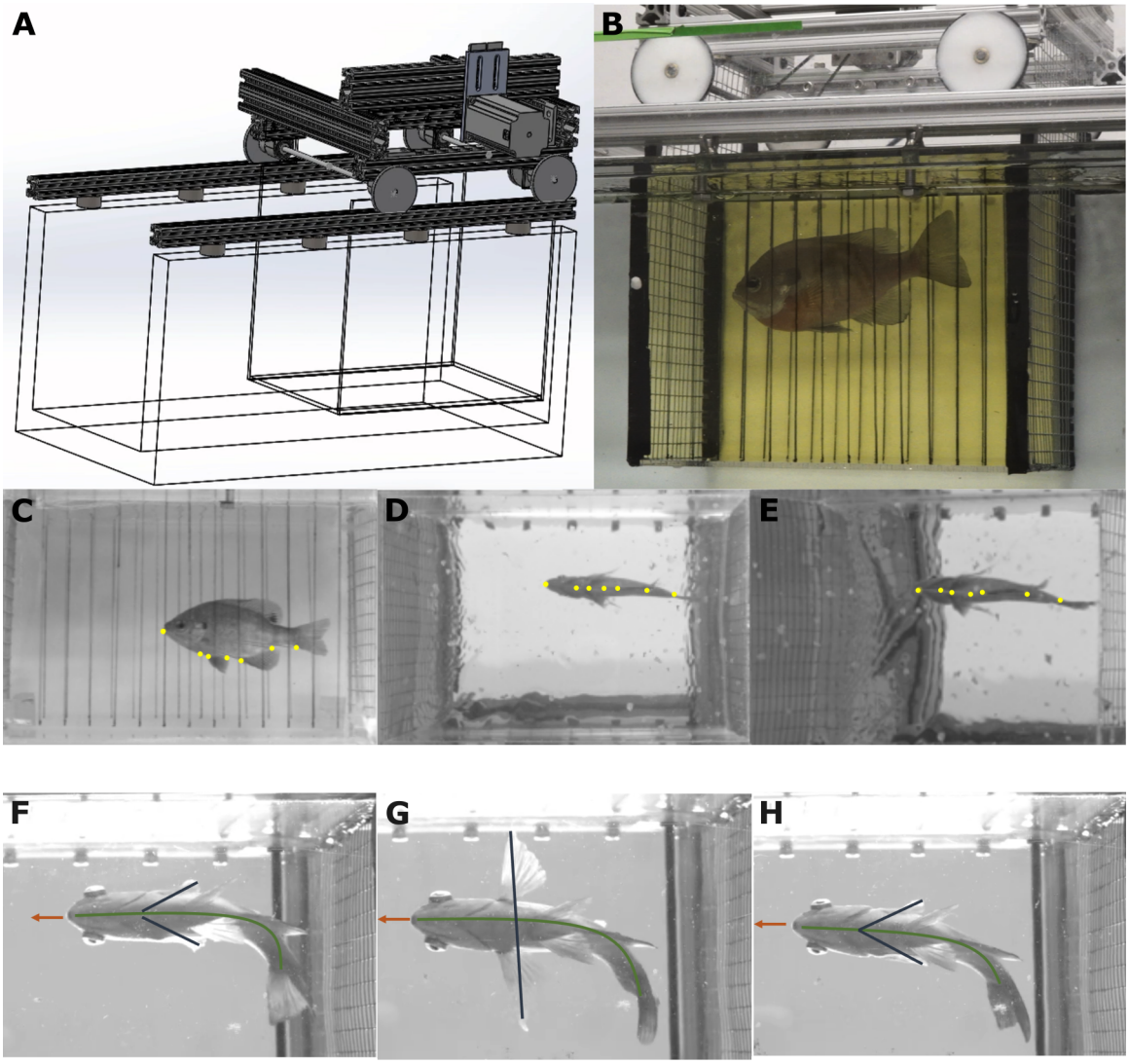

Figure 1: The programmable car elicits repeatable turns. (A) A 3D solidworks model of the system (available in supplementary material). (B) A bluegill swimming in the chamber. (C, D, E) I filmed using an orthogonal lateral camera (C), an orthogonal ventral camera (D), and an off axis ventral camera (E). The yellow points represent digitized points along the body. Light gray lines show the skeleton used for training (the snout to all other points to form a shallow tree). (F, G, H) Three consecutive turns show similar kinematics from the ventral view.

Inspired by the system used by Marcoux and Korsmeyer (2019) I developed an oscillatory device to repeatably induce unsteady behaviors (Figure 1 A,B). I mounted a Teknic ClearPath-SDSK servo motor (part number CPM-SDSK-2310S-EQN) to an 80/20 chassis with an attached acrylic flow-through chamber that is 20.3cm wide by 30cm long and 30.5cm tall. When on top of the flow tank, the water level sits about 19.3cm above the bottom of the flow through chamber. This results in a function volume that is 20.3cm wide, 30cm

long, and 19.3cm tall. This device drove forwards and backwards at programmable rates controlled by an Arduino Uno. The flow-through chamber had metal grates on either end to keep the fish inside and translucent plastic sheets taped on either side with vertical lines drawn on them to provide a visual stimulus for the fish. The wheels of the car ran in a metal track. Since the fish is contained by the grates of the car, when the car reverses direction, the fish must turn at roughly the same rate. In general, for each trial, fish adapted to the movement in the car within 1 or 2 car cycles, after which point I collected my data. I ran all my experiments over the course of a few hours, but recorded each series of slow and fast turns in around 10 minutes or less.

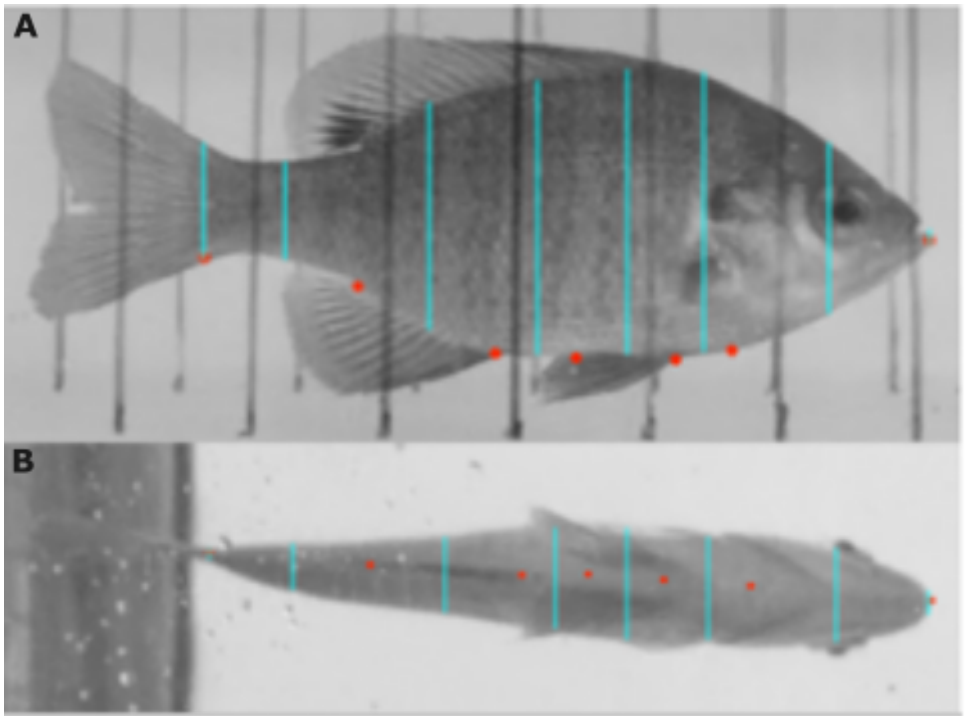

Figure 2: Mass was estimated using images of each bluegill. (A, B) Points were added to their respective locations along the length of the body (red dots). Lines were then drawn from vertical edge to vertical edge of the fish in the lateral view (A) and lateral edge to lateral edge of the fish in the ventral view (B) (light blue lines). FIJI was then used to measure each of the lines and the distance between them in the ventral view. The known length of the fish was used to set the scale.

These turns were repeatable (see Figure 2 C-E for an example) and their consistency allowed me to collect multiple trials with similar performance. For all trials, I kept the water still while the car moved along the track and ran the car at either a low speed (around 1 body lengths L per second at peak speed) or a high speed (either 2.5 or 3.5 L/sec at peak speed) to elicit slow and fast turns respectively. When the fish refused to remain centered in the flow through chamber, it was gently encouraged to move with a wooden dowel. I defined the start of each turn as the first observable movement of the snout in the direction of the turn, and the end as when the fish's snout was oriented in the opposite direction (an approximately 180 degree turn).

Filming and digitizing

To film the kinematics, I set up two Phantom Miro M340 high-speed cameras and one Phantom Miro M120 high-speed camera. I positioned two cameras orthogonal to each other: one directly below the working section of the tank and one directly lateral to the working section of the tank, with one positioned ventrally and at an angle to the rear to the other cameras. I filmed all videos at 60 frames per second. I calibrated

videos by using a ChArUco board (Garrido-Jurado et al., 2014) and the aniposelib package from the Anipose toolkit (Karashchuk et al., 2021).

I used SLEAP (Pereira et al., 2022) to digitize seven points along the midline on the bottom of the fish: the snout, a point in line with the posterior portion of the gills, a point between the pelvic fin insertions, a point halfway between the pelvic fin insertions and the anal fin insertion, the anal fin insertion, a point halfway between the anal fin insertion and the peduncle, and the peduncle (Figure S1 C-E). I wrote custom code to use a ChArUco board to calibrate the filming space and triangulated all digitized points from SLEAP into 3D coordinates in centimeters. I then rotated all points such that they conformed to axes defined by the flow-through section of the apparatus, where the x axis is forward, the y axis is to the fish's left, and the z axis is up. Finally, I used the projections of the 3D points into the x, y for all analyses, since those were the primary axes in which the turns took place. This allowed me to look at the turns in the important axes while correcting for parallax introduced if the fish was at different vertical locations.

I smoothed the x and y locations of all digitized points individually using a 9th order low pass Butterworth filter with a cut off frequency of 8 Hz for fast turns and 4 Hz for slow turns. I then used a cubic smoothing spline to spline the points along the body, interpolating locations that are evenly spaced along the body.

Snout and tail angle and angular velocity

I estimated snout angle by first drawing a line from the center of the pelvic fin insertions to the snout, and tail angle similarly with peduncle and the point halfway between the base of the anal fin and the peduncle. The angle between this vector and the horizontal x axis (θ) is then $\theta = \text{atan2}(y_1 - y_2, x_1 - x_2)$, where y_1 and x_1 are the y and x positions of the snout and y_2 and x_2 are the y and x positions of the pelvic point, respectively. I used the same methods to calculate the tail angle, but using the peduncle point instead of the snout point and the base of the anal fin point instead of the pelvic point.

I then smoothed the angles using a low pass Butterworth filter with a threshold of 4 Hz before numerically differentiating the angle with respect to time by estimating the central difference between points (Smith, 1985). Positive angular velocity values denote movement in the direction of the turn while negative angular velocity values denote movement in the direction opposite the turn.

Moment of inertia

To estimate the volume of each segment along the body, I first used FIJI (Schindelin et al., 2012) to measure height, width, and length of each segment of the fish. I then estimated volume by approximating each segment as a truncated elliptical cone and approximated mass by assuming the fish's density is constant (Fath et al., 2023). Here, w and h are width and height of the fish's body segments, with w as the blue lines in Figure S2 B and h as the blue lines in Figure S2 A. I drew each segment line halfway between two adjacent points down the length of the body, with the exception of the snout and peduncle point where I drew one segment line at the point. For each point along the body, I used the width and height of the body segment line directly anterior to the point (w_i and h_i) and the width and height of the body segment line directly posterior to the point (w_{i+1} and h_{i+1}).

The volume V_i of each segment is thus

$$V_i = \pi \Delta l (w_i h_i + \frac{1}{2}\Delta w h_i + \frac{1}{2}\Delta h w_i + \frac{1}{3}\Delta w \Delta h) \tag{0.4}$$

where Δl is the distance between segments, $\Delta w = w_{i+1} - w_i$ and $\Delta h = h_{i+1} - h_i$, and the mass of each segment is then $m_i = \rho V_i$. Finally, I approximated each segment's mass as a point mass located at the digitized points splined along the body such that the distances between them were consistent with the known distances along the body of the fish.

The moment of inertia (Equation 0.2) was then estimated, assuming the center of rotation was the whole body center of mass (X_M, Y_M), which I estimated as

$$X_M = \frac{\sum x_i m_i}{m_t} \qquad \text{and} \qquad Y_M = \frac{\sum y_i m_i}{m_t} \tag{0.5}$$

where m_i is the mass of each segment. Using Equation 0.2, I then estimated moment of inertia, assuming a constant density of 1 (see discussion in Fath et al., 2023). In this way, I calculated moment of inertia using the volume center of mass (Roche et al., 2023). I then normalized moment of inertia by dividing by the moment of inertia for each individual when its body was straight.

Torque

I estimated the whole body torque of the fish based on of the sum of the torques of the segments. In a non-rigid body, torque is the time derivative of moment of inertia of each body segment (I_i) multiplied by its corresponding angular velocity (ω_i):

$$\tau = \sum \frac{d}{dt} (I_i \omega_i) \tag{0.6}$$

The moment of inertia I_i for each segment is equal to the segment's mass multiplied by the square of its distance to the center of rotation (r_i). Further applying the chain rules gives me the whole body torque of the fish:

$$\tau = \sum m_i (2 r_i \omega \dot{r}_i + r_i^2 \dot{\omega}_i) \tag{0.7}$$

Pectoral fins

I manually digitized the start of all pectoral fin strokes that occurred during the turn. Working with only ventral orthogonal videos, I identified the frames in which each pectoral fin was maximally extended away from the body, immediately before the fish pulled it back towards the body to take a stroke. I digitized the tips of each pectoral fin when it was extended in a frame and the bases of both pectoral fins in all frames in which either fin was extended. In many instances, bluegill seem to be taking "backing" strokes in which they pushed their pectoral fins far towards their snout to produce a backwards force on that side. For my analyses, I considered every pectoral fin stroke greater than 90 degrees (maximally extended) to be a backing stroke.

Momentum

I estimated the linear momentum p_l of the fish during turning as

$$p_l = m_t v_l \tag{0.8}$$

where linear velocity v_l is the central difference of the position of the whole body mass centroid differentiated with respect to time and m_t is the total mass of each fish. Because maximum velocity tends to be proportional to body length L, and body mass is proportional to L^3, momentum should be proportional to

L^4. To control for individual size differences, I therefore divided momentum by L^4. I estimated angular momentum p_θ as

$$p_\theta = Iv_\theta \tag{0.9}$$

where I is the moment of inertia I estimated using Equation 0.2 and v_θ is the angular velocity of the fish's snout as estimated above.

For both linear and angular momentum, I estimated the pre-turn momentum, defined as the mean of the momentum in the two frames leading up to the turn, the mean momentum during the first half of the turn and, and mean momentum during the second half of the turn. I divided the turns into halves according to total time of each turn.

Statistics

For all analysis and visualization, I used R version 4.3.3 with Rstudio version 2023.12.1.402 and the following packages: tidyverse version 2.0.0 (Wickham et al., 2019), lme4 version 1.1.35.1 (Bates et al., 2015), car version 3.1.2 (Fox and Weisberg, 2019), ggspatial version 1.1.9 (Dunnington et al., 2023), ggdist version 3.3.2 Kay (2024), and beeswarm version 0.4.0 (Eklund and Trimble, 2021).

When I used pairwise comparisons to look at the effect of the "slow" and "fast" speed groups, or to look at the significance between changes in momentum and turn portion, I used the Anova function from the car package and the lmer function from the lme4 package to run an ANOVA on a linear mixed-effects model with individual as a random effect. When I present linear and exponential fits, I similarly used the lmer function and fit the 1/x curve for Figure 9 C using ggplot2's geom_smooth function.

To see if the time differences between time of maximum torque and time of minimum moment of inertia were significant, I used emmeans (Lenth et al., 2025) to compare each group to 0 with individual as a random effect.

All means are provided plus or minus one standard deviation, unless otherwise noted.

Results

Angular velocity was higher when the car reversed faster

During fast car reversals (which I will call "fast turns"), fish turned 180 degrees in less time than they did during slow car reversals ("slow turns"), resulting in higher angular velocities (Figure 3). For each turn, I took the mean and maximum angular velocity over the duration of the turn. Then, I examined the means of these values across all turns. Both mean of the mean and the mean maximum snout angular velocity were significantly higher in fast turns (mean = 181 $\pm$ 41 deg/s; max = 428 $\pm$ 84 deg/s) relative to slow turns (mean = 96 $\pm$ 35 deg/s, max 303 $\pm$ 89 deg/s) (for both mean and max, $p < 0.001$).

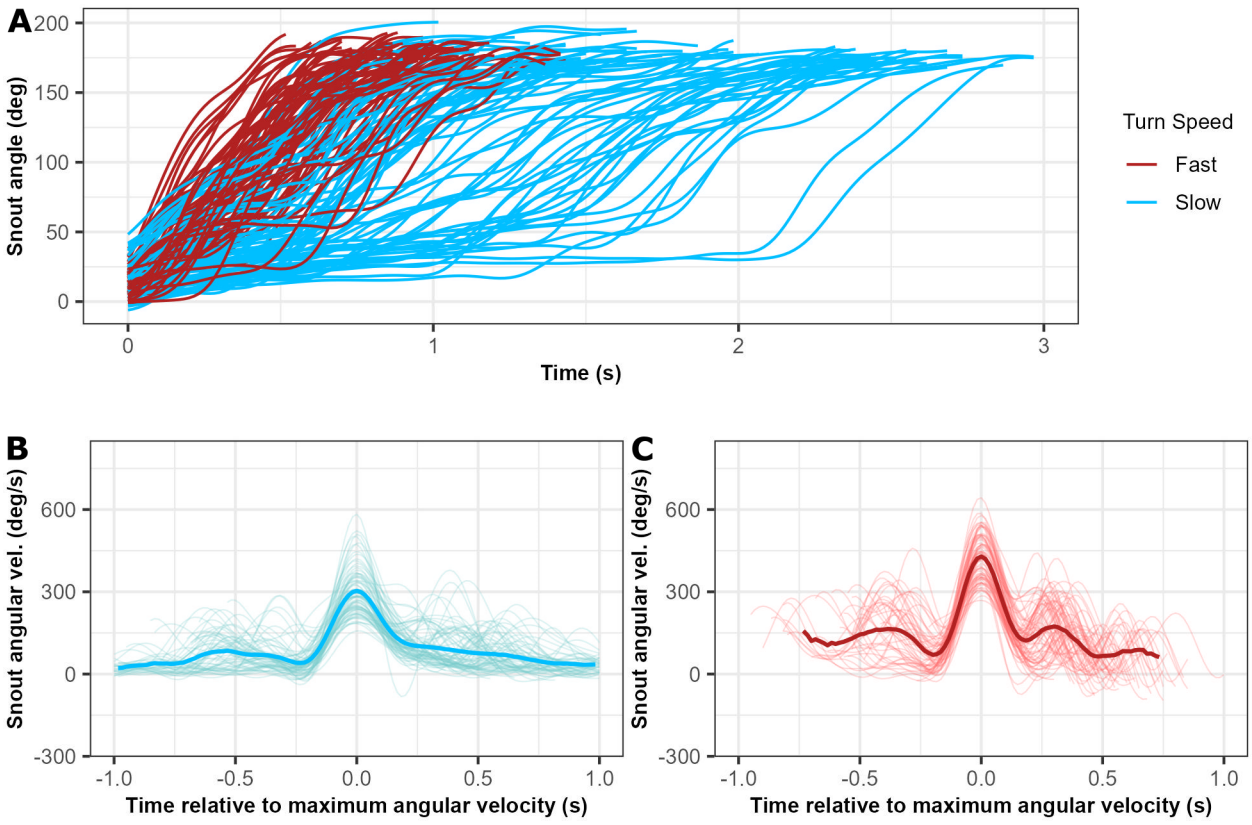

Figure 3: Angular velocities were higher when the car reversed faster. (A) Changes in snout angle for both slow turns in blue and fast turns in red using degrees over seconds. (B, C) Angular velocity with slow turns in blue (B) and fast turns in red (C)

Changes in snout angular velocity were driven by anterior bending

I found that when the snout was moving at its maximum angular velocity, the tail was moving at a significantly lower angular velocity ($p < 0.001$) and was close to 0 (Figure 4 B). The reverse was also true: when the tail was moving at its maximum angular velocity, the snout was moving at a significantly lower speed ($p < 0.001$) that was close to 0 (Figure 4 C).

Additionally, for all turns, fish asymmetrically beat their caudal fin and also simultaneously beat the median fins to that same side as the caudal fin. In about 1/3 of fast turns, fish bent and held their median fins to the side of the turn before beginning to beat their tails.

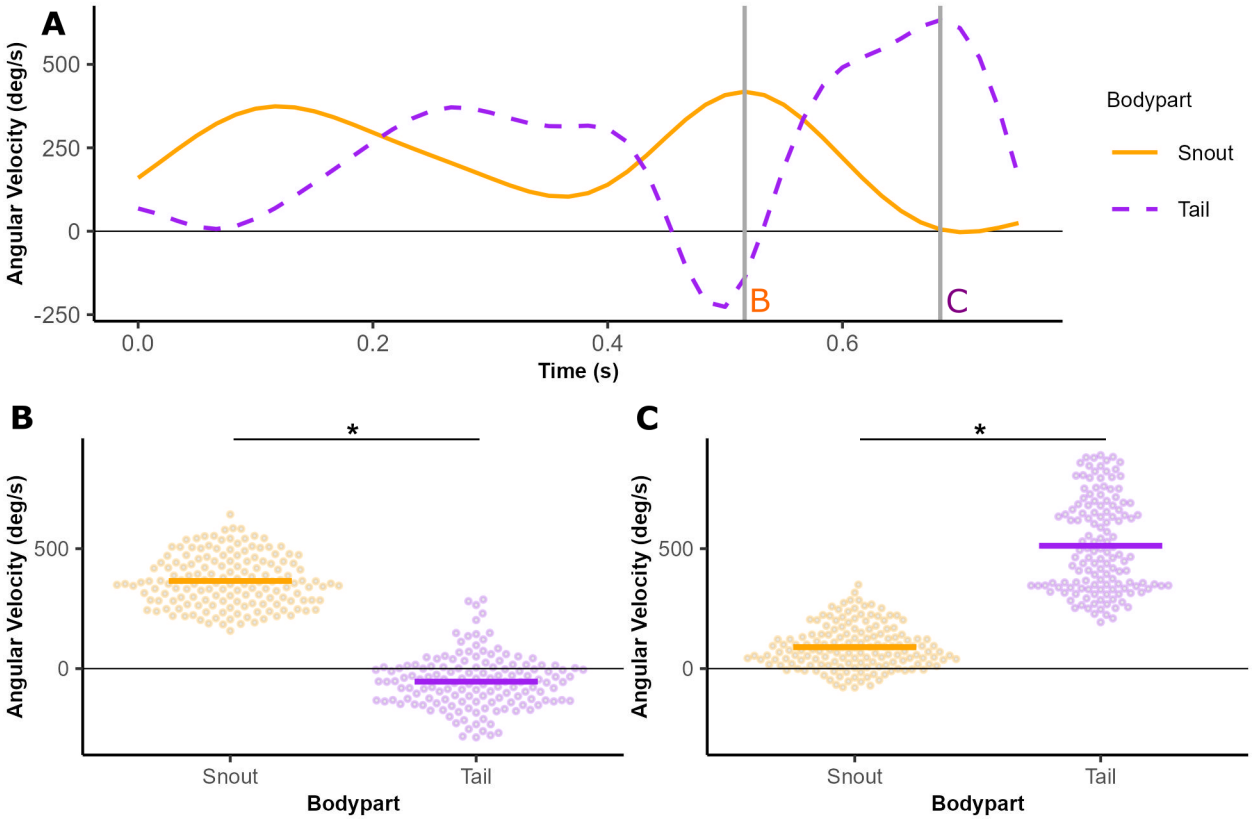

Figure 4: Snout and tail angular velocities across both slow and fast turns. (A) Representative traces of one trial's angular velocities over time for the snout (orange) and tail (purple). The representative turn is a fast turn. The gray lines represent the time of maximum angular velocity for the snout (orange "B") and tail (purple "C"). (B) Snout and tail angular velocities for each trial at the point where snout angular velocity is maximized (first gray line in A). Each point denotes the value for one trial. (C) Snout and tail angular velocities at the point where tail angular velocity is maximized (second gray line in A). Asterisks denote significance between groups.

The minimum moment of inertia was similar for slow and fast turns

Whether fish turned slowly or quickly, they bent their bodies by about the same amount, decreasing their moment of inertia to about the same value (0.9), despite different turning rates (Figure 5). The mean value of the minimum normalized moment of inertia across the duration of a slow turn was 0.9 ± 0.04 and for fast turns was 0.9 ± 0.03 ($p = 0.906$).

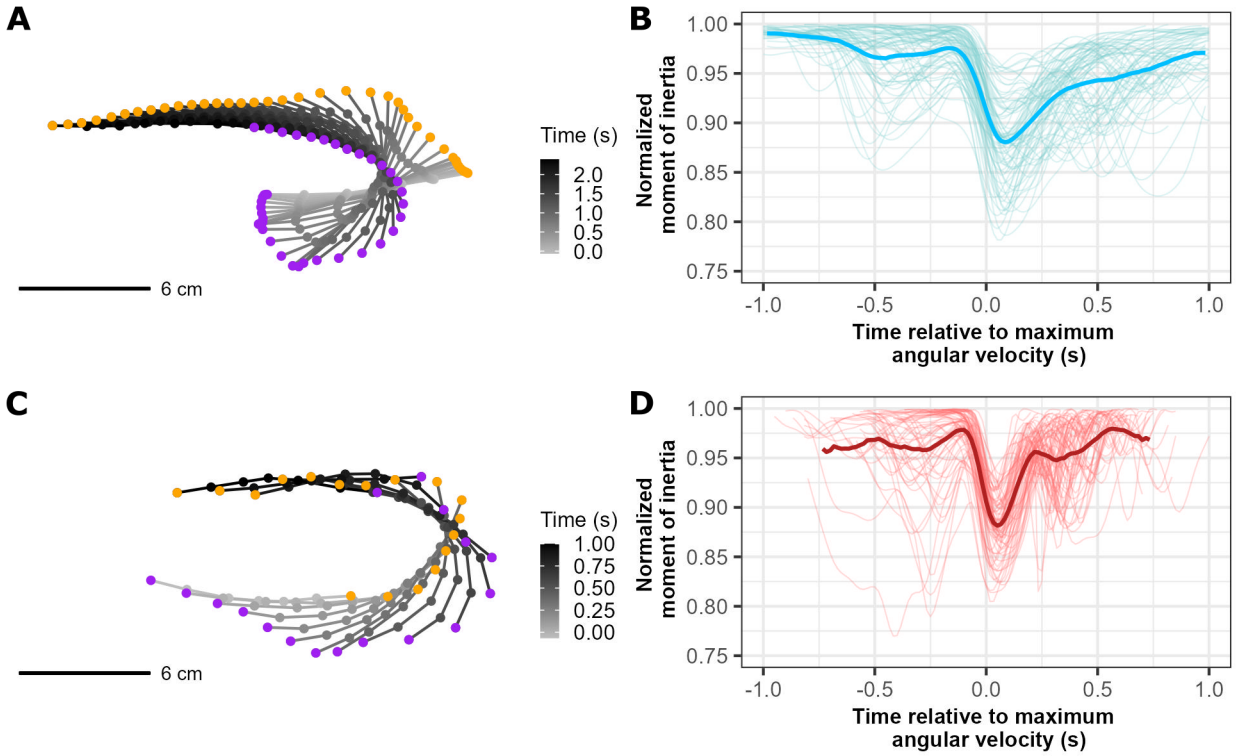

Figure 5: Fish bent their bodies to a similar degree in slow and fast turns. (A, C) Body traces of midlines for one individual for one slow (A) and one fast (C) turn. Points along the midlines denote digitized points, where the orange point is the snout and the purple point is the peduncle. Line color in (A) and (C) corresponds to the time course of the turn with lighter gray representing the beginning and darker gray representing the ending. Note the different time scale between fast and slow turns. (B, D) Normalized moment of inertia for slow (B) and fast (D) turns. Time is centered on the time of maximum angular velocity.

Lower moments of inertia resulted in higher angular velocities regardless within each turn speed

Overall, within each turn speed group, fish that bent their bodies more or held the bend longer over the course of the entire turn (resulting in a lower mean moment of inertia) turned with higher mean angular velocities (Figure 6). Fitting with a linear mixed effects regression with individual as a random effect yielded a significant negative slope for both slow ($p < 0.001$) and fast ($p < 0.001$) turns. The slopes were the same for both types of turns ($p = 0.408$). As with minimum moment of inertia, the mean moment of inertia over the entire turn did not differ significantly between slow and fast turns (0.95 ± 0.02 for both, $p = 0.114$), but the mean angular velocity was higher in fast turns (Figure 3).

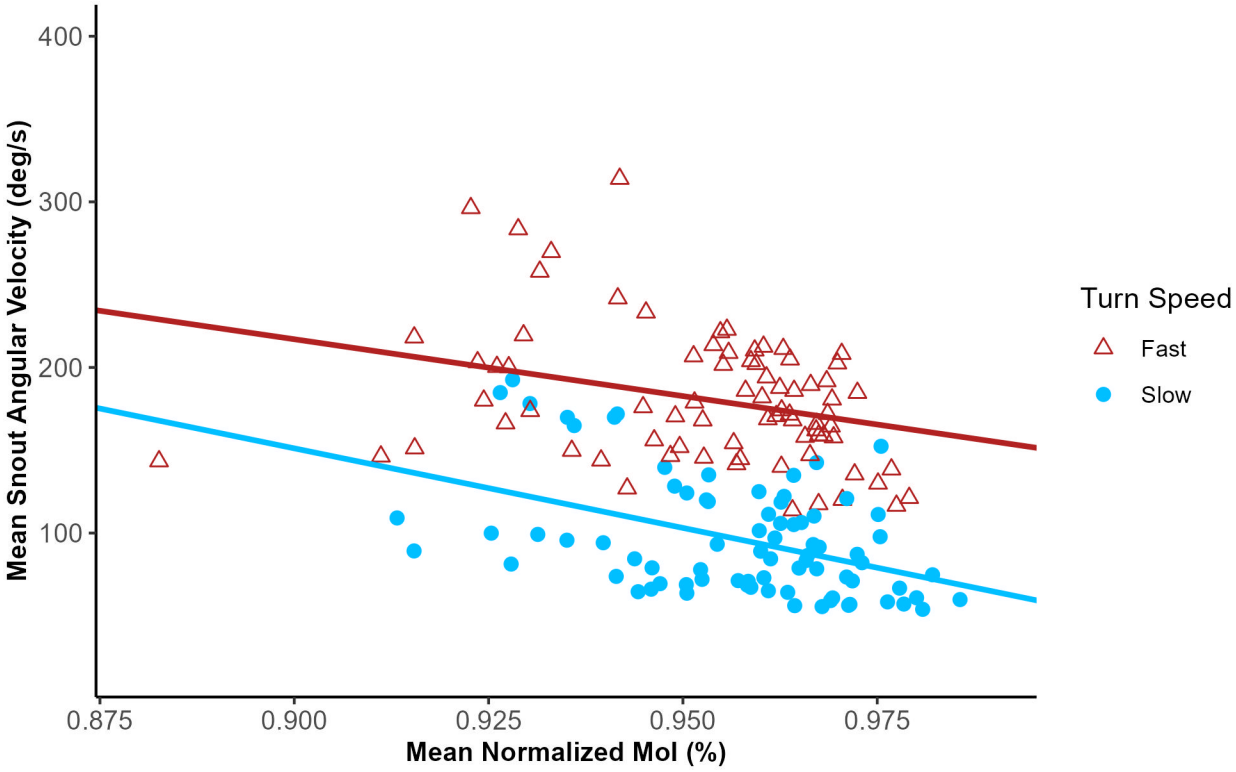

Figure 6: Within each turn speed, bluegill that bent their bodies more generated higher angular velocities. Mean moment of inertia per trial, normalized by the maximum moment of inertia for that trial, plotted against mean snout angular velocity of that trial. Data is shown for both slow (in blue) and fast turns (in red). Linear regressions for slow (light blue) and fast (red) turns are shown as dashed lines.

For the vast majority of trials (130 of 139), fish reached their maximum angular velocity before they fully minimized their moment of inertia (points in the bottom right shaded region in Figure 7). Both slow and fast turns followed this pattern with few exceptions.

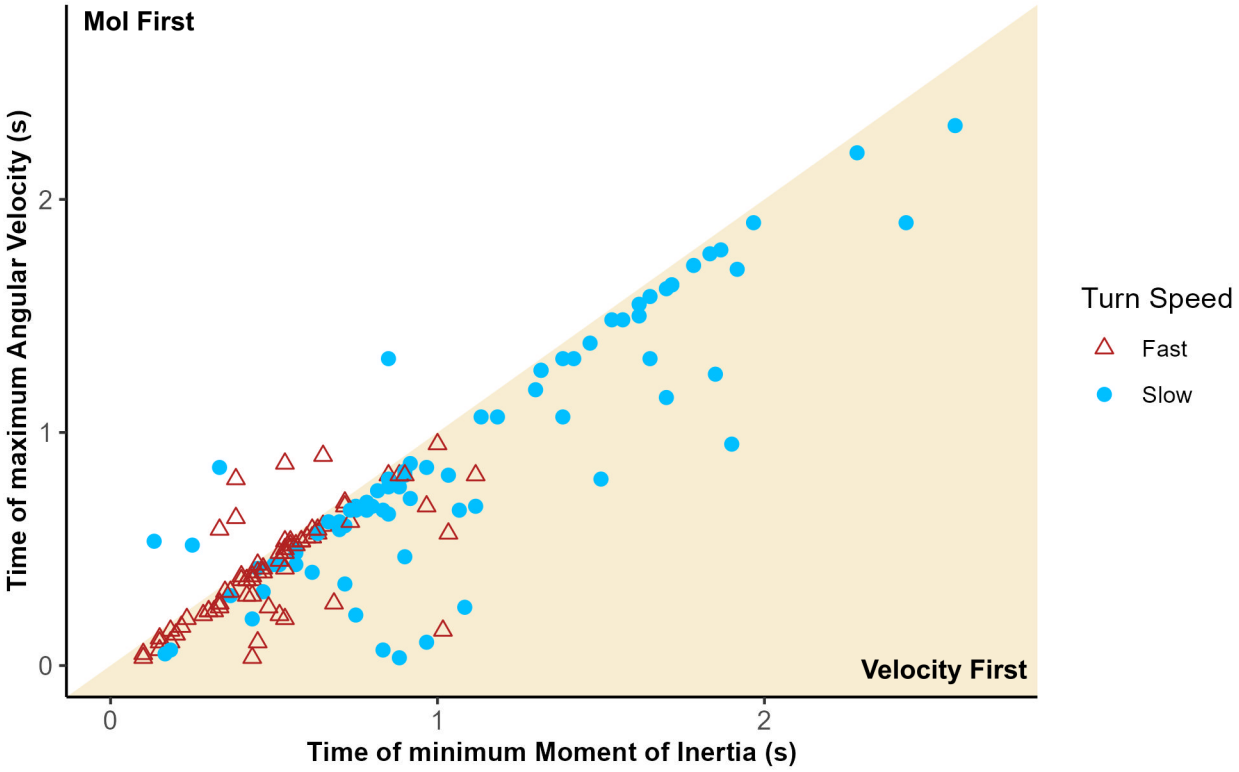

Figure 7: Bluegill consistently maximized angular velocity before minimizing moment of inertia. The time at which moment of inertia was minimized during a turn is plotted against the time at which angular velocity was maximized during that turn for both slow (blue) and fast (red) turns. The yellow shaded region is where the fish maximized its angular velocity before minimizing its moment of inertia, while the unshaded region is where the fish minimized its moment of inertia before maximizing its angular velocity.

Fast turns traded off linear and angular momentum

Linear momentum differed between the two types of turns (Figure 8 A, C), while angular momentum showed a similar pattern across the turns. Pre-turning linear momentum was significantly higher in fast turns than it was in slow turns ($p < 0.001$). For fast turns, linear momentum then significantly *decreased* in both the first and second half of the turn ($p < 0.001$ in both cases). However, for slow turns, it did not change significantly in the first half of the turn ($p = 0.141$) and significantly *increased* in the second half of the turn compared to pre turning phase ($p < 0.001$). In other words, in fast turns, bluegill initially started with higher linear momentum, which decreased during the entire turn, corresponding to an increase in angular momentum (Figure 8 B). In slow turns, bluegill initially started with low linear momentum (Figure 8 A), increased angular momentum in the first half of the turn while maintaining linear momentum, then increased linear momentum in the second half of the turn as angular momentum decreased (Figure 8 a, B).

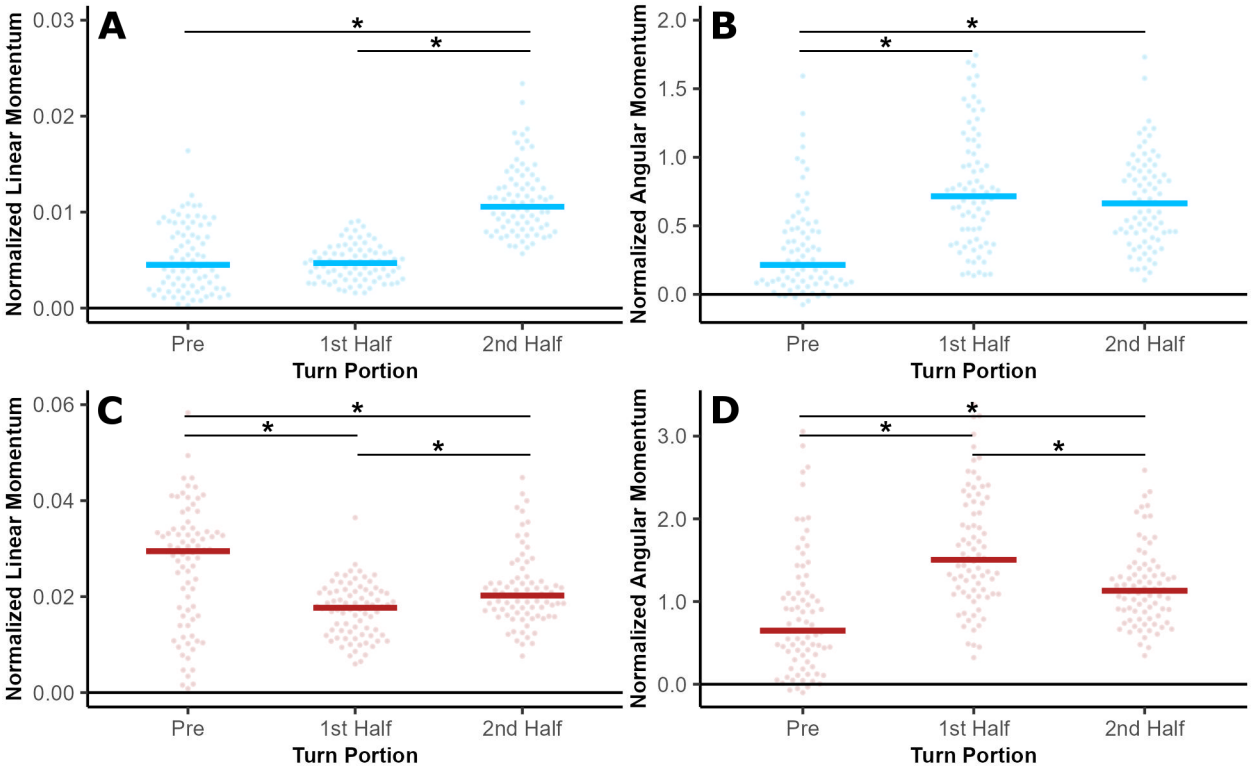

Figure 8: Bluegill converted linear to angular momentum in fast turns but not slow ones. (A,B) Linear (A) and angular (B) momentum for slow (blue) turns before the turn, during the first half of the turn, and during the second half of the turn. (C,D) Linear (C) and angular (D) momentum for fast (red) turns before the turn, during the first half of the turn, and during the second half of the turn. Asterisks denote significance between groups.

Bluegill used their pectoral fins differently during fast turns

Bluegill took more strokes with their pectoral fins in slower turns (based on a significant positive slope on the regression: $p < 0.001$) (Figure 9 A), but beat their pectoral fins at a higher mean frequency in fast turns (based on a significant inverse relationship on the regression: $p < 0.001$) (Figure 9 B). During slow turns, fish beat both their inside and outside pectoral fins at a similar amplitude ($p = 0.378$), but during fast turns, fish beat their inside fin at a higher amplitude than their outside fin ($p < 0.001$) (Figure 9 C). The inside fin amplitudes did not differ between slow and fast turns ($p = 0.643$) (Figure 9 C). Finally, bluegill take fewer backing strokes during fast turns ($p < 0.001$) (Figure 9 D). All individuals used their pectoral fins in all turns.

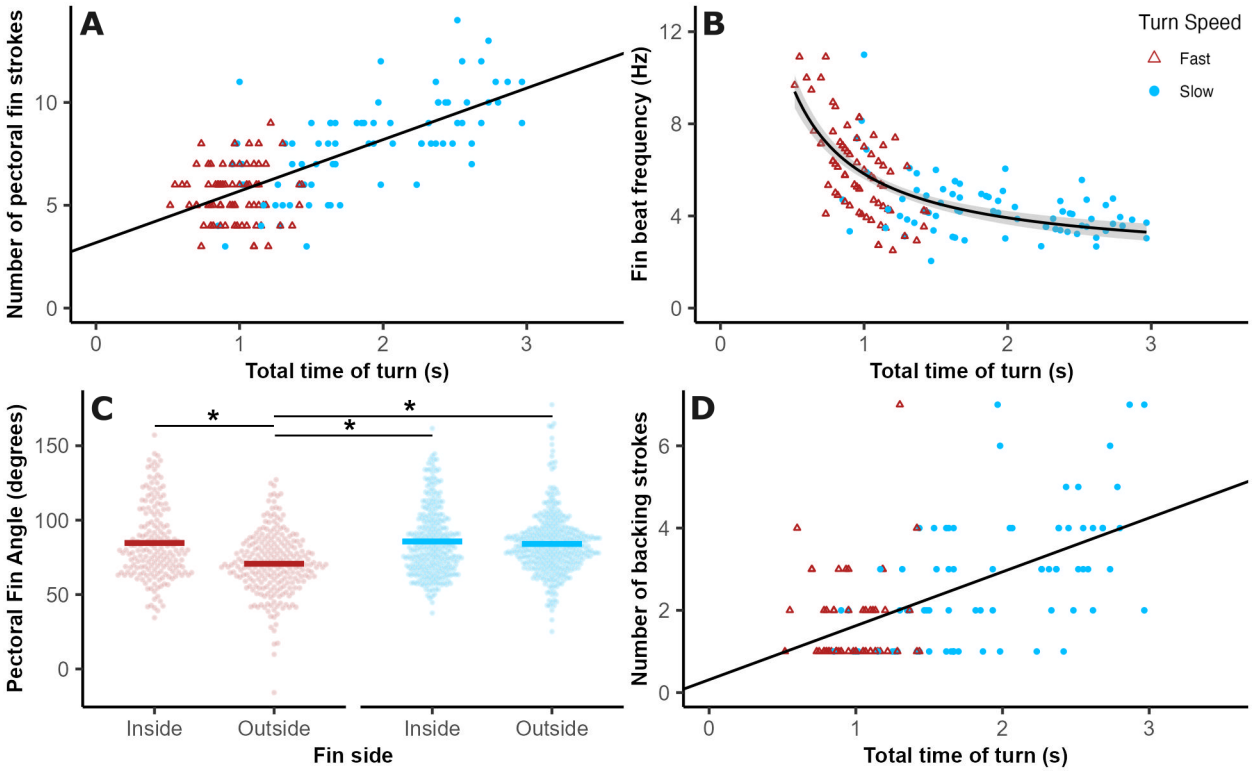

Figure 9: Bluegill used their pectoral fins differently at different speeds. Pectoral fin data for slow (blue circles) and fast (red triangles) turns. (A) Total number of pectoral fin beats increases for longer turns. The black line is the linear fit. (B) Fin beat frequency decreased for longer turns with a 1/x model shown by the black line. (C) Fin amplitude for the inside and outside fins in slow and fast turns. (D) Number of backing strokes increased for longer turns. The black line shows the linear fit. Asterisks denote significance between groups.

Timing of maximum torque and minimum moment of inertia differed based on turn speed

The timing of the estimated maximum torque relative to moment of inertia was different for slow and fast turns. For 51 of 79 slow turns fish maximized torque before minimizing moment of inertia. In contrast, for 54 of 78 fast turns, they minimized moment of inertia first. For slow turns, fish minimized their moment of inertia a mean of 0.06 $\pm$ 0.3s *after* maximizing torque, which was significantly different than fast turns, where fish minimized moment of inertia 0.2 $\pm$ 0.3s *before* maximizing torque ($p < 0.001$) (Figure 10). For slow turning fish, the difference between the time at which they maximized torque and minimized moment of inertia (Figure 10 B) was negative (torque first), but not significantly different from zero ($p = 0.093$), whereas for fast turning fish, the difference was significantly positive (torque second) ($p > 0.001$).

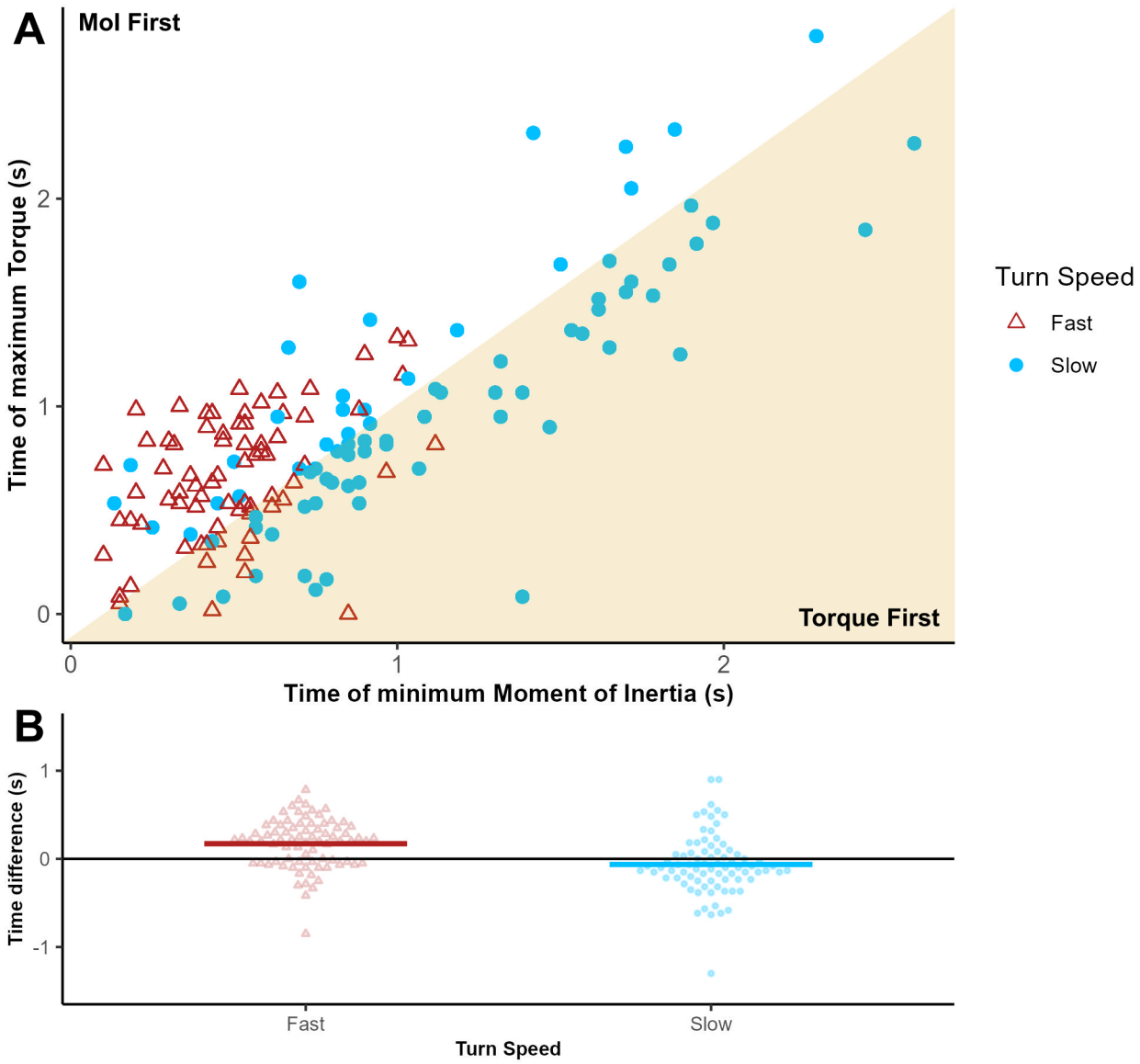

Figure 10: Slow and fast turns differed in their timing of maximum torque and minimum moment of inertia. (A) The time at which moment of inertia was minimized during a turn is plotted against the time at which torque was maximized during that turn for both slow (blue) and fast (red) turns. The yellow shaded region is where the fish maximized its torque before minimizing its moment of inertia, while the unshaded region is where the fish minimized its moment of inertia before maximizing its torque. (B) The difference between the time that the bluegill maximized their torque and minimized their moment of inertia is show for both fast (red) and slow (blue) turns. The solid black line represents the theoretical point at which both events would occur at the same time.

Discussion

Fast turns are not sped up slow turns

Fast turns are not sped up slow turns, but are kinematically distinct. During slow turns, bluegill behaved similarly to jellyfish and zebrafish as studied by Dabiri et al (2020), reaching similar angular velocities and maximizing torque before minimizing moment of inertia. However during fast turns, bluegill did something different, reaching higher angular velocities and maximizing torque after minimizing moment of inertia. This change in timing coupled with the discrete differences in how linear momentum changes during turning suggests that fish change their kinematics based on some threshold of turn speed (Figure 10 and Figure 8).

Physically, it makes sense that bluegill change their timing of torque and moment of inertia. Due to how torque scales with r (Equation 0.3), while moment of inertia scales inversely with r^2 (Equation 0.2), a reduction in r decreases moment of inertia more than torque. Therefore, bluegill prioritized minimizing moment of inertia early to maximize angular acceleration at the start. For slower turns, they can instead turn how Dabiri et al (2020) found and maximize torque at the beginning with a straighter body before bending to accelerate through the turn.

My results contrast with those of Howe and Astley (2020) in that I found discrete differences based on speed while they did not. I believe this was because all of the turns they studied would fall into my category of "fast turns". They did not control the heading change, and therefore most of the turns they studied were much smaller than those presented here. The largest was 120 deg (Howe and Astley, 2020), which is below the 180 degree turns I studied. However, even the turns that had a small angular change had high angular velocities, and would fall into my fast turn category. Their routine turns had maximum angular velocities of around 600 deg/s, which is greater than the maximum angular velocities in my fast turns, which averaged around 430 deg/s.

The slow turns then represent a qualitatively different behavior than fast turns, and than the turns studied by Howe and Astley (2020). I believe they represent the type of behavior that fish might use to maneuver in a controlled manner around an obstacle or while grazing. For example, coelacanths make similar slow turns when maneuvering around an obstacle (Fricke and Hissmann, 1992).

Fast turns are not C-starts

Importantly, the turns I measured were not C-starts. Compared to C-starts, even the fast turns took much longer to complete. The shortest turn in my study (0.6sec long) took much longer than the longest C-start (0.21sec) in Domenici and Blake's (1997) review. The turns also had much lower maximum angular velocities, of around 600 deg/s, compared to 2000 deg/s or more in fast starts (Tytell and Lauder, 2008). Moreover, in fast starts, fish tend to swing the head to one side (during the "C") and back toward the other side as they kick out of the turn (Domenici and Blake, 1997), meaning that the head angular velocity has a positive and a negative peak. In the turns I measured, the fish only swung their heads to one side, meaning that angular velocity only had a positive peak (Figure 3). During turning, bluegill in my study also reached a maximum snout linear velocity of 4.7 L/s, which is less than half of maximums that have been reported during bluegill C-starts (Webb, 1978).

But fast turns share some similarities with slow turns

Despite the distinct differences in the timing of maximum torque and minimum moment of inertia (Figure 10 B), slow and fast turns share many similar features. Whether bluegill were performing a slow or fast turn, they began turning with an anterior body movement, similar to what Gray (1933) saw in turning whiting. More recently, Thandiackal and Lauder (2020) found that the anterior and posterior body in zebrafish produce substantial positive work during turning, "planting" the tail and using it to drive the anterior body around through the turn.

Fast and slow turns were also quantitatively similar across a range of variables. First of all, regardless of whether bluegill turn slowly or quickly, they did not change how much they maximally bent their bodies, resulting in similar minimum moments of inertia (Figure 5). This may be a physical constraint based on the shape and thickness of the body.

Additionally, in both slow and fast turns, bluegill maximized their angular velocity around the same time that they minimized moment of inertia (Figure 7), similar to what Dabiri et al (Dabiri et al., 2020) found, likely as a result of the physics of angular acceleration (Equation 0.1). Bluegill also consistently used a similar ratcheting behavior as tuna (Downs et al., 2023), suggesting that turning involves similar kinematics among different species.

Pectoral fins and momentum may drive differences

There were both continuous and discrete differences in how bluegill used their pectoral fins during slow and fast turns. Pectoral fins played a greater role *continuously* during a slow turn, where fish tended to take more strokes, but a greater role *instantaneously* during a fast turn, where fish tended to take faster strokes that would produce higher torque (Figure 9). Additionally, many of these pectoral fin strokes were backing strokes. These occured when bluegill extended their inner fin far towards their heads during turning. These backing strokes were likely pushing water anteriorly to help the fish rotate. Drucker and Lauder (2001) quantified pectoral fin forces during turning bluegill and found that during turning pectoral fins act asymmetrically, and that both the turning side and weak side fins generate strong lateral and posterior forces respectively. Importantly, they studied bluegill turning slightly to avoid an obstacle (Drucker and Lauder, 2001) whereas I studied full 180 degree turns, suggesting that to turn more extremely, bluegill may also use their pectoral fins to generate backing forces. Finally, the backing behavior that I saw has previously been observed in coelacanths who couple a backwards stroke of their inner pectoral fin with a forwards stroke of their outer pectoral fin during turning (Fricke and Hissmann, 1992).

Additionally, bluegill traded off linear and angular momentum differently in slow and fast turns. In both slow and fast turns, bluegill began with little angular momentum and needed to increase it to complete the turn (Figure 8 B, D). For fast turns, the angular momentum seemed to come in part from their starting linear momentum, as linear momentum decreased at the same time that angular momentum increased (Figure 8 C, D). In contrast, during slow turns, bluegill did not start with as high linear momentum and subsequently increased both linear and angular momentum in order to turn around and accelerate in the opposite direction. This means they needed to accelerate, gaining both linear and angular velocity.

Future directions

I studied a species thought to be specialized for maneuvering (Webb, 1984b), with a deep body and large pectoral fins. The tradeoff I highlighted between torque production and moment of inertia is likely to be different for different species, akin to how maneuverability and agility are different for different species. For more fusiform fishes, such as bass, the moment of inertia for the straight body should be higher, making it more important to reduce the inertia for turning and more challenging to turn in a tighter radius. In that case, it might be that they would not perform a kinematically distinct slow turn as I have defined it. Even more

elongate fishes, such as eels, likely turn in a different way again. My analysis was based on the idea that the body flexes in a single curve, and that the whole body rotates around a single center of rotation. For eels, their bodies are so flexible that they can pass a point or multiple points of flexion along the body so that different portions can rotate independently (Gray, 1933), which may circumvent the tradeoff that other less flexible fishes face. Finally, organisms like boxfish which are rigid (Walker, 2000) and rays which are laterally rigid (Parson et al., 2011) and are thus less able to modulate their moments of inertia, again potentially needing to find find alternate solutions to effectively turn around. However, despite their lateral rigidity, rays are still able to faster than other rigid bodied species of similar lengths (Fish et al., 2018). Furthermore, Dabiri et al (2020) found consistencies in the patterns even between zebrafish and jellyfish. Therefore, future studies could expand this speed dependent research to better understand and quantify how different morphologies allow fish or other aquatic organisms to resolve the tradeoff between moment of inertia and torque production.

Additionally, I found that that fast turns are not sped up slow turns and are kinematically distinct, but there are some components that vary continuously. Therefore more work could be done to determine exactly when a slow turn becomes a fast turn. Is the transition gradual or discrete? Future experimental work, similar to mine, could address when this transition occurs for bluegill, and whether it differs for different species of fish. Moreover, robotic and modelling studies could help us understand what aspects of body and fin motion drive the shift from slow to fast turns, and which are consequences of the change in speed, since such methods can directly control all features of how their "fish" turn and can compare both the continuously varying parameters and discrete differences.

While my work quantifies differences in slow and fast turns and highlights several mechanisms driving these differences, I was not able to distinguish the individual contributions of each fin. These could be substantial, especially given how active the median fins are in turning bluegill and dolphin fish (Webb and Keyes, 1981) Therefore I advocate for detailed PIV during turning with a focus on what each fin is doing. In spontaneous routine turns, this is not feasible, because fish may not turn consistently in the laser light sheet necessary for PIV. However, my setup means that fish turn in a controlled and repeatable way in a known position, which may make such flow measurements possible. Specifically, I showed that bluegill use their pectoral and paired median fins extensively during turning. Therefore to better characterize turning and turning performance in fishes, I propose that future studies use PIV to focus on the pectoral and paired median fins during turning.

Finally, while my programmable car was effective at eliciting repeatable turns, it was different from a

fish's natural habitat. While the "car" triggers a turn, the fish did not interact physically with the car in any way. Thus, I argue that, if a fish were to perform a 180deg turn without the car, it would do it in the same way. Even so, it would be useful to compare my results to laboratory experiments of spontaneous turning or to studies conducted in the wild, which could show whether fish spontaneously perform turns similar to those I have measured here, or could identify other ways that fish in natural environments might cope with the tradeoff between high torque and low moment of inertia.

Acknowledgements

I would like to acknowledge Dr. Barry Trimmer, Dr. Erik Dopman, Dr. Frank Fish, Dr. Yordano Jimenez, Dr. Mike Fath, and Dr. Ben Tidswell for their support and guidance on this project. I would also like to acknowledge the Tytell lab members for all of their help.

Competing Interests

The authors declare no competing interests.

Funding

I received funding from NSF IOS 1652582 and ARO W911NF-17-1-0234.

Data Availability

Code and data are available through Zenodo (DOI to be generated upon acceptance). For review purposes, the code is available directly on Github at https://github.com/andrewdclark/BluegillTurning.

References

Ashraf, I., Wassenbergh, S. V. and Verma, S. (2020). Burst-and-coast swimming is not always energetically beneficial in fish (*Hemigrammus bleheri*). *Bioinspiration & Biomimetics* **16**, 016002. doi: 10.1088/1748-3190/abb521.

Bates, D., Mächler, M., Bolker, B. and Walker, S. (2015). Fitting linear mixed-effects models using Lme4. *Journal of Statistical Software* **67**, 1–48. doi: 10.18637/jss.v067.i01.

Coughlin, D. J. and Dutterer, M. D. (2024). Intermittent swimming and muscle power output in brook trout, *Salvelinus fontinalis*. *Journal of Experimental Zoology Part A: Ecological and Integrative Physiology* **341**, 896–902. doi: 10.1002/jez.2844.

Coughlin, D. J., Chrostek, J. D. and Ellerby, D. J. (2022). Intermittent propulsion in largemouth bass, *Micropterus salmoides*, increases power production at low swimming speeds. *Biology Letters* **18**, 20210658. doi: 10.1098/rsbl.2021.0658.

Coughlin, D. J., Santarcangelo, K., Wilcock, E., Tum Suden, D. J. and Ellerby, D. J. (2023). Muscle power production during intermittent swimming in bluegill sunfish. *Journal of Experimental Zoology Part A: Ecological and Integrative Physiology* **339**, 1026–1035. doi: 10.1002/jez.2751.

Dabiri, J. O., Colin, S. P., Gemmell, B. J., Lucas, K. N., Leftwich, M. C. and Costello, J. H. (2020). Jellyfish and fish solve the challenges of turning dynamics similarly to achieve high maneuverability. *Fluids* **5**, 106. doi: 10.3390/fluids5030106.

Domenici, P. and Blake, R. W. (1997). The kinematics and performance of fish fast-start swimming. *Journal of Experimental Biology* **200**, 1165–1178. doi: 10.1242/jeb.200.8.1165.

Domenici, P. and Hale, M. E. (2019). Escape responses of fish: A review of the diversity in motor control, kinematics and behaviour. *Journal of Experimental Biology* **222**, jeb166009. doi: 10.1242/jeb.166009.

Downs, A. M., Kolpas, A., Block, B. A. and Fish, F. E. (2023). Multiple behaviors for turning performance of Pacific bluefin tuna (*Thunnus orientalis*). *Journal of Experimental Biology* **226**, jeb244144. doi: 10.1242/jeb.244144.

Drucker, E. G. and Lauder, G. V. (2001). Wake Dynamics and Fluid Forces of Turning Maneuvers in Sunfish. *Journal of Experimental Biology* **204**, 431–442. doi: 10.1242/jeb.204.3.431.

Dunnington, D., Thorne, B. and Hernangómez, D. (2023). Ggspatial: Spatial data framework for Ggplot2. url: https://cran.r-project.org/web/packages/ggspatial/index.html.

Eklund, A. and Trimble, J. (2021). Beeswarm: The bee swarm plot, an alternative to stripchart. url: https://cran.r-project.org/web/packages/beeswarm/index.html.

Fath, M. A., Nguyen, S. V., Donahue, J., McMenamin, S. K. and Tytell, E. D. (2023). Static stability and swim bladder volume in the bluegill sunfish (*Lepomis macrochirus*). *Integrative Organismal Biology* **5**, obad005. doi: 10.1093/iob/obad005.

Feldmeth, C. R. (1983). Costs of aggression in trout and pupfish. In *Behavioral energetics*, pp. 117–138. Columbus, OH: Ohio State University Press.

Fish, F. E. (2020). Advantages of aquatic animals as models for bio-inspired drones over present AUV technology. *Bioinspiration & Biomimetics* **15**, 025001. doi: 10.1088/1748-3190/ab5a34.

Fish, F. E., Kolpas, A., Crossett, A., Dudas, M. A., Moored, K. W. and Bart-Smith, H. (2018). Kinematics of swimming of the manta ray: Three-dimensional analysis of open-water maneuverability. *Journal of Experimental Biology* **221**, jeb166041. doi: 10.1242/jeb.166041.

Flammang, B. E. and Lauder, G. V. (2013). Pectoral fins aid in navigation of a complex environment by bluegill sunfish under sensory deprivation conditions. *Journal of Experimental Biology* **216**, 3084–3089. doi: 10.1242/jeb.080077.

Fox, J. and Weisberg, S. (2019). *An R Companion to Applied Regression*. Third edition. Thousand Oaks CA: Sage.

Fricke, H. and Hissmann, K. (1992). Locomotion, fin coordination and body form of the living coelacanth *Latimeria chalumnae*. *Environmental Biology of Fishes* **34**, 329–356. doi: 10.1007/BF00004739.

Fuiman, L. A. and Webb, P. W. (1988). Ontogeny of routine swimming activity and performance in zebra danios (Teleostei: Cyprinidae). *Animal Behaviour* **36**, 250–261. doi: 10.1016/S0003-3472(88)80268-9.

Garrido-Jurado, S., Muñoz-Salinas, R., Madrid-Cuevas, F. J. and Marín-Jiménez, M. J. (2014). Automatic generation and detection of highly reliable fiducial markers under occlusion. *Pattern Recognition* **47**, 2280–2292. doi: 10.1016/j.patcog.2014.01.005.

Gray, J. (1933). Directional control of fish movement. *Proceedings of the Royal Society B: Biological Sciences* 115–125. doi: 10.1098/rspb.1933.0035.

Higham, T. E. (2007). Feeding, fins and braking maneuvers: Locomotion during prey capture in centrarchid fishes. *Journal of Experimental Biology* **210**, 107–117. doi: 10.1242/jeb.02634.

Hitchcock, A. C., Chen, T., Connolly, E., Darakananda, K., Jeong, J., Quist, A., Robbins, A. and Ellerby, D. J. (2015). Trade-offs between performance and variability in the escape responses of bluegill

sunfish (*Lepomis macrochirus*). *Biology Open* **4**, 743–751. doi: 10.1242/bio.201511577.

Howe, S. P. and Astley, H. C. (2020). The control of routine fish maneuvers: Connecting midline kinematics to turn outcomes. *Journal of Experimental Zoology Part A: Ecological and Integrative Physiology* **333**, 579–594. doi: 10.1002/jez.2398.

Karashchuk, P., Rupp, K. L., Dickinson, E. S., Walling-Bell, S., Sanders, E., Azim, E., Brunton, B. W. and Tuthill, J. C. (2021). Anipose: A toolkit for robust markerless 3D pose estimation. *Cell Reports* **36**, 109730. doi: 10.1016/j.celrep.2021.109730.

Kay, M. (2024). Ggdist: Visualizations of distributions and uncertainty in the grammar of graphics. *IEEE Transactions on Visualization and Computer Graphics* **30**, 414–424. doi: 10.1109/TVCG.2023.3327195.

Kay, M. and Wiernik, B. M. (2024). Ggdist: Visualizations of distributions and uncertainty. url: https://cloud.r-project.org/web/packages/ggdist/index.html.

Lenth, R. V., Banfai, B., Bolker, B., Buerkner, P., Giné-Vázquez, I., Herve, M., Jung, M., Love, J., Miguez, F., Piaskowski, J., et al. (2025). Emmeans: Estimated marginal means, aka least-squares means. url: https://cran.r-project.org/web/packages/emmeans/index.html.

Marcoux, T. M. and Korsmeyer, K. E. (2019). Energetics and behavior of coral reef fishes during oscillatory swimming in a simulated wave surge. *Journal of Experimental Biology* **222**, jeb191791. doi: 10.1242/jeb.191791.

Parson, J. M., Fish, F. E. and Nicastro, A. J. (2011). Turning performance of batoids: Limitations of a rigid body. *Journal of Experimental Marine Biology and Ecology* **402**, 12–18. doi: 10.1016/j.jembe.2011.03.010.

Pereira, T. D., Tabris, N., Matsliah, A., Turner, D. M., Li, J., Ravindranath, S., Papadoyannis, E. S., Normand, E., Deutsch, D. S., Wang, Z. Y., et al. (2022). SLEAP: A deep learning system for multi-animal pose tracking. *Nature Methods* **19**, 486–495. doi: 10.1038/s41592-022-01426-1.

Porter, M. E., Roque, C. M. and Long Jr., J. H. (2009). Turning maneuvers in sharks: Predicting body curvature from axial morphology. *Journal of Morphology* **270**, 954–965. doi: 10.1002/jmor.10732.

Porter, M. E., Roque, C. M. and Long, J. H. (2011). Swimming fundamentals: Turning performance of leopard sharks (*Triakis semifasciata*) is predicted by body shape and postural reconfiguration. *Zoology* **114**, 348–359. doi: 10.1016/j.zool.2011.06.001.

Puckett, K. J. and Dill, L. M. (1984). Cost of sustained and burst swimming to juvenile coho salmon (*Oncorhynchus kisutch*). *Canadian Journal of Fisheries and Aquatic Sciences* **41**, 1546–1551. doi:

10.1139/f84-192.

Roche, D. G., Tytell, E. D. and Domenici, P. (2023). Kinematics and behaviour in fish escape responses: Guidelines for conducting, analysing and reporting experiments. *Journal of Experimental Biology* **226**, jeb245686. doi: 10.1242/jeb.245686.

Schindelin, J., Arganda-Carreras, I., Frise, E., Kaynig, V., Longair, M., Pietzsch, T., Preibisch, S., Rueden, C., Saalfeld, S., Schmid, B., et al. (2012). Fiji: An open-source platform for biological-image analysis. *Nature Methods* **9**, 676–682. doi: 10.1038/nmeth.2019.

Smith, G. D. (1985). *Numerical Solution of Partial Differential Equations: Finite Difference Methods*. Clarendon Press.

Thandiackal, R. and Lauder, G. V. (2020). How zebrafish turn: Analysis of pressure force dynamics and mechanical work. *Journal of Experimental Biology* **223**, jeb223230. doi: 10.1242/jeb.223230.

Tytell, E. D. and Lauder, G. V. (2008). Hydrodynamics of the escape response in bluegill sunfish, *Lepomis macrochirus*. *Journal of Experimental Biology* **211**, 3359–3369. doi: 10.1242/jeb.020917.

Walker, J. A. (2000). Does a Rigid Body Limit Maneuverability? *Journal of Experimental Biology* **203**, 3391–3396. doi: 10.1242/jeb.203.22.3391.

Webb, P. W. (1978). Fast-start performance and body form in seven species of teleost fish. *Journal of Experimental Biology* **74**, 211–226. doi: 10.1242/jeb.74.1.211.

Webb, P. W. (1983). Speed, acceleration and manoeuvrability of two teleost fishes. *Journal of Experimental Biology* **102**, 115–122. doi: 10.1242/jeb.102.1.115.

Webb, P. W. (1984a). Form and function in fish swimming. *Scientific American* **251**, 72–83.

Webb, P. W. (1984b). Body and fin form and strike tactics of four teleost predators attacking fathead minnow (*Pimephales promelas*). *Canadian Journal of Fisheries and Aquatic Sciences* **41**, 157–165. doi: 10.1139/f84-016.

Webb, P. W. (1986). Effect of body form and response threshold on the vulnerability of four species of teleost prey attacked by largemouth bass (*Micropterus salmoides*). *Canadian Journal of Fisheries and Aquatic Sciences* **43**, 763–771. doi: 10.1139/f86-094.

Webb, P. W. (1991). Composition and mechanics of routine swimming of rainbow trout, *Oncorhynchus mykiss*. *Canadian Journal of Fisheries and Aquatic Sciences* **48**, 583–590. doi: 10.1139/f91-074.

Webb, P. W. and Keyes, R. S. (1981). Division of labor between median fins in swimming dolphin (Pisces: Coryphaenidae). *Copeia* **1981**, 901–904. doi: 10.2307/1444198.

Weihs, D. (1973). The mechanism of rapid starting of slender fish. *Biorheology* **10**, 343–350. doi: 10.3233/BIR-1973-10308.

Weihs, D., Keyes, R. S. and Stalls, D. M. (1981). Voluntary swimming speeds of two species of large carcharhinid sharks. *Copeia* **1981**, 219–222. doi: 10.2307/1444062.

Wickham, H., Averick, M., Bryan, J., Chang, W., McGowan, L. D., François, R., Grolemund, G., Hayes, A., Henry, L., Hester, J., et al. (2019). Welcome to the Tidyverse. *Journal of Open Source Software* **4**, 1686. doi: 10.21105/joss.01686.

Prospectus

When looking back at my work and at my time at Tufts, there are two main things I want to address in the prospectus: the science, and the PhD in general. Obviously the science merits a profound discussion, but it is only one part of the whole story, and in this section, I hope to also highlight the PhD outside of the science.

The science

What worked and what did not

Going into Tufts, I was coming from the University of St Andrews where I had conducted some research into larger evolutionary trends. Before that, I had spent some time in various biomechanics labs, focusing specifically on kinematics and on how to collect and analyze kinematic data. Therefore it comes as no surprise that when I began my journey at Tufts, I started by collecting large scale kinematic data with the goal of assembling a massive dataset for analysis. While this ended up being a generally successful path for me, it was also one of my biggest pitfalls. Large scale kinematic data is very powerful for asking and answering important questions, but is incredibly difficult to collect and incredibly time consuming to analyze.

As I began my PhD with hundreds of videos, I was very quickly faced with the challenge of digitizing hundreds of thousands of frames. This situation was a very strange mix of something that worked very well and something that worked horribly. On the one hand, it allowed me to conduct some good and powerful analysis. On the other hand, it loomed over me like an arduous mountain and slowed me down, precluded me from progressing the way I wanted to. If I could go back in time and talk to myself in the first year of my PhD, I would encourage myself to focus on something that did not require as much digitizing, so that I could take a few smaller steps before making a big leap.

Another challenging, yet rewarding aspect of my PhD was how disparate it rapidly became. When I initially started at Tufts, I began with the turning project: a challenging and long term project that I could have

easily broken down into several dissertation chapters had I truly focused in on it. Instead, I very quickly became a mentor on a project on EKGs in swimming bluegill, dove into the field of deceleration, and eventually branched into species-level comparisons of steady swimming. While I am grateful for all of these projects, I also spread myself very thin and instead of being able to dedicate my time to one field, I needed to address 4. Thus, it felt like I was doing 4 PhDs, instead of just 1. This both worked well and was a challenge, because while I am proud of all of the work that came out of my PhD, I do wish I had narrowed my sights ever so slightly.

Future directions

Going forward I feel there are a few opportunities to build on the work that I have done. First of all, as with many projects, there is yet more data to analyze and refine. It was a gargantuan task to analyze the data that I have already had the opportunity to analyze, and still more remains untouched. There may be a full second PhD's worth of work that remains.

I view the most promising opportunities to be in some of my deceleration trials where I operated FISHCAR at a maximum speed with no oncoming flow and stopped it in the middle of its progress along the track. This created a situation in which the bluegill needed to stop quite rapidly, exhibiting behaviors not observed in the more gradual decelerations that I analyzed. In these maximal brakes, it was apparent that bluegill were heavily dependent on every single one of their fins and I expect the results would line up quite well with the larger body of literature on rapid braking in fishes. I also suspect that it could further contextualize and develop the ideas that I explored in my deceleration chapter. While I did not have the time or opportunity to analyze this data during my PhD, I strongly believe that this could be a very powerful future direction.

I also hope that the lab (likely Olivia) continues to collect and analyze kinematic data of swimming bluegill and pumpkinseed. Currently, the dataset consists of only 3 individuals, but the trends have previously been shown to be very consistent and repeatable – particularly keeping Stephen Michaels' senior thesis on differences in accelerating bluegill and pumpkinseed in mind. I believe that by adding more individuals, we can better understand the differences between these two morphologically similar species. I also think there are a lot of ways in which this study can grow, including EMGs, which would give us insight into how the two fish might be different with respect to how maximally they need to use their bodies, and how their body stiffness might change. Overall, further analysis could provide some very interesting results that could help us disentangle the differences in steady swimming between these two species.

I also believe there is a lot of potential to advance all of these projects by looking beyond the kinematics. Due to my set of skills and to the questions I was asking, kinematic studies fit best and so those are the ones that I conducted. However, while my experiments quantified how fish behave, they do very little to move beyond that. In particular, physical and evolutionary links are addressed, but could be expanded. For example, EMG and PIV experiments would provide a window directly connecting the kinematics to the physics, and would reduce some of the conjecture. To address evolutionary confounds and explore the development of fish over long periods of time, we could conduct these experiments in a larger array of species. My previous work has taught me the importance of evolution in understanding anything about biology, and while I kept that in mind during this PhD, by using at most 2 species, I really have not been able to address the evolutionary influence on the observed kinematics. I would love to see future studies on individuals across the phylogenetic tree to understand how locomotion evolved in addition to how it is employed.

Overall, unsteady behaviors constitute a field that bears further analysis, not only because they help us understand the organisms that we study, but also because they offer us promise for future engineering applications. Despite being so complex, unsteady locomotion is quite regular and without an in depth analysis and understanding of it, we necessarily limit ourselves to what is easy and to what is less informative. Unsteady locomotion could be critical to our development of our own ideas and designs and as a result, bears future consideration.

The PhD

Everyone tells you that when you are at the end of your PhD, you look back and you realize you could have done the whole thing in far less time. While that is certainly true, it ignores the significance of the journey. Time is a strange thing when you are doing a PhD: it seems endless, but before you know it, it is all too finite. Thinking back to who I was at the beginning and to who I am at the end, it is hard to know what I did wrong, what I did right, and what I wish I had done differently because everything I did was an integral part of the journey. That being said, there are a few things I wish I had known at the start, that would have helped me along the way.

Going into the PhD, I assumed that the main challenges I would face would be scientific in nature; that I would confront experimental complications and learn how to overcome them. The challenging parts of the PhD were not scientific in nature at all. In particular one thing I would have made clear to my younger self

is how academia works. I expected academia to be dominated by the research and focused on the science and on how to turn the science into something of value. But while the science was certainly a large portion of the PhD, it was absolutely not the most prominent. Instead, much of my time was taken up by mentoring, by teaching, by interacting with my fellow students, and by grappling with my own inner battle to stick with the PhD despite the physical, emotional, and financial costs. At the start, I thought the PhD was a job, but in actuality, it was a learning opportunity.

I would also encourage myself to view my time as more valuable than I did. It is so easy to spend all of your time helping others, especially in an academic institution. As a result, it is often easy to lose track of where your time is going. If I could go back, I would tell myself to be a little bit more protective of my time so that I could get my own work done. While I was able to manage a lot of projects and to help a lot of people achieve their dreams, it often felt like I did so at a cost to myself where I was not able to do what I needed to do in the time that I needed to do it, thereby making things more challenging for me at the end.

An additional complication is that, by supporting others' projects, I spread my own research across a large range of sometimes loosely related fields. This made it difficult to master any one of them. I am grateful for the opportunity to grow in so many different ways and to gain so much widespread knowledge. Nonetheless, I still gravitate toward the idea of a more focused and centralized project, especially considering the ultimate goal of the PhD is to produce a dissertation and to defend it, with everything else seemingly secondary to that objective.

One thing that I would not change is my commitment to going to and giving presentations. Science is nothing if it is not communicated, and while the writing is often very difficult for me, presenting and speaking feels natural. I will never regret all the time I spent preparing and giving presentations and I am very grateful for all the opportunities I have had to hone my craft. Whether I was presenting at regional or general SICB meetings, or going up to Lowell to present at UMOVE, I feel that the act of sharing my work with my colleagues and connecting with them has served me very well over the years.

Overall, my PhD has been an incredible journey. It has had as many ups as it has downs, but at the end of the day, I am grateful for such a wonderful opportunity and for an impactful six years. My overall message to my younger self and to future PhD students is to go in prepared for an experience, not a job, to always keep the end goal in mind, and to connect with others as much as possible, because that is where the true value lies.